UNIVERSITY OF CALIFORNIA

Los Angeles

Analyticity and Acausality of Nonlocal Quantum Field Theory

A dissertation submitted in partial satisfaction

of the requirements for the degree

Doctor of Philosophy in Physics

by

Paokuan Chin

2022

© Copyright by
Paokuan Chin
2022

ABSTRACT OF THE DISSERTATION

Analyticity and Acausality of Nonlocal Quantum Field Theory

by

Paokuan Chin
Doctor of Philosophy in Physics
University of California, Los Angeles, 2022
Professor Terry Tomboulis, Chair

In this dissertation, we study nonlocal quantum field theories obtained by delocalizing the fields in the interaction terms of some local Lagrangian. The delocalization kernels in momentum space are exponentials of entire functions, thus no additional mass poles are introduced, but they ensure UV finiteness of loop integrals of Feynman diagrams. The transition matrix is defined in the Euclidean regime, followed by analytic continuation of the external momenta. Because of the delocalization kernels, manipulations valid in local theories are prohibited in the nonlocal theories, including Wick rotation and dispersion relation. We study the analyticity structure of the transition matrix of such theories at the perturbative level, using the Landau equations. The result shows that singularities that occur in local theories are also present in the nonlocal theories, except for singularities of the second type. The Cutkosky rule is then derived using Cutkosky's original argument, and the unitarity condition follows as an application of the rule. We then quantify the acausality present in such nonlocal theories using the Bogoliubov causality condition (BCC). First we study the acausality of the effective propagator, which is shown to be exponentially suppressed for large space-time separation. Mellin transform is introduced to help find the asymptotic behavior of acausality. Next we prove that in local theories, for each diagram, the BCC equation amounts to a chain of retarded propagator between two vertices; while in nonlocal theories, the chain consists of $\tilde{\Delta}_R$, which is the retarded propagator delocalized by the non-

local kernel and is therefore no longer causal. The acausal amplitudes are then integrated over wave packets to make experimental predictions. We show that for a nonlocality scale of order Plank's length, the acausality will be experimentally immeasurable. Along the way, by extending the BCC to unitarity equations, we show that the theory defined directly in Minkowksi space is not unitary. This reaffirms that the theory has to be defined in the Euclidean regime and then analytically continued.

The dissertation of Paokuan Chin is approved.

Zvi Bern

Per Kraus

Mikhail Solon

Terry Tomboulis, Committee Chair

University of California, Los Angeles

2022

To my parents . . .

who have supported me through the ups and downs

of this deep rabbit hole.

Table of Contents

List of Figures . . . . . **ix**

Acknowledgments . . . . . **xi**

Curriculum Vitae . . . . . **xiii**

1 Introduction **1**

2 Defining the Theory **7**

2.1 The Feynman Amplitude 10

2.2 Relation between Euclidean and Minkowskian Theory 14

2.3 Other nonlocal kernels 18

2.3.1 Kernels that can be Wick-rotated 18

2.3.2 Kernels with polynomial decay 19

2.3.3 Kernels with compact support 19

3 Analyticity **22**

3.1 Parametric Representation 22

3.2 Landau equations and singularity structure 28

3.2.1 The Landau equations for the amplitudes 29

3.2.2 Singularity structure 34

4 Cutkosky discontinuity rule **41**

5 Acausality of the Effective Propagator **49**

5.1 Asymptotic Behavior for General Kernel 53

5.1.1 Asymptotic Expansion Using Mellin Transform 54
5.1.2 Asymptotic of (Minkowski) Fourier Transform 55
5.1.3 Asymptotic for Nonlocal Kernel and the Acausal Part of the Propagator 56
5.1.4 Kernels with polynomial decay 60

6 Amplitudes and causality 63
6.1 Bogoliubov Causality Condition 63
6.2 Tree Amplitudes 67
6.3 Causality violation for Tree Amplitudes 71
6.4 Loop amplitudes 80
6.4.1 One Loop Amplitudes 80
6.4.2 Unitarity of the Euclidean-defined theory 82
6.4.3 Multi-loop Amplitudes 85
6.5 Difference between Euclidean-defined and Minkowski-defined theory 85

A Non-vanishing of the Symanzik polynomial for the nonlocal theory . . . 90

B Equivalence of the Landau equations for the amplitudes in different forms 92

C Leading asymptotic behavior of the effective propagator 94

D Explicit asymptotic behavior of the acausal part of a particular effective propagator 96

E Fourier transform of Lorentz invariant functions 101

F Examples of asymptotic behavior using the Mellin Transform method . 103
F.1 Ordinary massive propagator 103

F.2 Bubble graph of massless particles 104

G BCC argument for all loop 106

Bibliography 112

List of Figures

2.1 The bubble diagramm. 12

2.2 The singularities and integration contour in the k^0 plane for the bubble amplitude when: (a) the zeroth component of the external momentum is purely imaginary, and (b) the external momentum rotates to real values. The contour is deformed from C_I to C 13

3.1 (a) The one-loop box graph; (b) one of the once-reduced graphs of (a) containing the anomalous thresholds; (c) one of the twice-reduced graphs of (a) containing the normal thresholds; (d) the acnode graph. Black circles denote nonlocal vertices. 35

4.1 (a) Original position of singularities with undistorted contour in q^2 plane; (b) singularity movement as $z \to z^0$ pinching the contour; (c) equivalent contour consisting of regular and a singular (circle) contribution. 43

4.2 Difference (circular contour) between continuing: (a) above and (b) below endpoint singularity. 45

4.3 Examples of eq. (4.9) for discontinuities involving: (a) three (anomalous threshold); and (b) four Cutkosky cuts (on-shell lines). 46

4.4 Discontinuity across normal threshold given by eq. (4.10). Energy flows from unshaded to shaded side of cut (on-shell) lines. Feynman rules on shaded side are those for $T^\dagger$. 47

5.1 The acausal part of a particular effective propagator. The analytic expression of its asymptotic (5.13) is compared to numerical evaluation using (5.16), and indeed they agree well for large x^2. The parameters are set to $m = 1$ and $\ell = 1/2$. 53

6.1 Propagation by a chain of Δ_R (arrowed segments) and Δ_{ac} (non-arrowed segments). (a) - (b): acausal propagation due to one or more Δ_{ac} segments; (c) - (d): carefully arranged space-time such that all Δ_{ac} have (nearly) null-like arguments connecting points with $|(x_1 - x_m)^2| \gg \ell^2$. 75

6.2 Contours for the bubble graph: blue for Minkowski-defined theory; green for Euclidean defined theory. Integration along the red contour gives the difference. 83

6.3 Integration along contour (red) giving the difference between Minkowski- and Euclidean-defined amplitude for the l.h.s. of (6.13). 84

D.1 Curves of steepest descent (in colors) and ascent (gray) of (D.4) in the complex u plane with $v = 0$. The saddle points (D.6) are located at the intersections. The original u contour of (D.2) can be deformed to $\mathcal{C}_1 \cup \mathcal{C}_2$. 98

G.1 Graphs with two internal propagators; external legs not explicitly shown. . . . 106

Acknowledgments

I am indebted to Terry Tomboulis for the years of guidance and for the care he has given me in his own way. I would also like to thank the committee members (past and present), Per Kraus, Zvi Bern, Mikhail Solon, and Roberto Peccei, for their advice and lessons in Physics. Lastly, I must thank Stephanie Krilov for handling the student affairs so smoothly.

I am extremely grateful for my parents, without whom I would not have been who I am today. I thank my family and friends in Taiwan, including Hsiao-Shan Chin, Hao-wei Huang, Yu-Shu Lin, Huei-Yu Liang, Hsiao-Tsu and Hsiao-En Wang, Chung-Nan Zhou, Ya-Feng Zhou, and Hsueh-Liang Tsai, who believed in me and provided mental and physical support. I thank my teachers Rong-hui Chen and Zheng-Liang Lu who pointed me to this fascinating world of Physics and who, to this day, are still my role models as Physics teachers.

I could not have made it through my graduate student life were it not for the wonderful friends I have, including (in alphabetical order) Gurleen Bal, Kevin Chen, Hsuan Chien, Kevin Hayakawa, Albert Hsu, Winson Huang, Dimitris Kosmopoulos, Yanyan Li, Lukas Lindwasser, Li-Chia Tai, Shawn Tang, and Wan Zhe. I am walking in the freezing dessert at night and they are my torch. Last but not least, I must thank Nanxi Yao for all the memorable and the mundane moments we share.

Words have failed me in expressing my appreciation of the aforementioned people. All my skill points in language have been used to express ideas in Physics, which is this dissertation. It would take an equal amount of skill points to express my deep appreciation. There are many more that I wish to thank, but due to length limitation, I apologize for failing to mention their names.

This work was supported by Mani L. Bhaumik Institute for Theoretical Physics.

Contribution of Authors

Chapters 3 and 4 are based on [1] in collaboration with Terry Tomboulis. Chapters 5 and

6 are based on [2] in collaboration with Terry Tomboulis. Chapters 1 and 2 are based on both [1, 2].

Curriculum Vitae

2011 - 2014	B.S. in Physics, University of California, Los Angeles (UCLA).
2015 - Present	Ph.D. candidate in Physics, University of California, Los Angeles (UCLA).
2015 - 2022	Teaching Assistant, University of California, Los Angeles (UCLA)

Publications

Paokuan Chin and Terry Tomboulis, *Nonlocal vertices and analyticity: Landau equations and general Cutkosky rule*, *JHEP* **06** (2018) 014, arXiv:1803.08899 [hep-th].

Paokuan Chin and Terry Tomboulis, *Nonlocal vertices and causality*, to be published (2022).

CHAPTER 1

Introduction

Nonlocal interaction vertices occur in a variety of nonlocal field theory models and in string field theory. A local field theory with some minimal resolution length ℓ also gives rise to a nonlocal field theory, using wavelet decomposition [3]. In this dissertation we study the analyticity properties of amplitudes and the extent of acausality in theories possessing such interactions.

In contrast to the finite order polynomial momenta dependence of local interactions, nonlocal interactions are described by nonpolynomial functions of the momenta. Such vertices must satisfy certain constraints to ensure sensible physical properties. Given such vertices, amplitudes can then be constructed that are well-defined as integrals along certain loop integration contours and in a certain regime of external momenta - this typically means the Euclidean regime. The object then is to analytically continue beyond that regime in the space of the external invariants, i.e., the various scalar products or, equivalently, invariant energy and momentum transfer variables (Mandelstam variables) formed out of the external momenta. The analytical structure of amplitudes as a function of the external invariants viewed as complex variables is, of course, a well-studied subject in local field theory [4]. We will examine this analytical structure in the case of nonlocal interactions.

In axiomatic field theory, causality is considered an essential requirement, but it is often replaced by analyticity because it is easier to work with [5]. Though we will show that the nonlocal theories considered here have the same analytic structure as the local theories, the closing of the contour in the dispersion relation is prohibited by the nonlocal vertices. Indeed causality is violated, as one would expect because the theory is nonlocal. Theories that are

acausal are not necessarily sick. In [6], it is shown that even classical electrodynamics imply acausal effects when considering the self-force of a charged particle. The macroscopic world is observed to be causal. To be consistent, the acausality predicted by a theory must be microscopic. Current collider experiments are at TeV scales, so the predicted acausal effects must be at scales much higher than that. To quantify acausality, we employ the Bogoliubov causality condition [7].

The content of the dissertation is as follows. In chapter 2 we introduce the class of nonlocal vertices we study. They are constrained by various requirements including analyticity in momentum space, Lorentz invariance and UV finiteness. Requiring UV finiteness, in particular, implies that such vertices must decrease sufficiently fast (exponentially, or more generally be functions of rapid decay) in certain directions in complex momentum space. These directions must include the Euclidean momenta so that loop integrations are well defined, and the Minkowski direction so that tree amplitudes don't diverge for large momentum. For nonpolynomial entire functions, however, this necessarily implies exponential (or fast) growth in other directions in the complex plane, thus, generally preventing the usual Wick rotation.

The types of vertices considered encompasses those encountered in string field theory Feynman rules and a wide class of nonlocal field models. We nominally consider such interactions within scalar field theory models but this is no real constraint - the inclusion of spin only alters vertices and propagator numerators by polynomials which cannot effect the analyticity structure nor acausality in any essential way.

Well-defined amplitudes are obtained originally in the Euclidean regime and are then to be analytically continued in the complex space of external invariants. It is important to note in this context that they satisfy the property of hermitian analyticity relating the matrix elements of the transfer matrix T to those of its hermitian conjugate $T^\dagger$. This holds in the case of the nonlocal vertices considered here just as it does in the local case (section 2.1).

Since Wick rotation is prohibited, many manipulations that are valid in local theories are invalid in nonlocal theories. To avoid confusion, in section 2.2, we start from defining the

theory and discuss how various common mathematical objects, such as correlation functions, are obtained from the definition, if the objects can be defined at all. Finally, some other possible nonlocal vertices and their feasibility are discussed in 2.3.

Parametric representations of amplitudes with local vertices are obtained by introducing Feynman or Schwinger parameters and integrating out the loop momenta. In the case of nonlocal vertices such explicit momenta integration after introduction of Feynman parameters is generally not possible. For a class of exponential vertices, however, such integration is possible after the introduction of (generalized) Schwinger parameters. This we do in section 3.1. This generalizes the parametric representation of the local theory which appears as the zero delocalization scale limit. We also give the correspondingly generalized topological rules for computing the Symanzik polynomials of the parametric representation.

The basic tool for analyzing the singularity structure of amplitudes are the Landau equations [8]. They locate the surfaces (algebraic varieties) in the complex space of external invariants on which singularities may reside. We obtain the Landau equations for the amplitudes in the momentum representation and in the parametric representation (section 3.2), with which one may proceed to examine the possible singularity structure. The central theme for us here is that any arguments or derivations that rely solely on 'local' deformations of momenta or parametric contours, i.e., deformations in the finite complex plane, apply in the nonlocal case just as they do in the local case. The parametric representation is particularly illuminating in this respect as it makes it apparent that the (appropriate) nonlocal vertices serve as UV regulators but do not modify the local structure. As a result, the Landau equations (section 3.2.1) reveal the rich analyticity structure of amplitudes familiar from local field theory: normal and anomalous thresholds as well as other singularities such as anodes, crunodes and Landau surface cusps. Some of the latter may, for appropriate range of the masses, appear as complex singularities even on the physical sheet. Singularities of the 'second type' [4] need special consideration for reasons explained below. This can be properly done through the parametric representation.

The amplitude discontinuities in going around singularities in the space of invariants are

given by the general Cutkosky rule [9]. There are several ways of arriving at cutting rules in local field theory. For the nonlocal theories under consideration here, however, only derivations involving local use of Cauchy's theorem are possible. The original Cutkosky argument does in fact fulfill this requirement, and we adopt it to present circumstances to derive the general rule in chapter 4. This general rule applies to the discontinuity corresponding to any given solution of the Landau equations, i.e., to 'cuts' across any subset of internal lines of a given graph. Its particular application to normal threshold discontinuities gives the unitarity condition (optical theorem) as discussed there.

A first look of acausality is studied in chapter 5. The class of nonlocal vertices considered here are factorizable (c.f 2.6), and thus we may view the Feynman rules as having ordinary vertices and effective propagators (5.1), which are ordinary propagators with factors of the nonlocal kernel. We will show that the effective propagator has the same asymptotic behavior as ordinary propagator in position space. The difference between those two will be the acausal part, but that is exponentially decaying in $|x^2|/\ell^2$, where ℓ is the scale of nonlocality. This is done in detail for a particular class of nonlocal kernel. To generalize, we introduce the Mellin transform method for finding asymptotic expansions. This is done in 5.1 and a self-contained derivation is included. Along the way we will also show that the nonlocal vertex is also exponentially decaying in $|x^2|/\ell^2$. The physical meaning is that though the interaction vertices are not point-like, the space-time point of the interacting fields must be within scale ℓ. A result of the Mellin transform method applied to Fourier Transforms of Lorentz invariant functions is stated in proposition 5.1.1 and will be used in later chapter as well.

In section 6.1, we introduce the Bogoliubov Causality condition (BCC) as the basis for detecting acausality. The condition on S-matrix is given by (6.1). Roughly speaking, it means perturbing the coupling at spacetime point x_2 should not affect the dynamics at x_1 if x_2 is in the future light-cone of x_1. Perturbatively, it amounts to demanding that the sum of certain cut diagrams should be zero when x_1 precedes x_2, as shown in (6.11). In local theory, this sum equals the same diagram but with a chain of retarded propagators from vertex x_2 to

vertex x_1, which satisfies the causality condition. For tree amplitudes in nonlocal theory, the sum (6.11) becomes a chain of $\tilde{\Delta}_R$ from x_2 to x_1. $\tilde{\Delta}_R$ (c.f. (6.7)) is similar to the ordinary retarded propagator Δ_R, but with the nonlocal factor attached, which prevents the closing of the contour at infinity when Fourier transforming it to position space. Thus $\tilde{\Delta}_R$ has support for both positive and negative time, unlike the ordinary Δ_R, and so (6.1) does not vanish. All this is derived in section 6.2 by induction. In section 6.3, we then calculate the physical measurement of the acausality of this chain of $\tilde{\Delta}_R$, by associating the incoming and outgoing particles with wave packets. For most experiments, the acausality will be exponentially suppressed in x^2/ℓ^2, where x^2 is the separation $x_2 - x_1$. However, for experiments that are carefully arranged so that all space-time points are null-separated (within the error of the nonlocality scale), we show that the acausality is at least polynomially suppressed in ℓ/L, where L is the size of the wave packets of the external particles. Though not like exponential suppression, the nonlocality scale may be as short as the Planck length, so suppression in powers of ℓ/L is still negligibly small.

In section 6.4, we apply the BCC analysis to loop diagrams. First we analyze it for the "Minkowski-defined" amplitudes, which are directly written in Minkowski momentum. (In contrast, the correct theory is first written in Euclidean momentum and then analytically continued to Minkowski momentum. See 2.2 for details of why they are different.) We point out that the Minkowski-defined theory is not UV-finite and not unitary, but its loop amplitudes are easier to manipulate. For this theory, we prove that the sum (6.11) is equal to diagrams in which there is always a chain of $\tilde{\Delta}_R$ from x_2 to x_1, plus diagrams that include closed loops of $\tilde{\Delta}_R$. The former is acausal but is suppressed like in the tree case; The latter is zero if the theory was local but also suppressed in the nonlocal theory. The derivation is done in 6.4.1 for 1-loop diagrams and in 6.4.3 for all loops. The derivation is inductive and involves repeated application of (6.8) and (6.9), which are derived from local deformation of integration contours. The derivation can be straightforwardly applied to local theories, which are indeed causal.

In section 6.5, we look at the difference between the Minkowski-defined theory and the

correct theory. This is shown to be suppressed for large space-time separation. Since the causality violation of the the "Minkowski-defined" theory is suppressed, the causality violation of the correct theory is also suppressed.

Unitarity is closely related to BCC. The sum of (6.1) and (6.2) gives (6.13), which is the unitarity condition. In terms of sums of cut diagrams, it is the L.H.S. of (6.14). In section 6.4.1 and 6.4.3, we also look at how the Minkowski-defined theory violates unitarity. The sum (6.14) is equal to diagrams that have closed loops of $\tilde{\Delta}_R$. Fortunately, the violation of unitarity is precisely the difference between the Minkowski-defined and the correct theory, as shown in section 6.4.2. We've therefore once again shown that the correct theory is unitary.

There has been some related recent work on theories with nonlocal interactions of the type considered here. In [10] the discontinuity due to pinching of contours responsible for normal thresholds is computed in theories with nonlocal interactions by a careful analysis of the difference $T - T^\dagger$ and shown to be given by the Cutkosky rule. In [11] some general arguments anticipating some of the results in the present paper are given but the main focus is on the classical initial value problem with some partial consideration of the corresponding quantum causality problem.

CHAPTER 2

Defining the Theory

We consider a scalar field ϕ with Lagrangian of the general form

$$\mathcal{L}(x) = \frac{1}{2}\partial_\mu\phi(x)\partial^\mu\phi(x) - \frac{1}{2}m^2\phi^2(x) - \sum_n V_n[x;\phi]\,. \tag{2.1}$$

The interactions $V^{(n)}$ at spacetime point x are taken to be functionals of the fields ϕ of the general form

$$V_n([x;\phi]) = \frac{\lambda_n}{n!}\int d^dy_1\cdots d^dy_n\,\hat{V}^{(n)}(x,y_1,\cdots,y_n)\,\phi(y_1)\cdots\phi(y_n)\,. \tag{2.2}$$

All couplings λ_n are real. The case of local interactions, including derivative interactions, e.g., $\phi^2\partial_\mu\phi\partial^\mu\phi$, corresponds to

$$\hat{V}^{(n)}(x,y_1,\cdots,y_n) = P\Big(\{\partial_y\}\Big)\prod_{i=1}^{n}\delta(x-y_i)\,, \tag{2.3}$$

where $P\Big(\{\partial_y\}\Big)$ is a polynomial in the ∂_{y_i} derivatives; the trivial (constant) polynomial being the non-derivative ϕ^n interaction. In general, the vertices $\hat{V}^{(n)}$ are generalized functions defined as the Fourier transforms of appropriate functions:

$$\hat{V}^{(n)}(x,y_1,\cdots,y_n) = \int\frac{d^dk_1}{(2\pi)^d}\cdots\frac{d^dk_n}{(2\pi)^d}\,V^{(n)}(k_1,\cdots,k_n)\,e^{-i[k_1(x-y_1)+\cdots+k_n(x-y_n)]}\,. \tag{2.4}$$

We require that *the momentum-space vertices $V^{(n)}(k_1,\cdots,k_n)$ are entire functions of all their arguments.*[1] Thus, they possess no singularities anywhere in the complex k_i-planes (except at the point at infinity). Local interactions then comprise the subclass in which these entire functions are polynomials. Nonlocal interactions result from non-polynomial entire $V^{(n)}$'s,

[1] More specifically, entire functions of order $\geq 1/2$.

which will be restricted by imposing further requirements, in particular, Lorentz invariance and perturbative UV finiteness. In all cases reality of the vertices (2.2) implies the complex conjugation property[2]

$$V^{(n)}(k_1^*, \cdots, k_n^*) = V^{(n)}(-k_1, \cdots, -k_n)^* \,. \tag{2.5}$$

The class of vertices given by

$$V^{(n)}(k_1, \cdots, k_n) = \prod_{i=1}^{n} F(k_i^2) \,, \tag{2.6}$$

where $F(z)$ is entire, is of particular interest. This form of factorized vertices arises naturally as local interactions of delocalized fields. A delocalized field $\tilde{\phi}(x)$ is a functional $\tilde{\Phi}$ of the field ϕ with dependence on the spacetime point x and generally represented by

$$\begin{aligned} \tilde{\phi}(x) &\equiv \tilde{\Phi}[x;\phi] \\ &= \int d^d y \hat{F}(x,y)\phi(y) \,. \end{aligned} \tag{2.7}$$

Here we take $\hat{F}$ to be a generalized function defined as the FT of an entire function $F(z)$:

$$\hat{F}(x,y) = \sum_{n=0}^{\infty} a_n \, \Box_x^n \, \delta^{(d)}(x-y) = \int \frac{d^d k}{(2\pi)^d} \, F(k^2) \, e^{-ik(x-y_1)} \tag{2.8}$$

If now in a local scalar field potential

$$V(\phi(x)) = \sum_n V_n(\phi(x)) \geq 0 \tag{2.9}$$

one replaces $\phi(x)$ with the delocalized field $\tilde{\phi}(x)$ one arrives at (2.1) with vertices (2.6). Vertices of the type (2.6) posses convenient properties while incorporating all the main features of nonlocal interactions. They occur in string field theory and have been used in previous investigations of model nonlocal field theories [11–14].

To ensure UV finiteness we require that each $V^{(n)}$ vanishes exponentially[3] when one or more k_i's go to infinity in certain directions in complex momentum space. Specifically, the

[2]This arises from the correspondence $\partial/\partial x_\mu \to -ik_\mu$.

[3]More generally, as functions of rapid decay.

vertices are required to vanish in this manner along the Euclidean directions. These may be specified as usual by taking purely imaginary time components: $k_r^0 = i\hat{k}_r^0$, with $-\infty < \hat{k}_r^0 < \infty$, and real space components $k_r^j = \hat{k}_r^j$, with $-\infty < \hat{k}_r^j < \infty$, and $j = 1, \ldots, (d-1)$, $r = 1, \ldots, n$. From the theory of entire functions (cf., e.g., [15]) we know that this necessarily implies that $V^{(n)}$ will diverge (exponentially) as k_i's go to infinity in other directions. This precludes the usual Wick rotation between Euclidean and Minkowski space.

Consider the function

$$F(k^2) = \exp[\ell^2 k^2]\,, \tag{2.10}$$

where ℓ is some given scale. This indeed vanishes exponentially in the Euclidean directions $k^2 = -[\sum_{\mu=0}^{(d-1)} \hat{k}_\mu^2]$ as any $\hat{k}_\mu \to \infty$, thus rendering loop integrals UV finite. For real Minkowski momenta, however, it vanishes exponentially only for spacelike momenta, while diverging exponentially for timelike momenta. This is unacceptable as it implies unphysical behavior in any process involving timelike exchange, e.g., in s-channel 2-to-2 scattering already at tree level. In complicated theories with several types of interactions, like string field theory, such unphysical behavior may be cancelled among the contributions from different vertices. For the model field theories (2.1) considered here we simply exclude such unphysical behavior by requiring that

$$F(k^2) = \exp[-\mathcal{P}(k^2)]\,, \tag{2.11}$$

where $\mathcal{P}(k^2)$ is an even degree polynomial in k^2 with real coefficients and positive highest coefficient. The minimal choice is then

$$\mathcal{P}(k^2) = -\frac{1}{2}\ell_1^2 k^2 + \frac{1}{4}\ell_2^4\,(k^2)^2\,. \tag{2.12}$$

It is natural to take the coefficients proportional to some common scale: $\ell_i = c_i\ell$, $i = 1, 2$, where ℓ is the basic nonlocality scale characterizing the model. (2.12) guarantees that the vertices asymptotically vanish exponentially inside cones around both the Euclidean and Minkowski directions. They diverge then exponentially in cones along the adjoining directions. The same holds, generally with more cone sectors, for (2.11) with higher even degree $\mathcal{P}$. For general vertices $V^{(n)}$ that do not necessarily factorize as in (2.6) we again take the

form (2.11) with even polynomials in variables k that now stand for linear combinations of the momenta on different legs of the vertex. In all cases, one may, furthermore, include polynomials multiplying the nonlocal $\exp[-\mathcal{P}(k^2)]$ factors. Such more general vertices encompass the various types of vertices one encounters in string field theory (cf. [10]) and a wide class of nonlocal field theories. Apart from some technical complications, however, these further elaborations, do not, in any essential way, alter the basic analyticity structure features already present in the simpler models.

We mention in passing that entire functions of the type considered above can be precisely characterized within the Gelfand-Shilov theory of generalized functions. Specifically, they and their FT are naturally treated within the theory of W spaces [16]. We will not, however, need to make use of this framework for the purposes of this thesis.

2.1 The Feynman Amplitude

The kinetic energy term in (2.1), being of the standard local form, gives the usual scalar propagator. The Feynman rules for (2.1) are then:
propagator $\dfrac{i}{(k^2-m^2+i\epsilon)}$ for each internal line of momentum k; and for each n-pronged vertex a factor: $-i\dfrac{\lambda_n}{n!}V^{(n)}(k_1,\cdots,k_n)$ with momentum conservation at each vertex. Since the vertices factorize as in (2.6), an equilvalent Feynman rule would be: a factor of

$$\frac{iF^2(k^2)}{k^2-m^2+i\epsilon} \tag{2.13}$$

for each internal line and a factor of $-i\frac{\lambda_n}{n!}$ for each n-pronged vertex. We will refer to (2.13) as the effective propagagtor.

We have so far considered a single scalar field, but one can straightforwardly extend (2.1) to multiple scalar fields including interactions between them of the same type (2.2). This allows one to consider different masses in the various propagators and external lines without altering the basic structure of the general L-loop graph (cf. (2.16) below) in any other way. This enhanced generality is very useful in discussing analyticity properties of amplitudes.

Consider a generic L-loop connected graph G with V vertices and I internal lines. One has $L = I - V + 1$. Let P_r denote the total external momentum flowing into the r-th vertex, $r = 1, \ldots, V$. All external momenta are taken to be incoming. By definition, $P_r = 0$ if all lines incident on the r-th vertex are internal. By overall momentum conservation we then have

$$\sum_{r=1}^{V} P_r = 0\,. \tag{2.14}$$

The internal momenta are labeled q_j, $j = 1, \ldots, I$. Each q_j is then a linear combination of the loop momenta l_k, $k = 1, \cdots, L$, and the external momenta P_r.

In the expression for the graph computed according to the above Feynman rules there is a factor of i from each propagator and $(-i)$ from each vertex. The corresponding transfer matrix T element (to the process described by graph G) is obtained by multiplying by an overall factor of i times a total momentum conservation delta-function. Here the transfer matrix T is defined from the S matrix by $S = I - iT$. Collecting the various factors of i gives $i^{I-V+1} = i^L$. Hence, we have

$$T_G = A_G\, \delta(\sum_{i=1}^{V} P_i)\,, \tag{2.15}$$

where the invariant amplitude A_G is given by

$$A_G(\{z_r\}) = C(G)\, i^L \int_C \prod_{k=1}^{L} \frac{d^d l_k}{(2\pi)^d} \prod_{j=1}^{I} \frac{1}{q_j^2 - m_j^2 + i\epsilon} \prod_{s=1}^{V} V_s^{(n_s)}(\{q, P\})\ . \tag{2.16}$$

Here $C(G)$ denotes the product of the various coupling and graph combinatorial factors, and q_j is the momentum flowing through line j. C denotes the loop momenta integration contours whose exact shape will be described below. The amplitude is a function of the various Lorentz invariants z_r constructed from the external momenta P_r. For parity invariant interactions these may be taken to be the set of all scalar products $P_r \cdot P_s$, including P_r^2. An alternative common choice is that of total energy and all sub-energies, momentum transfers and cross-energies $z_{ijk\ldots} = (P_i + P_j + P_k + \cdots)^2$. The Mandelstam s, t, u variables in 2-to-2 scattering is a familiar example. In general there are more invariants that can be formed

than independent variables among them. It is best for symmetry reasons to consider the amplitude as a function of all the invariants subject to relations among them.[4]

The amplitudes is only well-defined in "Euclidean" momentum space and can then be analytically continued to Minkowski space. In Euclidean space, the external momentum have imaginary zeroth component, $P_r^0 = iE_r$, where $E_r \in \mathbb{R}$, and the contour C of the zeroth component of loop momentum runs along the imaginary axis, denoted as C_{I}. (We retain the Minkowski signature while taking inner products.) The invariants z_r, as well as the q_j^2's of the propagators are then non-positive. These constrains the invariants $\{z_r\}$ to a subset of the full space. The amplitude is well-defined since no poles in the propagators are crossed and the loop integral is absolutely convergent due to the vanishing properties of the $V^{(n_s)}$'s.

To access the full z_r space, the P_r^0 are (simultaneously) Wick-rotated to reals $P_r^0 = iE_r \to E_r$ through the first or third quadrant, while keeping the endpoints of the l_i^0 contours fixed at $\pm i\infty$, since the vertices V diverge if any l_i^0 passes through certain cones at infinity. As P_r^0 rotates, singularities of the integrand of (2.16) moves in the l_i^0 plane and the contour needs to be deformed from $C_{\mathrm{I}} \to C$ to avoid them. Such deformation is always possible while P_r^0 is not real, but fails when P_r^0 approach certain real values, which gives rise to the singularity of $A_G(z)$. This is discussed in the next section.

As an explicit example (for full detail see [10]), we consider the bubble diagram as shown in Fig. 2.1. With the sum of incoming momentum defined as $p = p_1 + p_2$, the amplitude is

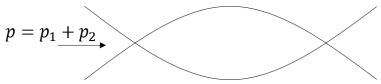


Figure 2.1: The bubble diagramm.

$$A_G(p^2) = -C(G) \int \frac{d^4k}{(2\pi)^4} \frac{F^2(k^2)}{k^2 - m^2} \frac{F^2((k-p)^2)}{(k-p)^2 - m^2} \,. \tag{2.17}$$

[4]Note that in d dimensions any set of $(d+1)$ or more vectors is linearly dependent. For an amplitude in d spacetime dimensions with E external legs and $E \geq d$, after imposing momentum conservation (2.14) and setting all E external legs on-shell, there are $\frac{1}{2}[2(d-1)E - d(d+1)]$ independent variables. E.g., in 4 dimensions with $E = 4$, there are 2 independent invariants, which can be any two among s, t, u with one relation between the three.

The theory is first defined with $p^0 = iE$, $E \in \mathbb{R}$, and the k^0 integration contour C_I is shown in Fig2.2(a). The singularities of the integrand are when the denominator of (2.17) vanishes, which are $k_0 = \pm\sqrt{\mathbf{k}^2 + m^2}, p^0 \pm \sqrt{(\mathbf{k}-\mathbf{p})^2 + m^2}$, away from the contour. As p^0 rotates to real values, the singularity $p^0 - \sqrt{(\mathbf{k}-\mathbf{p})^2 + m^2}$ may approach the contour (assuming $E > 0$), which is deformed to C to avoid it, as shown in Fig. 2.2(b). If for some particular choice of p, the singularity $p^0 - \sqrt{(\mathbf{k}-\mathbf{p})^2 + m^2}$ coincides $\sqrt{\mathbf{k}^2 + m^2}$, then the contour cannot e deformed away. This gives rise to a singularity of $A_G(p^2)$. The phenomenon will be discussed in general in chapter 3.

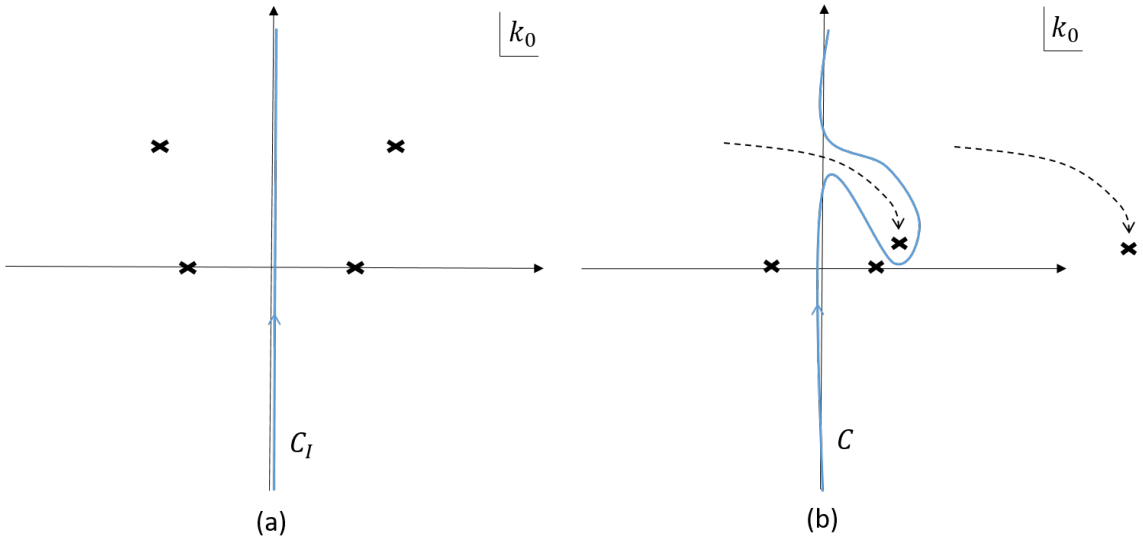


Figure 2.2: The singularities and integration contour in the k^0 plane for the bubble amplitude when: (a) the zeroth component of the external momentum is purely imaginary, and (b) the external momentum rotates to real values. The contour is deformed from C_I to C

The relation between the matrix elements of T and $T^\dagger$ is of basic importance. If T_{fi} is the T-matrix element between an initial state i and a final state f, one has $T^\dagger_{fi} = T^*_{if}$. We have the following result. Let the amplitude for T_{fi} be given by (2.16) with contour deformations $C_\mathrm{I} \to C$ as described above allowed. Then the amplitude for $T^\dagger_{fi}$ is obtained by complex conjugating all external momenta and all masses (for real masses this means $(m^2 - i\epsilon) \to (m^2 + i\epsilon)$) and changing the contour to $C^\dagger$. The contour $C^\dagger$ is obtained from C by first complex conjugating $C \to C^*$ and then restoring the original orientation. Note, in

particular, that $C_{\rm I}^\dagger = C_{\rm I}$.

This statement, which is easy to deduce by simple manipulations from (2.16), was proven in perturbation theory in local field theory in [17][5] and the proof in the presence of nonlocal vertices, already given in [10], is essentially the same. It is the statement of the fundamental property of *hermitian analyticity* [4], [17]. It will be invoked in sections 3.2.2 and chapter 4. Here we only remark that it shows T_{fi} and $T_{fi}^\dagger$ to be different values of the *same* analytic function. In this manner the behavior of scattering amplitudes is related to the singularity structure of a single analytic function of several complex variables $A_G(\{z_r\})$.

2.2 Relation between Euclidean and Minkowskian Theory

It will be helpful for what follows to first spell-out some facts concerning the relation of theories defined in Euclidean versus Minkowski space with respect to local versus nonlocal interactions, since some of these matters appear to have caused some confusion in the literature.

First recall some basic features of local quantum field theory. In local QFT a mathematically well-defined formulation at the nonperturbative level is provided by a convergent Euclidean path integral. Even within weak coupling perturbation theory amplitudes are given in terms of well-defined Feynman integrals strictly speaking only in Euclidean space - in Minkowski space the presence of the light cone renders such integrals ill-defined. Thus, e.g., rigorous power counting and bounds can only be obtained in Euclidean space. The n-point correlation functions of Euclidean fields, i.e., the Schwinger functions $S(x_1, \ldots, x_n) = \left\langle \phi(x_1) \cdots \phi(x_n) \right\rangle$ (after truncation of external legs) give, via Fourier transform, the Euclidean amplitudes $A^{(E)}(z_r)$, $z_r \leq 0$. The physical amplitude, denoted as $A(\{z_r\})$, $z_r \in \mathbb{R}$, is obtained by the analytic continuation of $A^{(E)}$ through the upper half planes of $\{z_r\}$. Then the FT of $A(\{z_r\})$ yield the position space n-point functions, which, modulo external leg truncations, represent the time-ordered correlations $\tau(x_1, \ldots, x_n)$ of Minkowski operator

[5] It holds also in the presence of fermions and complex couplings provided the Lagrangian is hermitian.

fields $\hat{\phi}$.

On the other hand, analytically continuing the Schwinger functions $S(x_1, \ldots, x_n)$ to Minkowski coordinate space yields the Wightman functions $W(x_1, \ldots, x_n)$. Given these functions, and a number of assumptions (on properties of W, existence of a vacuum, etc), one may then introduce operator fields $\hat{\phi}(x)$, a Hilbert space $\mathcal{H}$ and a Hamiltonian H, whose positivity follows from Reflection Positivity (positive transfer matrix) of the Euclidean theory. This is the content of the reconstruction theorems [18] that have been obtained at least for simple low-dimensional theories.[6] This general scheme in local QFT is depicted in the diagram:

$$
\begin{array}{ccc}
\text{Minkowski} & & \text{Euclidean} \\
\\
W(x_1, \ldots, x_n) & \longleftarrow a.c. \longrightarrow & S(x_1, \ldots, x_n) \\
\updownarrow & & \uparrow \\
\hat{\phi}(x),\, \mathcal{H},\, H & & \\
\downarrow & & FT \\
\tau(x_1, \ldots, x_n) & & \\
\updownarrow FT & & \downarrow \\
A(\{z_r\}) & \longleftarrow a.c. \longrightarrow & A^{(E)}(\{z_r\})
\end{array}
\tag{2.18}
$$

The possibility of Wick rotation of integration contours in Feynman integrals implies that, at least formally, the theory can be defined directly in Minkowski space, as done in elementary presentations of local QFT. The time-ordered correlation functions and amplitudes in perturbation theory defined directly in Minkowski space coincide with those obtained via analytic continuation from Euclidean space as described just above. This is *not* generally the

[6] No such constructions exist in four dimensions and certainly not for gauge theories, where the only gauge-invariant correlations are nonlocal (loops). The nonperturbative lattice Euclidean formulation is the only available for attempts at rigorous constructions of gauge theories.

case in the presence of nonlocal interactions. Since the nonlocal interaction vertices given by entire functions must necessarily diverge along certain directions in complex momentum space, that precludes the possibility of closing contours at infinity and preforming Wick rotations. The corresponding relation diagram for nonlocal theories then is as follows:

$$\begin{array}{ccccc} \text{Minkowski} & & & & \text{Euclidean} \\ W(x_1,\cdots,x_n)\,? & \longleftarrow & a.c. & \longleftarrow & S(x_1,\ldots,x_n) \\ & & & & \uparrow \\ A(x_1,...,x_n) & & & & FT \\ \updownarrow FT & & & & \downarrow \\ A(\{z_r\}) & \longleftarrow & a.c. & \longleftarrow & A^{(E)}(\{z_r\}) \end{array} \tag{2.19}$$

$A(x_1,...,x_n)$ is not the time-ordered correlation function of the field operators, which is undefined. It is simply the Fourier transform of $A(z_r)$, which can be understood as the (perfect but impossible) localization of incoming and outgoing particles using wavepackets. If, on the other hand, one analytically continues the Schwinger functions in position space from the Euclidean to Minkowski regime, the resulting would-be Wightman functions show in general singular unbounded behavior. Take for example, the amplitude of some 2-2 s-channel scattering, and let the nonlocal factor be $F = e^{-p^4/2\ell^4}$. The corresponding Schwinger function is

$$S(x) = \int_{\mathbb{R}^4} \frac{d^4p}{(2\pi)^4} \frac{e^{-p^4\ell^4}}{p^2+m^2} e^{-ipx} \tag{2.20}$$

where $x = x_2 - x_1$. To analytically continue this to the Wightman function, one rotates $x^0 \to ix^0$, but the contours of p need not and cannot be rotated simultaneously due to the vanishing and diverging properties of F at certain directions at infinity. The would-be Wightman function is then

$$W(x^0,\mathbf{x}) = S(ix^0,\mathbf{x}) = \int_{\mathbb{R}^4} \frac{d^4p}{(2\pi)^4} \frac{e^{-p^4\ell^4}}{p^2+m^2} e^{px^0 - i\mathbf{p}\cdot\mathbf{x}} \tag{2.21}$$

which grows exponentially in x^0.

Some attempts have been made to deal with this by extending the local theory Wightman axioms constructive approach with smearing by appropriate test function spaces, but no satisfactory scheme has emerged along these lines.[7]

The following question now arises concerning the last line in (2.19). Given some nonlocal theory Lagrangian we may always apply the corresponding Feynman rules written directly in Minkowski space to formally define amplitudes in perturbation theory directly in Minkowski space. (Assume, in particular, that we have vertices as in (2.6) with convergent behavior in cones both around the Euclidean and Minkowski axes, so that no extra issues with asymptotic behavior arise.) We may then construct an amplitude $A^{(M)}(\{z_r\})$ from these Minkowski space Feynman rules. Does this amplitude coincide with $A(\{z_r\})$ obtained by analytic continuation from Euclidean space? As already alluded to, in general it will not:

$$A^{(M)}(\{z_r\}) \neq A(\{z_r\}) \leftarrow a.c. \leftarrow A^{(E)}(\{z_r\}) \; . \tag{2.22}$$

The exception, where the equality does hold in (2.22), are tree-level amplitudes, where no loop integration contours are involved. For amplitudes involving loops, however, as noted above, (time component) integration contours must be pinned at $\pm i\infty$, since Wick rotations are not possible; and this results in the inequality in (2.22). This has several implications. One very important one is that, as we will show, the theory defined directly in Minkowski space is not even unitary. Some numerical evidence and arguments from the one-loop bubble diagram for this were presented in [19]. The amplitudes A_M, on the other hand, defined via the Euclidean continuation are known to be unitary [10, 19]. In section 6.5, we will estimate the size of the discrepancies implied by the inequality in (2.22).

[7] To illustrate the difficulties, we only note here that, for example, no usual notion of a Hamiltonian can be defined for nonlocal interactions, since no notion of evolution from data on a single time slice is possible. The only physical possibility is to define an effective Hamiltonian by smearing or averaging over time intervals longer than the nonlocal scale ℓ [11] aiming to regain, for appropriate rapidly-decaying vertices, the local theory as the effective theory at longer distances.

2.3 Other nonlocal kernels

In this thesis, we focus on nonlocal kernels of the type (2.11) with $\mathcal{P}$ being an even degree polynomial with positive highest coefficient. In this section we point out some other kernels that are also factorizable(c.f.(2.6)), and how they differ qualitatively from the one considered in this thesis. A particular variation that is *not* qualitatively different is $\mathcal{P}$ being exponential, e.g. $\mathcal{P}(k^2) = e^{k^4\ell^4} - 1$. $\mathcal{P}$ is entire and the kernel $\exp[-\mathcal{P}]$ decays faster than any power of $1/k$ in Euclidean and Minkwoski directions. All the features with polynomial $\mathcal{P}$ is also there for exponential $\mathcal{P}$.

2.3.1 Kernels that can be Wick-rotated

Here we consider kernels of the form (2.11), but $\mathcal{P}$ is such that the kernels decay with large momentum in the Minkowski and Euclidean direction and also along every direction in between. Mathematically, that means

$$\mathcal{P}(se^{i\theta}) \to \infty \quad \text{as} \quad s \to \infty \quad \text{and} \quad \theta \in [0, \pi]. \tag{2.23}$$

Since the kernel decays in the upper half plane of s, Wick rotation is possible. An example of such kernel would be

$$F(s) = \exp\left[-(s^2\ell^4)^\rho\right], \quad \rho < \frac{1}{4}\,. \tag{2.24}$$

Note this is not an entire function and we have to choose a Riemann sheet for which the theory is defined. The choice is given by the condition (2.23).

For theories with this type of kernels, loop amplitudes are UV-finite, and the zeroth component of the loop momentum need not be pinched at $\pm i\infty$, since Wick rotation is possible. For this reason, the scheme (2.18) is also valid like in local theories. Wightman functions can be defined and these theories fall under Jaffe's class of strictly-localizable fields [20].

In section 5.1, we'll see that for such theories, the delocalized vertex ((2.8)) and the acausal part of the effective propagator (5.8) decay polynomially in ℓ^2/x^2 for large x^2. In

contrast, those in theories where the kernels have polynomial $\mathcal{P}$ decay exponentially. In addition, the branch cuts of $\mathcal{P}$ may introduce extra complication in computing $T^\dagger$ when we discuss unitarity. For these reasons, we do not consider this type of kernel.

2.3.2 Kernels with polynomial decay

In this part we introduce kernels that are exponentials of entire functions, but they decay polynomially for large momentum along the Euclidean and Minkowski directions. An example would be

$$\begin{aligned} F(k^2) &= e^{-H(k^2)} \,, \\ H(k^2) &= \int_0^{\mathcal{P}(k^2)} \frac{1-\zeta(w)}{w}\, dw \,, \end{aligned} \tag{2.25}$$

where $\mathcal{P}$ is some even degree polynomial with $\mathcal{P}(0) = 0$; and $\zeta(w)$ is an entire function that's real on the real axis, $\zeta(0) = 1$, and $\zeta(w) \to 0$ as $w \to \infty$. A kernel approaches a constant as $k^2 \to 0$ and decays as $\frac{1}{\mathcal{P}(k^2)}$ for large space-like and time-like momentum. An explicit example would be $\mathcal{P} = k^4$ and $\zeta(w) = e^{-w}$. The kernel is thus

$$F(k^2) = \exp[-\Gamma(0, k^4) - \gamma - \ln k^4] \,, \tag{2.26}$$

where $\Gamma(s, x)$ is the incomplete gamma function and γ is the Euler's constant. While the kernel falls off as $\sim 1/k^4$ for large $|k^2|$, it grows exponentially for k^2 along the imaginary axis. Thus for amplitudes, the zeroth component of the loop momentum is also fixed to be at $\pm i\infty$. The delocalized vertex (i.e. 2.8) and the acausal part of the effective propagator (5.8) decay exponentially, which we will prove ini section 5.1.4.

2.3.3 Kernels with compact support

In (2.8), $\hat{F}(x, y)$ represents the extent of smearing of the delocalized field $\tilde{\phi}(x)$. For kernels of the type (2.11), although the delocalized field is centered at one point and has an exponentially decaying tail, it has infinite support. Here we discuss kernels that have compact

support (in the Euclidean space, where the theory is defined). An example would be

$$\hat{F}(x,y) = \frac{2}{\pi^2\ell^4}\Theta(\ell - \|x-y\|) \ , \tag{2.27}$$

where Θ is the Heaviside step function, $\|\cdot\|$ is the Euclidean norm, and ℓ would be the nonlocal scale. It is well-known that the Fourier transform of any function of compact support goes to 0 as the argument tends to infinity along the real direction, i.e.,

$$F(k) = \int d^4x \, \hat{F}(0,x) e^{ikx} \tag{2.28}$$

[8] goes to 0 as $k^2 \to +\infty$. (The inner products here are under Euclidean signature.) This feature is desired as it will render loop integrals UV finite. Another feature is that, by the Paley-Weiner Theorem [21], since $\hat{F}(0,x)$ is compact, $F(k)$ is an entire function. To go to Minkowski space, we simply let k^0 be purely imaginary. Unfortunately, it turns out that the kernel will grow exponentially for large time-like k^2, i.e. as $k^0 \to \pm i\infty$. This is unphysical since the s-channel 2-to-2 scattering amplitude will also grow unboundedly.

To prove that, we first state the Paley-Weiner Theorem.

Theorem 1 (Paley-Weiner) *If and only if an entire $F(k)$ on $\mathbb{C}^n$, for all $k \in \mathbb{C}^n$, satisfies*

$$F(k) \leq C(1+|k|)^N e^{\ell|\mathrm{Im}k|} \ , \tag{2.29}$$

for some constants C, N, ℓ, then $F(k)$ is the Fourier transform of some compact distribution $\hat{F}(x)$ supported in a ball $\{x| \, |x| \leq \ell\}$.

By rotational symmetry (Lorentz symmetry in Minkowski space), we can always choose $\mathrm{Im}k$ to be nonzero for only the 0th component. Then if $F(k) < e^{c|\mathrm{Im}k^0|}$ for sufficiently large k^0 for all $c > 0$, the inequality in the theorem is satisfied for arbitrarily small $\ell > 0$, meaning the inverse Fourier transform $\hat{F}(x)$ is compact within an arbitrarily small ball. This is a contradiction, so $F(k)$ must be $\sim e^{c|\mathrm{Im}k^0|}$ as $k^0 \to \pm i\infty$ for some $c > 0$.

[8] In this subsection we abuse the notation and denote $F(k)$, instead of $F(k^2)$, as the Fourier transform of $\hat{F}(x,y)$.

As a concrete example, consider the kernel (2.27). It can be worked out that, in 4d, the kernel in Euclidean momentum space is

$$F(k) = \frac{8}{\|k\|^2 \ell^2} J_2(\|k\| \ell) \ , \tag{2.30}$$

where J is the Bessel function of the first kind. If we rotate $\|k\|^2$ to negative values, we get

$$F(k) = -\frac{8}{k^2 \ell^2} I_2(\sqrt{k^2}\ell) \ , \tag{2.31}$$

where k^2 is now iin Minkowski signature and I is the Modified Bessel function of the first kind. Indeed $F(k)$ grows linearly with $\exp[\sqrt{k^2}\ell]$.

Because of the unphysical behavior at extremely high momentum, we do not consider this type of kernel in this thesis. However, if for some applications, such as lattice theory, one does not look at energy scale close to or above $1/\ell$, then the kernel is sensible.

CHAPTER 3

Analyticity

In this chapter, we study the analytic structure of the S-matrix amplitude perturbatively. We first introduce the parametric representation of Feynman amplitude, which turns out useful for our study. We then briefly introduce the Landau equations and then apply them to the amplitudes.

3.1 Parametric Representation

The use of Feynman or Schwinger parameters has been a very useful tool in investigating the analytic structure of amplitudes. Expressing the product of propagators in (2.16) by the introduction of Feynman parameters the amplitude may be written in the form

$$A_G(\{z_r\}) = C(G)\,\Gamma(I)\,i^L \int_{C_{\rm I}} \prod_{k=1}^{L} \frac{d^d l_k}{(2\pi)^d} \int_0^1 \prod_{i=1}^{I} d\alpha_i \, \frac{\delta(1-\sum_i \alpha_i)}{[\psi(\alpha,q,P)]^I} \prod_{s=1}^{V} V_s^{(n_s)}(\{q,P\})\,, \qquad (3.1)$$

where

$$\psi(\alpha,l,P) \equiv \sum_{i=1}^{I} \alpha_i (q_i^2 - m_i^2)\,. \qquad (3.2)$$

This 'mixed' form (3.1), involving integrations over both loop momenta and Feynman parameters, has proved convenient for arriving at the Landau equations (cf. below) and discussing analyticity properties.

In the case of local vertices, where all $V_s^{(n_s)}$ factors are polynomials in the momenta, it is possible to carry out the integrations over the loop momenta in (3.1) explicitly resulting in the well-known Feynman parameter representation. In the case of nonlocal vertices carrying out the loop momenta integrations in (3.1) in closed form is, in general, no longer possible. For vertices of exponential type, however, it is natural to use Schwinger, rather

than Feynman, parameters. For a class of vertices considered above, in particular, the use of Schwinger parameters allows the loop integrations to be carried out explicitly resulting into a pure parametric representation. In the case of local vertices the Schwinger and Feynman parametric forms lead to equivalent expressions.

To obtain the parametric form of (2.16) by use of Schwinger parameters we proceed as follows. Let ε denotes the $V \times I$ incidence matrix given by :

$$\varepsilon_{ri} = \begin{cases} 1 & \text{if } q_i \text{ leaves vertex } r \\ -1 & \text{if } q_i \text{ enters vertex } r \\ 0 & \text{if } q_i \text{ not incident on vertex } r \end{cases} \tag{3.3}$$

Momentum conservation at each vertex then implies

$$P_r - \sum_{j=1}^{I} \varepsilon_{rj} q_j = 0 \,. \tag{3.4}$$

Noting that for fixed line j only two of the elements of ε are non-vanishing and of opposite sign, one obtains

$$\left[\sum_{r=1}^{V} \varepsilon_{rj} \right] = 0 \,. \tag{3.5}$$

(3.5) implies that the rank of ε for a connected graph is $V-1$. Conservation of the external momenta (2.14) then follows from (3.4) by summing over the vertex index r and using (3.5), which is in fact a necessary and sufficient condition for the compatibility of the system (3.4).

Recall that the amplitude is defined in Euclidean space. (See the second paragraph after (2.16).) We denote $P_r^0 = i\hat{P}_r^0$ and $l_i^0 = i\hat{l}_i^0$, where $\hat{P}_r^0$ and $\hat{l}_i^0$ are reals, and $z_r = -\hat{z}_r$, $\hat{z}_r > 0$. Furthermore, use of the incidence matrix allows us to take the I internal momenta q_j (rather than singling out L independent loop momenta) as integration variables subject to the constraint (3.4). Thus, with vertices of type (2.6), we can write (2.16) in the form:

$$\begin{aligned} & A_G(-\{\hat{z}_r\})\,(2\pi)^d \delta^{(d)}\Big(\sum_r \hat{P}_r\Big) \\ = \;& C(G)(-1)^{I+L} \int \prod_{k=1}^{I} \frac{d^d \hat{q}_k}{(2\pi)^d} \prod_{j=1}^{I} \frac{[F(-\hat{q}^2)]^2}{\hat{q}_j^2 + m_j^2} \prod_{r=1}^{V} (2\pi)^d \delta^{(d)}\Big(\hat{P}_r - \sum_{j=1}^{I} \varepsilon_{rj} \hat{q}_j\Big) \,, \end{aligned} \tag{3.6}$$

with all momenta now being Euclidean. We introduce Schwinger parameters α_i, $i = 1, \cdots, I$, for each of the propagator factors in (3.6) using the following well-known identity,

$$\frac{1}{\hat{q}^2 + m^2} = \int_0^\infty e^{-\alpha(\hat{q}^2+m^2)}\, d\alpha \,. \tag{3.7}$$

For the particular vertex factor of type (2.12), we also introduce parameters β_i, $i = 1, \cdots, I$, to rewrite the vertex factors as

$$\begin{aligned} [F(-\hat{q}^2)]^2 &= e^{-\ell_1^2\hat{q}^2 - \frac{1}{2}(\ell_2^2\hat{q}^2)^2} \\ &= \int_{-\infty}^{\infty} \frac{d\beta}{\sqrt{2\pi}}\, e^{-\ell_1^2\hat{q}^2 - i\beta\ell^2\hat{q}^2 - \frac{1}{2}\beta^2} \\ &= \left(\frac{e}{2\pi}\right)^{\frac{1}{2}} \int_{-\infty}^{\infty} d\beta\, e^{-\ell_1^2\hat{q}^2 - \ell_2^2\hat{q}^2 - i\beta\ell_2^2\hat{q}^2 + i\beta - \frac{1}{2}\beta^2} \,. \end{aligned} \tag{3.8}$$

The last line in (3.8) is obtained by displacing the integration contour in the complex β-plane from the real axis to $(-\infty - i, +\infty - i)$. We also write the delta functions in (3.6) in their exponential integral representation. Thus,

$$\begin{aligned} &\prod_{j=1}^{I} \frac{[F(-\hat{q}^2)]^2}{q_j^2 + m_j^2} \prod_{s=1}^{V} (2\pi)^d \delta^{(d)}\Big(\hat{P}_r - \sum_j \varepsilon_{rj} q_j\Big) \\ &= \left(\frac{e}{2\pi}\right)^{\frac{I}{2}} \int_{-\infty}^{\infty} \prod_{s=1}^{V} d^d x_s \int_0^\infty \prod_{k=1}^{I} d\alpha_k \int_{-\infty}^{\infty} \prod_{l=1}^{I} d\beta_l \;\exp\left[\sum_{j=1}^{I}\Big(-\alpha_j(\hat{q}_j^2 + m_j^2)\Big)\right] \\ &\quad \cdot \exp\left[\sum_{i=1}^{I}\left(-(\ell_1^2 + \ell_2^2 + i\ell_2^2\beta_i)\hat{q}_i^2 + i\beta_i - \frac{1}{2}\beta_i^2\right)\right] \exp\left[-i\left(\sum_{r=1}^{V} x_r(\hat{P}_r - \sum_{i=1}^{I}\varepsilon_{ri}\hat{q}_i)\right)\right] . \end{aligned} \tag{3.9}$$

Inserting (3.9) in (3.6) the q_k-integrations may be straightforwardly performed. To next carry out the x_s-integrations perform first a shift of integration variables:

$$x_s = y_s + x_V \qquad \text{for} \quad s = 1, \cdots, (V-1)\,. \tag{3.10}$$

This, as it is easily seen, has the effect that, by (3.5), x_V couples only to the external momenta P_r. Integration over x_V then gives a delta function factor $(2\pi)^d\delta^{(d)}(\sum_r \hat{P}_r)$ enforcing overall momentum conservation. The $(V-1)$ remaining y_s integrations can then be carried out.

The final result assumes the form:

$$A_G(\{z_r\}) = C(G)\left(\frac{e}{2\pi}\right)^{\frac{I}{2}} I\left(\frac{1}{4\pi}\right)^{Ld/2}(-1)^{I+L}\int_0^\infty \prod_{k=1}^{I} d\alpha_k \int_{-\infty}^{\infty}\prod_{l=1}^{I} d\beta_l \, \frac{\exp\left[J(\alpha,\beta;P)\right]}{\Delta(w)^{d/2}}\,. \tag{3.11}$$

Here we introduced the notation

$$w_j = \alpha_j + \bar{\ell}^{\,2} + i\ell_2^2\,\beta_j\,, \qquad j = 1,\cdots,I\,, \tag{3.12}$$

with

$$\bar{\ell}^{\,2} \equiv \ell_1^2 + \ell_2^2\,. \tag{3.13}$$

Then, in (3.11):

$$\Delta(w) \equiv \Big(\prod_{j=1}^{I} w_j\Big)\det d(w) \tag{3.14}$$

where $d(w)$ is the $(V-1)\times(V-1)$ matrix, of rank $(V-1)$, given by

$$d(w)_{rs} \equiv \sum_{i=1}^{I} \varepsilon_{ri}^{(V)}\,\frac{1}{w_i}\,(\varepsilon^{(V)})_{is}^{T}\,. \tag{3.15}$$

In (3.15) $\varepsilon^{(V)}$ denotes the incidence matrix with the V-th row deleted. Finally, $J(\alpha,\beta;P)$ in (3.11) is given by

$$J(\alpha,\beta;P) = Q(w;P) - \sum_{i=1}^{I}(\alpha_i m_i^2 - i\beta_i) - \frac{1}{2}\sum_{i=1}^{I}\beta_i^2\,, \tag{3.16}$$

where $Q(w;P)$ denotes the quadratic form:

$$Q(w;P) = \sum_{r,s=1}^{V-1} P_r d^{-1}(w)_{rs} P_s\,. \tag{3.17}$$

(3.11) is written in terms of Minkowski scalar products for general (complex) momenta P_r, but was derived above in the Euclidean regime, i.e., for momenta $\hat{P}_r$ related by $P_r^0 = i\hat{P}_r^0$ and thus $P_r\cdot P_s = -\hat{P}_r\cdot\hat{P}_s$, $z_r = -\hat{z}_r$.

For a given diagram G, $\Delta(w)$ and $Q(w;P)$ may be computed directly from their definitions (3.14) and (3.17), respectively. Alternatively, the expressions for them can be conveniently obtained from the topology of the graph. To give a precise statement of these

topological prescriptions we need a few basic graph theory notions. Consider the Feynman diagram G as a graph defined by V vertices and I edges (the internal lines).[1] A tree in G is a subgraph that contains no loops (circuits, in common graph theory terminology). The number of vertices V_T and edges I_T of tree T are related by $V_T = I_T + 1$. A spanning tree T in G is a subgraph that is a tree and contains all the vertices of G, i.e., $V_T = V$. Note that then $I - I_T = L$. The complement T^* of a spanning tree T in G is called a co-tree (or the 'chord set' corresponding to T). Thus, $I_{T^*} = I - I_T = L$. A 2-tree $T^{(2)}$ is a spanning tree with one edge removed. Removing one edge of a spanning tree leaves two vertex-disjoint connected subgraphs $T^{(2)}_\pm$ making up the 2-tree: $T^{(2)} = T^{(2)}_+ \cup T^{(2)}_-$. Note that, from its definition, a 2-tree contains all the vertices of G and that one of the subgraphs $T^{(2)}_\pm$ may be an isolated vertex.[2] The compliment of a 2-tree in G is the corresponding 2-co-tree $T^{(2)*}$.

We can now give a precise statement of the topological rules for obtaining $\Delta(w)$ and $Q(w;P)$. The determinant of the matrix $d(w)$ defined in (3.15) is given by

$$\det d(w) = \sum_{T\subset G} \prod_{i\in T} \frac{1}{w_i}\,. \tag{3.18}$$

It follows from (3.14) that

$$\Delta(w) = \sum_{T\subset G} \prod_{i\in T^*} w_i\,. \tag{3.19}$$

As seen from (3.19) $\Delta(w)$ is a homogeneous polynomial in the w_i's of degree L. $Q(w;P)$ is then obtained from

$$\Delta(w)\,Q(w;P) = \sum_{T^{(2)}\subset G} z_{T^{(2)}} \prod_{i\in T^{(2)*}} w_i\,. \tag{3.20}$$

The variables $z_{T^{(2)}}$ denote the square of the sum of the momenta P entering either of $T^{(2)}_\pm$:

$$z_{T^{(2)}} = \left(\sum_{r\in T^{(2)}_+} P_r\right)^2 = \left(\sum_{r\in T^{(2)}_-} P_r\right)^2\,. \tag{3.21}$$

[1] External lines of G are irrelevant for the graph-theoretic considerations here.

[2] More generally, an n-tree $T^{(n)}$ is a spanning tree with $(n-1)$ edges removed. Thus a spanning tree is a 1-tree. An n-tree contains all vertices of G and consists of n connected components.

The r.h.s. of (3.20) is a homogeneous polynomial in the w_i's of degree $L+1$. Thus $Q(w;P)$ is given by the ratio of two polynomials and is homogeneous of degree 1. The relation (3.18) is well-known from the theory of circuits. The proof of (3.20), following [22], is more involved.[3]

Furthermore, one has the important fact that

$$|\Delta(w)| \neq 0, \quad \text{for} \quad \bar{\ell}^2 \neq 0 \tag{3.22}$$

for all $\alpha_i \geq 0$, $-\infty < \beta_i < \infty$. We prove (3.22) in Appendix A.

The local case is obtained by setting $\ell_1 = \ell_2 = 0$:

$$A_G(\{z_r\}) = C(G) \left(\frac{1}{4\pi}\right)^{Ld/2} (-1)^{I+L} \int_0^\infty \prod_{k=1}^{I} d\alpha_k \frac{\exp\left[J(\alpha,0;P)\right]}{\Delta(\alpha)^{d/2}} \,. \tag{3.23}$$

Rescaling $\alpha_i \to \rho\alpha_i$ in (3.23) and integrating over $\rho \in (0,\infty)$ gives the same result that is obtained from (3.1), with $V_s = 1$ vertex factors, by integrating over the loop momenta. Explicitly, the result is given by (3.45) below with $s = 0$ and $\rho_0 = 0$ (so only the $k = 0$ term survives on the r.h.s. of (3.45)). These manipulations are valid provided (3.23) and the local (3.1) version are UV convergent, which will be the case for $(I - \frac{d}{2}L) > 0$. Otherwise, as it well known, there is UV divergence from the $\alpha_i = 0$ Schwinger parameter integration endpoint where $\Delta(\alpha) = 0$, as evident from (3.19) with $w_i = \alpha_i$. In the local case then, (3.22) can be violated. This divergence can be regulated by cutting off the low end of the Schwinger parameter integration range. We now see explicitly from the representation (3.11) that this is precisely what the nonlocal vertices accomplish: *they render (3.11) UV finite by the introduction of the nonlocality scale ℓ.* This effects the shift $\alpha_i \to \alpha_i + \bar{l}^2$, cf. (3.12), thus ensuring (3.22) (cf. Appendix A). *Otherwise, the analyticity structure of the amplitude in the finite complex plane remains unaffected* as it is seen by examining the Landau equations for it, which we do next.

[3]The quantities $\Delta(a)$ and $\Delta(\alpha)Q(\alpha,P)$ are known as Symanzik polynomials. Here they are generalized to complex parameters w.

3.2 Landau equations and singularity structure

Let us briefly recall the general procedure whose application leads to the Landau equations. Consider a function $I(z)$ of a set of complex variables $z = \{z_r\}$, $r = 1, 2, \ldots$, given by an integral representation

$$I(z) = \int_C dw\, f(w, z) \tag{3.24}$$

for some contour C in the space of the complex integration variables $w = \{w_s\}$, $s = 1, 2, \ldots$, and some domain R in z-space for which the integral (3.24) is well-defined. One may then extend the definition of $I(z)$ outside R by analytic continuation. A general method for doing this goes back to [23], and was elaborated in the physics literature in [24], [25]; for a mathematically more rigorous homology-based approach see [26]. The integrand in (3.24) may have singularities at $\mathbf{w} = \mathbf{w}_i(z)$, $i = 1, 2, \ldots$, which depend on z. For z in the region R, the singularities should be away from the contour C to ensure that the integral converges. As z moves outside of R, the singularities move in the complex w-space and may approach C, which may then need to be deformed to avoid them. The contour deformation cease to be possible either if two or more of these singularities pinch the contour or if a singularity hits the fixed boundary of C. A general formulation encompassing these possibilities is given as follows [24], [25]. Let the location of singularities of the integrand be given by a set of equations $S_i(w, z) = 0$, $i = 1, 2, \ldots, n$; and let the boundaries of the contour be specified by another set $\tilde{S}_j = 0$, $j = 1, 2, \ldots, m$. Introduce corresponding parameters λ_i, $i = 1, \ldots, n$, and $\tilde{\lambda}_j$, $j = 1, \ldots, m$. The critical hypersurfaces on which the singularities of $I(z)$ are located are then specified by the solutions of the following conditions [24], [25]:

(i)

$$\lambda_i S_i(w, z) = 0\,, \qquad i = 1, 2, \ldots, n\,; \tag{3.25}$$

(ii)

$$\tilde{\lambda}_j \tilde{S}_j(w, z) = 0\,, \qquad j = 1, 2, \ldots, m\,; \tag{3.26}$$

(iii)

$$\frac{\partial}{\partial w_k}\Big(\sum_i \lambda_i S_i(w,z) + \sum_j \tilde{\lambda}_j \tilde{S}_j(w,z)\Big) = 0 \qquad \text{for each } k\ . \tag{3.27}$$

The nice feature of the method is that one has only to examine the integrand for its singularities in complex space and apply these conditions. Working out their implications, however, can be highly nontrivial.

Application of conditions (i) - (iii) to the Feynman integral representation of an amplitude $A(\{z_r\})$ gives the Landau equations [8], also [27]. Depending on which form of the Feynman integral one uses these equations are given in different equivalent forms.

3.2.1 The Landau equations for the amplitudes

The first form of the Landau equations is obtained from the representation (2.16) in which there are no integration boundaries. With all vertex factors $V^{(n_s)}$ given by entire functions, the only singularities in the integrand can only come from the denominators: $S_i = (q_i^2 - m_i^2)$. Hence, application of (3.25) gives

$$\lambda_i(q_i^2 - m_i^2) = 0\,, \qquad \text{each } i\ , \tag{3.28}$$

i.e.,

$$\text{either} \quad q_i^2 = m_i^2\,, \qquad \text{or} \quad \lambda_i = 0 \qquad \text{for each } i\,, \tag{3.29}$$

where $i = 1, \ldots, I$ enumerates the internal lines. From (3.27) and noting that each internal momentum q_i is a linear combination of the loop momenta and the external momenta one obtains

$$\sum_{i \in C_k} \lambda_i q_i = 0\ , \qquad \text{for each } k\,. \tag{3.30}$$

In (3.30) the sum runs around the loop C_k, where $k = 1, \cdots, L$ enumerates a set $\{C_1, \cdots, C_L\}$ of L independent loops in the graph.

(3.29) and (3.30) are the Landau equations for the graph G (in what is often referred to as the first representation). The important point for us here is that they are independent of the form of the vertices as long, of course, as the vertices are entire functions: polynomials

in the local case and transcendental functions (such as (2.11)) in the nonlocal case. In either case, they, being entire, introduce no other singular points in the integrand and thus lead to the same form (3.29) and (3.30) of the Landau equations. Strictly speaking we have so far considered only the finite complex plane. In the extended complex plane singularities may occur at the point at infinity, which then require special consideration. These are in fact the so-called singularities of the second type. We will return to them below.

According to (3.29) and (3.30) singularities arise from configurations where either an internal line is on shell or the corresponding parameter $\lambda_i = 0$. For a given graph the solution with all $\lambda_i \neq 0$ gives its leading singularity. Those with some of the $\lambda_i = 0$ are the non-leading (or lower order) singularities. A non-leading singularity is the leading singularity of the corresponding so-called reduced graph, i.e., the graph obtained from the given graph by contracting each internal line with $\lambda_i = 0$ to a point.

One may alternatively use the 'mixed' form (3.1). To discuss analyticity properties using the representation (3.1) first note that the α-integration can be extended to $+\infty$ since the delta-function enforces $\alpha_i \leq 1$. We then multiply (3.1) by $1 = \int_0^\infty d\rho\, e^{-\rho}$ and rescale $\alpha_i \to \alpha_i/\rho$. Carrying out the ρ integration (3.1) is recast in the form

$$A_G(\{z_r\}) =$$
$$C(G)\,\Gamma(I)\,i^L \int_{C_{\rm I}} \prod_{k=1}^{L} \frac{d^d l_k}{(2\pi)^d} \int_0^\infty \prod_{i=1}^{I} d\alpha_i \, \frac{(\sum_{j=1}^I \alpha_j)\, e^{-(\sum_{j=1}^I \alpha_j)}}{[\psi(\alpha, q, P)]^I} \prod_{s=1}^{V} V_s^{(n_s)}(\{q, P\})\,. \tag{3.31}$$

With entire vertices there is now only one singularity surface $S = \psi(\alpha, q, P)$, and boundary surfaces $\tilde{S}_i = \alpha_i$. Straight application of conditions (i) - (iii) then gives a set of equations which are easily reduced to

$$\alpha_i(q_i^2 - m_i^2) \;=\; 0\,, \qquad \text{each } i = 1, \cdots, I \tag{3.32}$$
$$\sum_{i \in C_j} \alpha_i q_i \;=\; 0\,, \qquad \text{each } j = 1, \cdots, L\,,\ , \tag{3.33}$$

These are again the Landau equations (3.28) and (3.30) (with the relabeling $\lambda_i = \alpha_i$). For future reference we note that (3.32) - (3.33) can also be expressed as:

$$\psi = 0\,, \quad \text{and} \quad \frac{\partial \psi}{\partial l_j} = 0 \qquad \text{each } j \tag{3.34}$$

and

$$\alpha_i \frac{\partial \psi}{\partial \alpha_i} = 0 \qquad \text{each } i\,. \tag{3.35}$$

The parametric form of the Landau equations, after having performed the momentum integrations, is obtained from (3.11). Let $\zeta_i \equiv \bar{\ell}^2 + i\bar{\beta}_i$, with $\bar{\beta}_i \equiv \ell_2^2 \beta_i$, so that $w_i = \alpha_i + \zeta_i$, and also $Q_{,i\ldots j}(w) \equiv \dfrac{\partial Q(w)}{\partial w_i \ldots \partial w_j}$. Now,

$$Q(w) = Q(\alpha) + \sum_{i=1}^{I} \zeta_i Q_{,i}(\alpha) + \sum_{i,j=1}^{I} \zeta_i \zeta_j \int_0^1 ds \int_0^s dt\, Q_{,ij}(\alpha + t\zeta)\,. \tag{3.36}$$

Since $Q(w)$ is a homogeneous function of degree 1, $Q_{,i}$ and $Q_{,ij}$ are homogeneous of degree 0 and -1, respectively. To examine the large β regime, consider the rescaling $\beta_i \to \rho\beta_i$. From (3.36) one has

$$\begin{aligned} Q(\alpha + \bar{\ell}^2 + i\bar{\beta}) = Q(\alpha) + \bar{\ell}^2 \sum_{i=1}^{I} Q_{,i}(\alpha) + i2\bar{\ell}^2 \sum_{i,j=1}^{I} \bar{\beta}_i \int_0^1 ds \int_0^s dt\, Q_{,ij}\Big(\frac{\alpha + \bar{\ell}^2}{\rho} + it\bar{\beta}\Big) \\ + \rho \left[i \sum_{i=1}^{I} \bar{\beta}_i Q_{,i}(\alpha) - \sum_{i,j=1}^{I} \bar{\beta}_i \bar{\beta}_j \int_0^1 ds \int_0^s dt\, Q_{,ij}\Big(\frac{\alpha + \bar{\ell}^2}{\rho} + it\bar{\beta}\Big) \right]. \end{aligned} \tag{3.37}$$

Hence, $Q(w)$ grows at most linearly with ρ, plus $O(1)$ and $O(1/\rho)$ corrections. The large β behavior of $J(\alpha, \beta; P)$ is then always controlled by the $-\frac{1}{2}(\sum_i \beta_i^2)$ term, thus resulting in convergent behavior for $\beta_i \to \pm\infty$.

On the other hand, from (3.36), under $\alpha_i \to \rho\alpha_i$ one has

$$Q(\rho\alpha + \zeta) = \rho Q(\alpha) + \sum_{i=1}^{I} \zeta_i Q_{,i}(\alpha) + \frac{1}{\rho} \sum_{i,j=1}^{I} \zeta_i \zeta_j \int_0^1 ds \int_0^s dt\, Q_{,ij}(\alpha + t\zeta/\rho) \tag{3.38}$$

and, hence, for $\rho \to \infty$:

$$J(\alpha, \beta; P) = \rho \left[Q(\alpha; P) - \sum_{i=1}^{I} \alpha_i m_i^2 \right] + Const. + O(\frac{1}{\rho}) \tag{3.39}$$

For large α_i then convergence requires that

$$S \equiv Q(\alpha; P) - \sum_{i=1}^{I} \alpha_i m_i^2 \tag{3.40}$$

satisfies $S < 0$. This is the case for Euclidean momenta, and $\alpha_i \geq 0$, for which the parametric representation was derived. This identifies $S = 0$ as a singularity surface.

Note that the region of both α and β simultaneously large, i.e., $\alpha_i \to \rho\alpha_i$, $\beta_i \to \rho\beta_i$, $\rho \to \infty$, gives nothing new - it is equivalent to the large β regime.

We may in fact single out the contribution of non-vanishing α parameters in (3.11) explicitly by inserting a delta function in the integrand. Omitting numerical factors this contribution is given by

$$I = \int_0^\infty \prod_{k=1}^I d\alpha_k \int_{-\infty}^\infty \prod_{l=1}^I d\beta_l \int_{\rho_0}^\infty d\rho\, \delta(\rho - \sum_{i=1}^I \alpha_i) \\ \frac{1}{\Delta(w)^{d/2}} \exp\left[Q(w;P) - \sum_{i=1}^I (\alpha_i m_i^2 - i\beta_i) - \frac{1}{2}\sum_{i=1}^I \beta_i^2\right], \quad (3.41)$$

with $\rho_0 > 0$. The delta function constraints one or more α_i parameters to be nonzero, the actual value of ρ_0 being irrelevant for this purpose. Rescaling $\alpha_i \to \rho\alpha_i$, using (3.38) together with

$$\Delta(\rho\alpha + \bar{\ell}^2 + i\ell_2^2\beta) = \rho^L \Delta(\alpha + \frac{\bar{\ell}^2 + i\ell_2^2\beta}{\rho}), \quad (3.42)$$

and expanding in powers of $1/\rho$, one obtains a series of integrals over ρ of the form

$$I_s \equiv \int_{\rho_0}^\infty d\rho \rho^{[I-\frac{d}{2}L-1]} \left(\frac{1}{\rho}\right)^s \exp\left[-\rho\left[-Q(\alpha;P) + \sum_{i=1}^I \alpha_i m_i^2\right]\right] \quad (3.43)$$

with integer $s \geq 0$. Carrying out the ρ integration for Euclidean momenta, for which $Q(\alpha;P) < 0$, i.e., $S < 0$, and with[4]

$$q \equiv I - \frac{d}{2}L - s, \quad (3.44)$$

one obtains:

$$I_s = e^{\rho_0 S(\alpha;P)} \sum_{k=0}^{q-1} \frac{\Gamma(q)}{k!} \frac{\rho_0^k}{[-S(\alpha;P)]^{(q-k)}}, \qquad \text{for} \quad q > 0\,; \quad (3.45)$$

[4]Even d is assumed so q is integer.

$$I_s = -\,\mathrm{Ei}(\rho_0 S(\alpha;P))\,, \qquad \text{for} \quad q=0\,; \tag{3.46}$$

$$\begin{aligned} I_s =& \frac{(-1)^{|q|+1}}{\Gamma(|q|+1)}[-S(\alpha;P)]^{|q|}\,\mathrm{Ei}(\rho_0 S(\alpha;P)) \\ &+ \frac{e^{\rho_0 S(\alpha;P)}}{\rho_0^{|q|}} \sum_{k=0}^{|q|-1} \frac{(-1)^k \rho_0^k\,[-S(\alpha;P)]^k}{|q|(|q|-1)\cdots(|q|-k)}\,, \qquad \text{for} \quad q<0\,, \end{aligned} \tag{3.47}$$

where

$$\mathrm{Ei}(x) = \gamma + \ln(\pm x) + \sum_{k=1}^{\infty} \frac{x^k}{k k!}\,, \qquad x \gtrless 0 \tag{3.48}$$

is the exponential integral function with γ denoting Euler's constant. As seen directly from (3.45), (3.46) then, upon continuation $S=0$ is indeed the singularity surface. I_s is regular for sufficiently large s as evident from (3.47).

Note that the $s=0$ contribution is the exact result for the local theory obtained by setting $\ell_1 = \ell_2 = 0$, i.e., $V_s^{(n_s)} = 1$, in the Schwinger parametric representation (3.11). As pointed out right after (3.23) this is identical to the result obtained by carrying out the momentum integrations in the Feynman parameter representation (3.1), provided the integral is UV convergent; otherwise it will have to be UV regulated. In the nonlocal case the transcendental entire vertices automatically provide such regularization, whereas the singularity structure defined by the S surface remains intact.

Applying the conditions (i) - (iii), with, again, $\alpha_i = 0$ defining the contour boundaries, we now have:[5]

$$S(\alpha,P) = 0 \tag{3.49}$$

$$\tilde{\lambda}_i \alpha_i = 0 \tag{3.50}$$

$$\frac{\partial}{\partial \alpha_i}\Big(\lambda S + \sum_{k=1}^{I} \tilde{\lambda}_k \alpha_k\Big) = 0\,, \qquad \text{each } i\,. \tag{3.51}$$

Hence, either $\tilde{\lambda}_i = 0$ and $\partial S/\partial\alpha_i = 0$, or $\alpha_i = 0$. But

$$S = \sum_{i=1}^{I} \alpha_i \frac{\partial S}{\partial \alpha_i}\,, \tag{3.52}$$

[5]We disregard the trivial $\lambda = 0$ case in the $\lambda S(\alpha,P)=0$ equation.

since S is homogeneous of degree one in the α_i. Thus one concludes that

$$\text{either:} \qquad \alpha_i = 0 \tag{3.53}$$

$$\text{or:} \qquad \frac{\partial S}{\partial \alpha_i} = 0\,, \qquad \text{each} \quad i\,. \tag{3.54}$$

In either case then (3.49) is automatically satisfied. For many purposes the parametric form of the Landau equations (3.53) - (3.54) turns out to be the most convenient form for analyzing the analyticity properties of amplitudes.

The parametric form of the Landau equations (3.53) - (3.54) is equivalent to that given by (3.34) - (3.35). This is shown in the Appendix B. Note that this implies that the former are in fact of general validity even though they were obtained within the vertex subclass used in deriving the parametric representation.

3.2.2 Singularity structure

Eliminating the λ or α parameters from the Landau equations one obtains the equations for the Landau surfaces (algebraic varieties) in the multi-dimensional space of the external invariants z_r. This can be done by forming the inner product of (3.30), or, equivalently, (3.33), with q_j giving a set of simultaneous equations for the λ, or, respectively, α, parameters. The condition for non-trivial solution of this set gives the Landau surface equations. Equivalently, they may be derived from the condition for non-trivial solution of the system of equations given by (3.54). In this manner the equations for the leading Landau surface $\Sigma(z_r)$ may be given in the form

$$\det Y = 0\,, \tag{3.55}$$

where $Y(z_r)$ is a matrix with entries depending on the external momenta invariants z_r. The lower order surfaces $\Sigma_{ij\ldots}(z_r)$, corresponding to solutions with a subset of the α_i's (resp., λ's) equal to zero, are then given by the vanishing of the appropriate minors of Y.

Thus, for example, for the basic square box diagram in Fig. 3.1(a), with external masses M_i, internal masses m_i and external legs on shell, there are two independent invariants, the familiar s and t Mandelstam variables. Proceeding as indicated above one straightforwardly

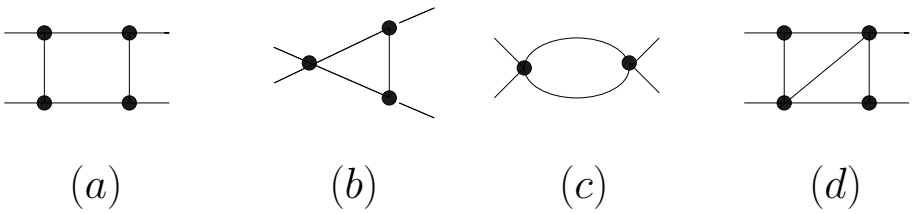


Figure 3.1: (a) The one-loop box graph; (b) one of the once-reduced graphs of (a) containing the anomalous thresholds; (c) one of the twice-reduced graphs of (a) containing the normal thresholds; (d) the acnode graph. Black circles denote nonlocal vertices.

finds the leading singularity Landau surface Σ given by (3.55), where

$$Y_{ij}(z_r) = -\frac{z_{ij} - m_i^2 - m_j^2}{2m_i m_j}\,, \quad i \neq j\,; \qquad Y_{ii} = 1\,. \tag{3.56}$$

Here $z_{ij} = (\sum_{r\subset ij} P_r)^2$ denotes the square of the sum of the external momenta entering between lines i and j. Thus, $z_{13} = (P_1 + P_4)^2 = t$, $z_{24} = (P_1 + P_2)^2 = s$, whereas $z_{ij} = z_{ji} = P_j^2 = M_j^2$ for adjacent i and j with $i < j$ in cyclic order clockwise around the graph. The invariants formed by the squares of the external momenta have been set on shell; considering them as variables amounts then to continuation in the dependence on the external masses. The surfaces for the subleading singularities are found from the corresponding reduced graphs. Setting one α parameter to zero gives the triangle graphs in Fig. 3.1(b), whose leading singularities are the 'anomalous' thresholds. Each of their Landau surfaces Σ_i, $i = 1, 2, 3, 4$, may be obtained from the corresponding reduced graph and, as easily seen, is given by

$$\det Y[i, i] = 0\,, \tag{3.57}$$

where $Y[i, i]$ denotes the submatrix of Y obtained by deleting the i-th row and i-th column of Y; i.e., Σ_i is given by the vanishing of the (i, i)-minor of Y.

Similarly, solutions with two α parameters equal to zero correspond to Landau surfaces Σ_{ij} given by

$$\det Y[ij, ij] = 0\,, \tag{3.58}$$

where $Y[ij, ij]$ denotes the submatrix obtained by deleting the i-th and j-th rows and the

i-th and j-th columns of Y. In the case of the square graph these are the leading singularities of the reduced graphs in Fig. 3.1(c), which include the usual normal thresholds, and (3.58) results, respectively, in:

$$s = (m_2 \pm m_4)^2 \,, \qquad \text{and} \qquad t = (m_1 \pm m_3)^2 \,. \tag{3.59}$$

Landau surfaces generally have rather intricate structure with multiple components in the multi-dimensional space of the external invariants. This is true even for the simplest diagrams, such as the square graph and the reduced triangle graphs in Fig. 3.1(b)[6] given by (3.56). Such examples have been extensively studied, cf. [4] for a review. One typically starts with the solution for the real section of the surface in the complex space of the invariants, e.g., the intersection of Σ with the real (s,t) plane in the example of the box diagram above; this section will, in general, consists of several components. The complex parts attached to the real sections are then determined by the searchline technique [28]. This can be a rather laborious procedure. Having determined the shape of the surfaces on which potential singularities lie, there remains the nontrivial task of determining which parts are actually singular on which Riemann sheet. In the present context, however, the main point, once more, is that the resulting local singularity structure is not affected by replacing polynomial by transcendental entire vertices, since, as we saw, except for providing UV regularization, this leaves the Landau equations unaffected.

It will be useful for our discussion to recall here some aspects of this singularity structure. Despite the generally complicated form of the Landau surfaces some general features are present that are crucial for the structure of physical amplitudes. The physical sheet is defined by attaching a small imaginary part $-i\epsilon$ to each internal mass m_i^2 and integrating over undistorted integration contours in (3.1) or, equivalently, (3.11). Now, from (3.20),

$$\mathrm{Im}\, S(\alpha, P) = \frac{1}{\Delta(\alpha)} \sum_{T^{(2)} \subset G} \mathrm{Im}\, z_{T^{(2)}} \prod_{i \in T^{(2)*}} \alpha_i + (\sum_{i=1}^{I} \alpha_i)\, \epsilon \,. \tag{3.60}$$

[6]The triangle may of course be viewed in its own right as a form factor depending on general complex $z_i = P_i^2$, i.e., a 6-dimensional space.

For real positive α's (undistorted contours), this does not vanish for $\mathrm{Im}\, z_r \geq 0$. The same, of course, holds for the imaginary part of the extremized form (3.2) (w.r.t. the loop momenta) which equals S, see Appendix B. Hence, one may continue through this region of complex z_r space without the potential singularity $S = 0$ or $\psi = 0$ in the integrands forcing a distortion of the contour. The physical amplitude is obtained in the limit $\mathrm{Im}\, z_r \to 0^+$. This defines the direction of approach to the subspace of real z_r in which one may encounter singularities. We know, however, that there is a region R in real z_r subspace, which includes Euclidean momenta, where $S \neq 0$. The boundaries of this region will be determined by those parts of the real sections of the Landau surfaces $\Sigma, \Sigma_i, \Sigma_{ij}, \ldots$ that correspond to real, positive α solutions of the Landau equations. The common situation is that the normal thresholds provide the boundaries of this analyticity region R; at the boundary provided by the first threshold for two particle intermediate state the amplitude acquires a cut, followed by additional cuts at the onset of three and higher intermediate states. This is the familiar singularity structure expected from unitarity. The general situation, however, can be rather more complicated due to the existence of the anomalous thresholds and other, nastier types of singularities. These, upon continuation in the z_r, may move to replace the normal thresholds as boundaries.

The 1-loop box diagram of Fig. 3.1(a) provides an instructive example. One has

$$S(\alpha; s, t) = \frac{\alpha_1\alpha_2 M_2^2 + \alpha_1\alpha_4 M_1^2 + \alpha_1\alpha_3\, t + \alpha_2\alpha_4\, s + \alpha_2\alpha_3 M_3^2 + \alpha_3\alpha_4 M_4^2}{\alpha_1 + \alpha_2 + \alpha_3 + \alpha_4} - \sum_{i=1}^{4} \alpha_i m_i^2\,. \quad (3.61)$$

One chooses the external masses to be stable against decay into pairs of the internal masses, i.e., $M_1 < m_1 + m_4$, etc. Then for sufficiently small masses[7] one can show that $S < 0$ for $s < (m_2 + m_4)^2$ and $t < (m_1 + m_3)^2$. Thus the boundaries of the region R in this case are given by the normal threshold surfaces Σ_{13}, Σ_{24}. This, however, changes drastically as the masses are increased [29]. As the external masses are increased one of the triangle surfaces, say Σ_2, moves to collide with the normal threshold surface Σ_{24} and then separate. As a

[7]More precisely, for masses such that none of the Σ_i surfaces corresponds to a solution of the non-leading triangle Landau equations with real positive α. The effect of subsequent increases in the masses violating this condition successively for each Σ_i is described in the main text.

result the boundary of R now consists of Σ_{13} and Σ_2 and an anomalous threshold singularity appears on the physical sheet. Increasing the external masses further another Σ_i moves up to and then away from Σ_{13} and the region R is now bounded by two anomalous threshold surfaces Σ_i. Further increases of the masses leads to collision of the Σ_i's with the leading surface Σ. The R boundary is now formed by part of Σ and the Σ_i and this is accompanied by the onset of complex singularities on the physical sheet [29]. This disturbing appearance of physical sheet complex singularities originates here in the movement of the anomalous thresholds as function of the masses.

Unfortunately, this is not the only known mechanism by which complex singularities can appear on the physical sheet. Investigation of the 2-loop box diagram shown in Fig. 3.1(d), the infamous acnode graph, reveals a new phenomenon [30], [31]. In addition to the continuous parts of the real section of surface Σ, as some external mass is increased beyond a certain value isolated points, known as acnodes, appear on the real (s,t) plane. There are singular complex pieces of the surface, of complicated shape, intersecting the real plane only through these acnodes. The acnodes move as the masses are further increased till they meet the continuous part of the real surface section creating a crunode (self-intersection point) as well as cusps in Σ. The physical interpretation of such physical sheet complex singularities and their effect on physical amplitudes remains obscure.[8] [30]

Whatever the boundaries of the real region R of analyticity may be, its existence has some important consequences. Analytic continuation in z_r-space out of R along a path P to some point z_r is related to that along the complex-conjugate path P^* to point z_r^* by complex conjugation. Thus, any distortion of integration contours made necessary during the continuation along P implies the complex-conjugate distortion along P^*. If, therefore, analyticity can be proven in one region, it is guaranteed to hold also in the complex conjugate region. Furthermore, a path out of R with $\mathrm{Im}\, z_r > 0$ to an endpoint with $\mathrm{Im}\, z_r = \epsilon^+$, i.e., on the physical sheet, and the complex conjugate path to the conjugate point relate the

[8] Their appearance is what prevents the general validity of the Mandelstam representation in the case of local (polynomial) vertices

amplitude for the transfer matrix T to that for $T^\dagger$ by continuation of the *same* analytic function. This is the content of the hermitian analyticity property of section 2.1 above. The introduction of nonlocal entire function vertices does not in any way interfere with these fundamental properties.

The existence of the real analyticity region R, in fact, generally implies extension to a larger region of analyticity [32]. First note that since $S < 0$ with undistorted contours for $z_r \in R$, S cannot vanish if one continues to complex z_r such that $\mathrm{Re}\, z_r \in R$. Thus the amplitude is analytic in a tube in the complex z_r-space whose real section is R. Furthermore, given a fixed point $z_r^0 \in R$, consider the line in complex z_r-space given by $z_r(\zeta) = z_r^0 + \lambda_r \zeta$ with complex variable ζ and given numbers λ_r defining its direction. Now, since by (3.20) S is linear in z_r, for points on the line one has

$$S(\alpha;\zeta) = S(\alpha; z_r^0) + \mathcal{T}(\alpha)\,\zeta\,, \tag{3.62}$$

where $\mathcal{T}$ is a function of only the α. For α's real and positive, i.e., on the undistorted contours, one then has

$$\mathrm{Re}\, S(\alpha;\zeta) = S(\alpha; z_r^0) + \mathcal{T}(\alpha)\mathrm{Re}\,\zeta\,, \qquad \mathrm{Im}\, S(\alpha;\zeta) = \mathcal{T}(\alpha)\mathrm{Im}\,\zeta\,. \tag{3.63}$$

It follows from this that $S(\alpha;\zeta)$ cannot vanish when $\mathrm{Im}\,\zeta \neq 0$. Indeed, for it to vanish $\mathrm{Im}\, S = 0$, implying that $\mathcal{T} = 0$; and $\mathrm{Re}\, S = 0$, implying then that $S(\alpha; z_r^0) = 0$, which is not true, since $z_r^0 \in R$. Hence, the amplitude is analytic for all ζ such that $\mathrm{Im}\,\zeta \neq 0$ and all real values of $\zeta = x$ such that that $z_r(x) \in R$. Thus, if, for example, the boundaries of R are given by the normal thresholds, the amplitude is analytic in the entire ζ plane except for the normal threshold cuts along the real axis.

The result is independent of the type, polynomial or nonlocal entire functions, of the vertices. It immediately allows one to obtain single-variable dispersion relations *provided* contours in complex z_r-space can be closed at infinity.[9] This, modulo possible subtractions, is possible for polynomial interactions, but clearly not for nonlocal interactions. So, even

[9]For example, for 2-to-2 scattering, where $z_r = (s,t)$, one can choose the line through the region R in the above argument such that one obtains, say, a dispersion relation in s at fixed t.

though the singularity structure is the same in the finite complex z_r-space, the different behavior at the point at infinity in the nonlocal case does not allow one to use the above result to write such dispersion relations in any obvious way. For both classes of vertices, however, one may, of course, employ Cauchy's theorem by closing contours in the finite plane, as in fact is done in arriving at the Cutkosky discontinuity rule (cf. below).

Finally, there is the matter of the so-called second-type singularities [33], [9]. As originally discovered in the representation (2.16) with conventional polynomial interactions, these are singularities that appear to correspond to pinches of the loop integration contours at infinity. To make such discussions mathematically more well defined one has to make change of variables to convert these to finite points. A better discussion, which, most importantly for us here, can be equally well applied to nonlocal entire as well polynomial vertices, is given in the parametric representation. Second-type singularities can then be defined as solutions to the Landau equations (3.53) - (3.54), or, equivalently, (3.34) - (3.35), which *additionally* satisfy $\Delta(\alpha) = 0$. Now we proved (see Appendix A) that $\Delta(\alpha) \neq 0$ for all $\alpha_i \geq 0$. (In the local case, this holds only for $\alpha_i > 0$.) In fact, $\Delta(\alpha)$ could vanish only for some $\alpha_i < -\bar{\ell}^2$ due to the explicit UV regularization provided by the nonlocal vertices. Second-type singularities occur then due to pinches with distorted contours of negative α. In all known examples these negative α values imply that the singularity is not on the physical sheet. The general situation regarding the Riemann sheet properties of second-type singularities, however, is an open question.

CHAPTER 4

Cutkosky discontinuity rule

Consider the amplitude (2.16) and let $\{z_r\} = \{z_r^0\}$ denote a singularity given by a solution of the Landau equation with I_c lines on-shell and $(I - I_c)$ of the α parameters equal to zero. The Cutkosky rule provides a general formula for the discontinuity from going around the singularity z^0.

Let L_c be the number of independent loops in the reduced diagram obtained by contracting the $(I - I_c)$ lines with zero α. We can label lines and choose the loop momenta so that the reduced graph has internal line momenta q_i, $i = 1, \ldots, I_c$ and they depend only on the loop momenta l_j with $j = 1, \ldots, L_c$. Let us label loop momenta components by $l_{j\mu} \equiv l_A$ with A assuming dL_c values, and define the $I_c \times dL_c$ Jacobian matrix

$$J_{iA} = \frac{\partial q_i^2}{\partial l_A} \,. \tag{4.1}$$

Assume that $I_c \leq dL_c$ and that the rank of J equals I_c.[1] Then, following [9], one may introduce a change of variables replacing the loop momenta l_A on the contour C_I, i.e., Euclidean loop momenta, by the set ξ_A, where $\xi_i = \hat{q}_i^2 = -q_i^2$, $i = 1, \ldots, I_c$, and additional variables $\xi_a = \chi_a$, $a = 1, \ldots, (dL_c - I_c)$. The new variables may be visualized geometrically in d-dimensional Euclidean space as the construction of a simplex whose base is the polygon, closed by momentum conservation, formed by the vector diagram of the external momenta vectors. The rest of the oriented edges represent the I_c internal momenta vectors. The simplex on top of this base is built in such configuration of edges that momentum conservation is obeyed at each vertex of the reduced diagram. The variables $\xi_i = \hat{q}_i^2$ then represent the

[1] The argument may be extended to cases where these assumptions are violated, but there is no need to consider such cases in this paper.

squared lengths of the edges and the set χ_a represent the additional 'angle' variables needed to completely specify, for given $\hat{q}_i^2$, the allowed distortion/orientation degrees of freedom of the simplex in the dL_c-dimensional space. It may be that this latter set can be chosen in more than one way. This construction is always possible in Euclidean space showing that, under the above assumptions, this is a well-defined change of variables in (2.16).

The experts will recognize this as the first step in the construction of the so-called dual diagram for the graphical solution of the Landau equations.[2] Were one to additionally impose the Landau equations they would result into further relations between the edges that will, in general, not be possible to satisfy in Euclidean space and thus require complex or Minkowski vectors. This, of course, reflects the occurrence of singularities outside the original region of definition of the integral, which are encountered upon continuation in the external invariants.

In terms of the new variables (2.16) assumes the form

$$A_G(\{z_r\}) = \frac{C(G)\,(-1)^{(L_c+I_c)}i^{(L-L_c)}}{(2\pi)^{dL}} \prod_{i=1}^{I_c}\int_{a_i}^{b_i} dq_i^2 \int \prod_{a=1}^{(dL-I_c)} d\chi_a \int \prod_{j>L_c}^{L} dl_j \,\frac{1}{|J|} \cdot \prod_{k=1}^{I}\frac{1}{(q_k^2-m_k^2)} \prod_{s=1}^{V} V_s^{(n_s)}(\{q^2,\chi,l,P\})\,. \quad (4.2)$$

We choose to express (4.2) in terms of q_i^2 rather than $\hat{q}_i^2 = -q_i^2$ since we eventually want to consider complex q_i^2 contour deformations as the external invariants move out of the Euclidean region - cf. remark in the previous paragraph. Also, the masses m_k^2 are normally real with small negative imaginary parts, but, more generally, may be allowed to assume any complex values. The limits of integration a_i, b_i are determined by the extrema of q_i^2 w.r.t. the reduced graph loop momenta for fixed q_k^2, $k<i$, i.e., by extremizing

$$\phi(l,\gamma) = q_i^2 + \sum_{k<i}\gamma_k q_k^2 \quad (4.3)$$

w.r.t. to l_j $(1 \le l_j \le L_c)$ and Langrange multipliers γ. Note that one may always choose to label internal lines with $q_i = l_i$ for $i = 1, \cdots L_c$, so that for these lines one simply has $\hat{q}_i^2 = \hat{l}_i^2$ and, hence, $(a_i, b_i) = (-\infty, 0)$. (We necessarily have $1 \le L_c < I_c$). Subsequent a_i, b_i limits, however, will generally depend on the preceding q^2's and the z_r's.

[2] Also introduced in [8]. See [4] for references and examples.

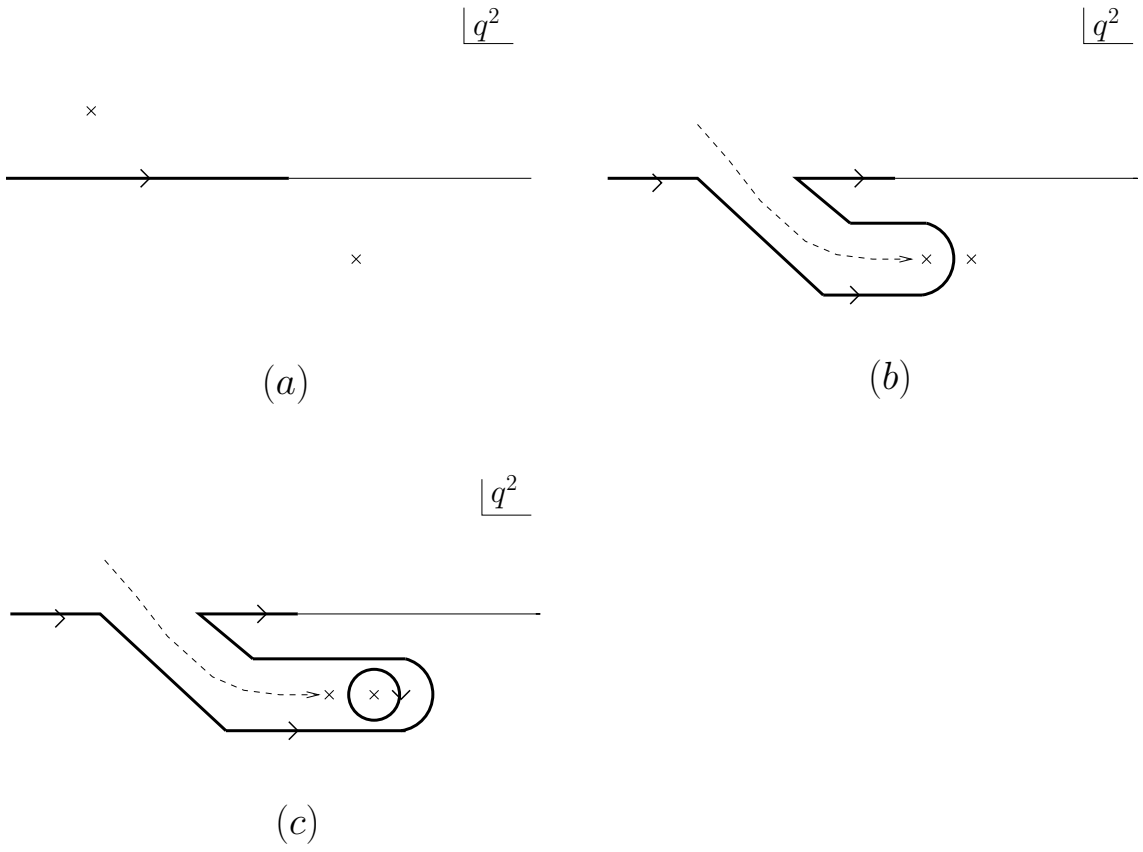


Figure 4.1: (a) Original position of singularities with undistorted contour in q^2 plane; (b) singularity movement as $z \to z^0$ pinching the contour; (c) equivalent contour consisting of regular and a singular (circle) contribution.

Now write (4.2) in the form

$$A_G(\{z_r\}) = K \int_{a_1}^{b_1} dq_1^2 \frac{1}{(q_1^2 - m_1^2)} I^{(1)}(q_1^2)\,, \tag{4.4}$$

where $K \equiv C(G)\,(-1)^{(L_c+I_c)} i^{(L-L_c)}/(2\pi)^{dL}$. The integrand $I^{(1)}(q_1^2)$ is the result of having integrated over all variables in (4.2) except q_1^2 and singling out the q_1^2-propagator factor explicitly - any corresponding q_1^2-dependent vertex factors (cf. structures as in (2.6)) have been lumped in the definition of $I^{(1)}(q_1^2)$. Note that, by the remark above, one can always have $a_1 = -\infty$, $b_1 = 0$.

By assumption, as $z \to z^0$ (4.2) has a singularity involving all I_c lines of the reduced graph being on-shell. The only way that this can happen in (4.4) then is if the pole at

$q_1^2 = m_1^2$ is pinched by a singularity in $I^{(1)}(q_1^2)$ as $z \to z^0$ (Fig. 4.1(b)). The distorted contour may be moved through the pole and split into two pieces: one on which the integral is regular and a small circle around the pole (Fig. 4.1(c)). The integral over the former, being regular, will not contribute to the discontinuity. The latter will be pinched and is the one that is singular. By the residue theorem it is given by

$$K(-2\pi i)\, I^{(1)}(m_1^2) = K(-2\pi i) \int_{a_2}^{b_2} dq_2^2 \frac{1}{(q_2^2 - m_2^2)} I^{(2)}(m_1^2, q_2^2)\,, \tag{4.5}$$

where $I^{(2)}(q_1^2, q_2^2)$ is the result of having integrated over all variables in (4.2) except q_1^2 and q_2^2 and after singling out the q_2^2- and q_1^2-propagator factors explicitly - (and , again, having lumped any corresponding vertex factors in $I^{(2)}(q_1^2, q_2^2)$).

The same argument can now be applied to $I^{(2)}(m_1^2, q_2^2)$. Iterating the argument $(I_c - 1)$ times, the singular part is found to be given by the expression

$$K(-2\pi i)^{(I_c-1)} \int_{a_{I_c}}^{b_{I_c}} dq_{I_c}^2 \frac{1}{(q_{I_c}^2 - m_{I_c}^2)} I^{(I_c)}(m_1^2, m_2^2, \cdots, m_{(I_c-1)}^2, q_{I_c}^2)\,. \tag{4.6}$$

The limits of integration are here given by the extrema of (4.3) with $i = I_c$. In this case, however, as it is easily seen,[3] the extremizing equations are identical to the Landau equations (3.32) and (3.33) for the leading singularity of the reduced graph, i.e., by assumption, the singularity z^0. Hence, in (4.6) the singularity is the result not of contour pinching but of an endpoint singularity: either b_{I_c} or a_{I_c} moves toward $q_{I_c}^2 = m_{I_c}^2$ as $z \to z^0$ thus giving rise to an endpoint singularity. The discontinuity from going around the endpoint singularity in (4.6) is then obtained as depicted in Fig. 4.2 and given by

$$\Delta A_G(\{z_r\}) = K(-2\pi i)^{I_c} I^{(I_c)}(m_1^2, \cdots, m_{I_c}^2)\,. \tag{4.7}$$

There are several remarks to be made concerning (4.7).

1. The above derivation, which harks back to the original Cutkosky argument, is well suited for extension in the presence of nonlocal vertices of the general type introduced in

[3] By rescaling of the α's one may always set one of them equal to one. The Lagrange multipliers γ are here the parameters α.



Figure 4.2: Difference (circular contour) between continuing: (a) above and (b) below end-point singularity.

section 2. The change of variables is well-defines in Euclidean space and the subsequent argument involves only local deformations of contours, i.e., in the finite complex plane, as the external invariants z_r are continued. This is in contrast to other ways of arriving at cutting-rules such as employing [34] the Feynman [35] or tree-loop theorems [36], which involve closing contours at infinity; or space-time techniques such as the largest-time equation [37] which are not suited to handle nonlocal interactions.

2. The usual case is that of real masses with small negative imaginary parts, $m_i^2 - i\epsilon$, corresponding to physical region (real momenta) singularities. In fact the figures above are drawn depicting this type of relative positioning of contours and singularities. In particular, all signs from evaluation of residues confirm to this situation. In this case then, reverting to the original variables (4.7) may be expressed in the form:

$$\begin{aligned}&\Delta A_G(\{z_r\})\\ &= C(G) i^L \int_C \prod_{k=1}^{L} \frac{d^d l_k}{(2\pi)^d} \prod_{j=1}^{I_c} (-2\pi i)\delta^+(q_j^2 - m_j^2) \prod_{i=I_c+1}^{I} \frac{1}{q_i^2 - m_i^2} \prod_{s=1}^{V} V_s^{(n_s)}(\{q, P\})\,. \end{aligned} \quad (4.8)$$

This is the Cutkosky discontinuity rule as usually stated. The contours C in (4.8) are specified as follows. The integration over loop momenta that circulate in the reduced graph may be taken over Minkowski space since the delta functions set these internal lines on-shell - they correspond to the little circular contours in figures 4.2, 4.3. The loop integrations in the parts of the graph that would be contracted in the reduced

graph must be along $C_{\rm I}$, i.e., Euclidean directions. The momenta external to these parts, which are either external lines or reduced graph internal lines, are then to be continued to Minkowski space. This pertains to point 4. below.

3. In the case of singularities at complex momenta (4.8) should be viewed merely as a mnemonic device for (4.7) since the delta functions in (4.7) are not immediately defined for complex arguments. The signs of some of the $(2\pi i)$ factors in (4.7) may need to change in this general situation. As we saw above such singularities may in certain circumstances occur even on the physical sheet. Explicit evaluation of the discontinuity in these cases may not be easy in practice.

4. A given singularity in the amplitude A for a given process is shared by all contributing Feynman graphs that can be contracted to the corresponding reduced graph. Each graph contributes to the discontinuity according to (4.8) so that the sum gives the complete discontinuity in the form

$$\Delta A(\{z_r\}) = i^{L_c} \int_C \prod_{k=1}^{L_c} \frac{d^d l_k}{(2\pi)^d} \prod_{j=1}^{I_c} (-2\pi i)\delta^+(q_j^2 - m_j^2) \prod_{i=1}^{V_c} A_i(q, P)\,, \tag{4.9}$$

where V_c is the number of vertices in the reduced graph, and the A_i's are the amplitudes represented by the blobs in the examples in Fig. 4.3. The following issue may now arise.

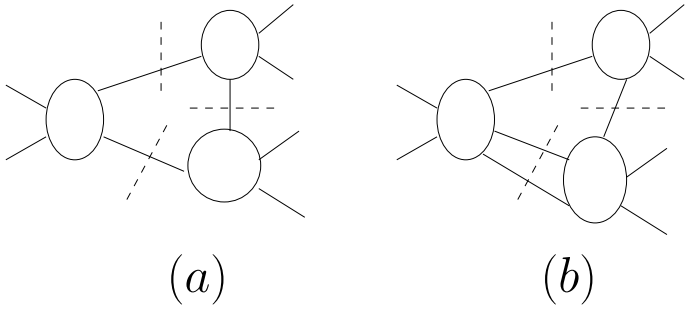


Figure 4.3: Examples of eq. (4.9) for discontinuities involving: (a) three (anomalous threshold); and (b) four Cutkosky cuts (on-shell lines).

(4.9) gives the discontinuity obtained by going around the singularity z^0 in question,

which is the leading singularity of the reduced graph. In doing so, however, it is not immediately clear what Riemann sheet each A_i may end up on; this will depend on whether or not one is simultaneously going around some singularity in A_i. To decide this requires a separate analysis in each particular case.

As a particular application consider the normal threshold singularity in a given channel s. It is specified as the Landau equations solution for the leading singularity of the (set of) reduced graph(s) such that a cut through the internal lines separates the graph(s) into two pieces along the direction of the given channel. Application of (4.9) then gives an expression for the discontinuity across this singularity. Noting that $i^{L_c}(-i)^{I_c} = i^{(-V_c+1)} = -i$ since here

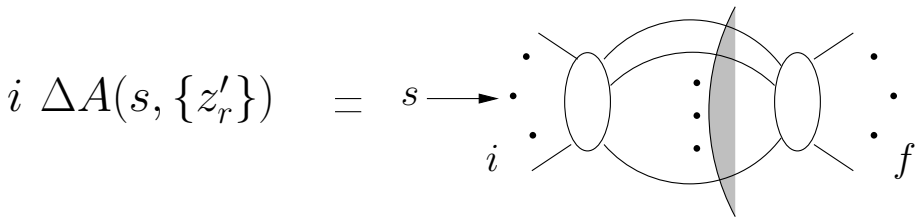


Figure 4.4: Discontinuity across normal threshold given by eq. (4.10). Energy flows from unshaded to shaded side of cut (on-shell) lines. Feynman rules on shaded side are those for $T^\dagger$.

$V_c = 2$, (4.9) gives (figure 4.4):

$$\Delta A(s,\{z'_r\}) = -i \int_C \prod_{k=1}^{n-1} \frac{d^d l_k}{(2\pi)^d}\, [A_{fn}] \left(\prod_{j=1}^{n} (-2\pi)\delta^+(q_j^2 - m_j^2) \right) A_{ni}\,. \tag{4.10}$$

In (4.10) we placed the outgoing A_{fn} 'blob' in square brackets to indicate that, as pointed out above, the general Cutkosky rule does not a-priori specify its sheet placement ($i\epsilon$ prescription). The total discontinuity in s for the amplitude A_{fi} between states i and f is given by summing over all possible intermediate state discontinuities (4.10) for the channel in question:

$$A_{fi}(s+i\epsilon,\{z'_r\}) - A_{fi}(s-i\epsilon,\{z'_r\}) = \sum \Delta A(s,\{z'_r\})\,. \tag{4.11}$$

So far we have simply applied the Cutkosky rule to the normal threshold discontinuity across a given channel s. This discontinuity is, of course, known to be related to the optical theorem.

We may arrive at this connection by the following indirect argument. The l.h.s. of (4.11) represents the difference between the amplitude where the real section in the space of the invariants is approached from above and that where it is approached from below. For the normal threshold singularity under consideration only the invariant s is discontinuous by definition. The property of hermitian analyticity (chapter 3) applied to all the contributing reduced graphs implies then

$$A_{fi}(s+i\epsilon,\{z'_r\}) - A_{fi}(s-i\epsilon,\{z'_r\}) = A_{fi}(s,\{z'_r\}) - A^\dagger_{fi}(s,\{z'_r\})\,. \tag{4.12}$$

Complex conjugating (4.12) shows that the only consistent choice for the factor in square brackets in (4.10) is $[A_{fn}] = A^\dagger_{fn}$, which results in the familiar form of the optical theorem. Note, however, that this is not a first principles derivation of unitarity. What the argument actually shows is that the normal threshold discontinuity as given by the Cutkosky rule combined with the hermitian analyticity of the contributing reduced graphs gives a statement of a form consistent with the optical theorem. Nonetheless, this type of indirect consistency argument invoking hermitian analyticity can be very useful. Thus, for example, specializing to the case of only 2-particle intermediate states it can be extended to conclude that these normal thresholds singularities can only be two-sheeted [38].[4]

To reiterate, for us the important point here is that, having obtained the general Cutkosky rule in the presence of nonlocal interactions, any of its various applications carry through as long as only local contour deformations are involved in the argument.

[4] n-particle normal threshold singularities with $n \geq 3$ are conjectured to be infinite-sheeted but no general argument is apparently known, cf. [4]

CHAPTER 5

Acausality of the Effective Propagator

In the following chapters we switch gears and study the extent of causality violation in nonlocal theories. We start by considering the simplest situation of free propagation of a particle between two general sources in the nonlocal theory. We envision this in the context of the general situation of production, scattering and detection of particles. Thus, a source may represent a nonlocal interaction vertex within the microscopic interaction region emitting a particle that is then propagating toward a detector acting as the absorbing source (sink); or an external source vertex producing an incoming particle traveling toward an interaction region, where it connects to a nonlocal vertex. We want to estimate the magnitude of any noncausal effects between such well separated sources. The nonlocal theory (2.1) has ordinary propagators $\Delta(x)$ and nonlocal vertices, which we take to be of the form (2.6). Thus, lumping the nonlocal vertex kernels with the propagator factor, propagation between two nonlocal sources is described by the effective propagator:

$$\tilde{\Delta}(p) = \frac{i}{p^2 - m^2 + i\epsilon}\mathcal{F}(p^2) \ , \tag{5.1}$$

where $\mathcal{F}(p^2) \equiv F^2(p^2)$. Henceforth, We conveniently normalize F so that $F(m^2) = 1$. The effective propagator may be written in position space as:

$$\tilde{\Delta}(x) = \mathcal{F}(-\Box)\Delta(x) \ . \tag{5.2}$$

We are then interested in the large x^2 behavior of $\tilde{\Delta}(x)$.

Now, it is a textbook result that the ordinary propagator $\Delta(x)$ has the explicit expression

$$\begin{aligned}\Delta(x) &= \int \frac{d^4p}{(2\pi)^4}\frac{i}{p^2-m^2+i\epsilon}e^{-ipx} \\ &= \frac{i}{4\pi}\delta(x^2)+\theta(x^2)\frac{im}{8\pi\sqrt{x^2}}H_1^{(2)}(m\sqrt{x^2})+\theta(-x^2)\frac{m}{4\pi^2\sqrt{-x^2}}K_1(m\sqrt{-x^2})\ ,\end{aligned} \tag{5.3}$$

where $H^{(2)}$ is the Hankel function of the second kind and K is the modified Bessel function of the second kind. The leading asymptotic behavior of (5.3) for large $|x^2|$ is:

$$\Delta(x) \sim \begin{cases} \sqrt{\frac{m}{32\pi^3}}\frac{1}{(x^2)^{3/4}}e^{-im\sqrt{x^2}-i\frac{3\pi}{4}} & x^2>0 \\ \sqrt{\frac{m}{32\pi^3}}\frac{1}{|x^2|^{3/4}}e^{-m\sqrt{|x^2|}} & x^2<0 \end{cases}\ . \tag{5.4}$$

Using (5.3) in (5.2) one sees that nonlocality results from the action of $\mathcal{F}(-\Box)$ on the delta and theta functions. Were $\mathcal{F}$ a polynomial, the result would be still local, modifying only the $x^2=0$ as discussed in [11]. Nonpolynomial $\mathcal{F}$, however, results in nonlocal smearing of these distributions and possible acausal tails. To examine the asymptotic behavior of the effective propagator $\tilde{\Delta}(x)$ we introduce Schwinger parameters and write

$$\tilde{\Delta}(x) = \int \frac{d^4p}{(2\pi)^4}\frac{i}{p^2-m^2+i\epsilon}\mathcal{F}(p^2)e^{-ipx} \tag{5.5}$$

$$= \int \frac{d^4p}{(2\pi)^4}\int_0^\infty d\alpha\,\mathcal{F}(p^2)e^{i\alpha(p^2-m^2+i\epsilon)}e^{-ipx}\ . \tag{5.6}$$

This allows use of stationary phase approximation to obtain the leading behavior in its asymptotic expansion. The computation is given in Appendix C. The result for large $x^2>0$ is:

$$\tilde{\Delta}(x) \sim \sqrt{\frac{m}{32\pi^3}}\frac{1}{(x^2)^{3/4}}\mathcal{F}(m^2)e^{-im\sqrt{x^2}-i\frac{3\pi}{4}}\ . \tag{5.7}$$

Since $\mathcal{F}(m^2)=1$ by the normalization, comparing with (5.4), we see that the leading asymptotic behavior of the effective propagator for large timelike separations, $x^2>0$, is the same as for the ordinary propagator $\Delta(x)$. For spacelike x^2, the computation is more involved, because the saddle point is now in the complex hyperplane of p and α, and the contour needs to be carefully deformed to pass through the saddle point. We will simply assert here that the same result holds true for large space-like x^2 as well. This is in any

case implied by the general results on asymptotic expansions obtained in section 5.1. We thus conclude that *the ordinary propagator* $\Delta(x)$ *and the effective propagator* $\tilde{\Delta}(x)$ *of the nonlocal theory, given by (5.5), have the same leading asymptotic behavior for large* $|x^2|$.

Any acausal effects must then reside in the non-leading contributions of the asymptotic expansion of $\tilde{\Delta}(x)$. The ordinary propagator $\Delta(x)$ is causal, so we define the 'acausal part' of the effective propagator by

$$\Delta_{ac}(x) \equiv \tilde{\Delta}(x) - \Delta(x) \tag{5.8}$$

$$= \int \frac{d^4p}{(2\pi)^4} \frac{i}{p^2 - m^2 + i\epsilon} (\mathcal{F}(p^2) - 1) \, . \tag{5.9}$$

Note that, by our leading behavior result, $\Delta_{ac}(x)$ indeed includes only non-leading asymptotic terms.[1] In the next section we obtain a general result on the asymptotic behavior of general kernels, in particular kernels of the general type (2.11), which allows us to determine the asymptotic behavior $\Delta_{ac}(x)$. It is instructive, however, to obtain the asymptotic behavior of $\Delta_{ac}(x)$ by direct explicit computation for the special case of the prototype kernel $\mathcal{F}(p^2) = e^{-\ell^4(p^4 - m^4)}$. Using the identity

$$e^{-(p^4 - m^4)\ell^4} - 1 = \int_0^1 d\xi \, e^{\xi(-p^4 + m^4)\ell^4} (-p^4 + m^4)\ell^4 \, , \tag{5.10}$$

(5.9) becomes

$$\Delta_{ac}(x) = -i\ell^4 \int_0^1 d\xi \int \frac{d^4p}{(2\pi)^4} e^{-\xi(p^4 - m^4)\ell^4} (p^2 + m^2) e^{-ipx} \, . \tag{5.11}$$

One can then compute the momentum integral in (5.11) by the method of steepest descents. See e.g. [39] for a detailed explanation of the method. The detailed steps are in Appendix D. For $x^2 > 0$, the leading asymptotic behavior of (5.11) is

$$\Delta_{ac} \sim i\ell^4 \int_0^1 d\xi \, \frac{e^{\xi m^4 \ell^4}}{8\pi^2\sqrt{3}} \frac{1}{(4x^2\xi^4\ell^{16})^{1/3}} \exp\left[-\frac{3}{2} \left(\frac{x^4}{256\xi\ell^4} \right)^{1/3} \right] \cos\left[\frac{3\sqrt{3}}{2} \left(\frac{x^4}{256\xi\ell^4} \right)^{1/3} + \frac{\pi}{6} \right] . \tag{5.12}$$

[1] We will in fact show using BCC in section 6.1 that the difference (5.9) constitutes precisely the acausal part of $\tilde{\Delta}$.

To do the remaining ξ integral, we perform a change of variable $\zeta = \xi^{-1/3}$ and apply Laplace's method. The result is

$$\Delta_{ac}(x) \sim -i\frac{e^{m^4\ell^4}}{2\pi^2\sqrt{3}|x^2|}\exp\left[-\frac{3}{2}\left(\frac{|x^2|}{16\ell^2}\right)^{2/3}\right]\sin\left[\frac{3\sqrt{3}}{2}\left(\frac{|x^2|}{16\ell^2}\right)^{2/3}\right] . \tag{5.13}$$

An analogous derivation holds for space-like x^2, giving the same (5.13), which is expressed in $|x^2|$ for this reason. One sees that, indeed, the acausal part $\Delta_{ac}(x)$ of $\tilde{\Delta}(x)$ is exponentially suppressed for large separation and decays faster than its leading, causal part, which it has in common with $\Delta(x)$. Note that (5.13) does not depend on the mass. Indeed one can show that with the same nonlocal kernel, the massless effective propagtor, which we will denote by $\tilde{D}(x)$, has the same acausal asymptotic behavior. In fact, $\tilde{D}$ has been worked out in closed form in terms of the MeijerG functions ([13, 40]):

$$\tilde{D}(x) = \frac{-1}{4\pi x^2} + \frac{i}{8\pi^4|x^2|}\left[2\pi^2 G^{4,1}_{3,6}\left(\begin{matrix}0,-\frac{1}{4},\frac{1}{4}\\ 0,0,\frac{1}{2},\frac{1}{2},-\frac{1}{4},\frac{1}{4}\end{matrix}\middle|\frac{x^4}{256\ell_2^4}\right) + G^{4,1}_{2,5}\left(\begin{matrix}0\\ 0,0,\frac{1}{2},\frac{1}{2}\end{matrix}\middle|\frac{x^4}{256\ell_2^4}\right)\right] . \tag{5.14}$$

Its acausal part $D_{ac}(x)$, which is (5.14) minus the ordinary massless propagator $D(x)$, has indeed (5.13) as its leading asymptotic behavior.

We have also carried out numerical calculation as a check. We first split (5.5) into the pole part and the principal value part of the p^0 integral:

$$\tilde{\Delta}(x) = I_{PV} + I_{pole}. \tag{5.15}$$

At the pole, the nonlocal factor is $\mathcal{F}(m^2) = 1$, so I_{pole} contributes to $\tilde{\Delta}(x)$ as it would to $\Delta(x)$. It is also the real part of the ordinary as well as the effective propagators, i.e $I_{pole} = \mathrm{Re}(\Delta(x)) = \mathrm{Re}(\tilde{\Delta}(x))$. the principal value part, which is purely imaginary, one can integrate out the angular integrals of p, as detailed in Appendix E, and get

$$I_{PV}(x^2>0) = \frac{i}{(2\pi)^3\sqrt{x^2}}\mathrm{PV}\int_0^\infty dp\, p^2\left[2\pi\frac{\mathcal{F}(p^2)}{p^2-m^2}Y_1\left(p\sqrt{x^2}\right) + 4\frac{\mathcal{F}(-p^2)}{p^2+m^2}K_1\left(p\sqrt{x^2}\right)\right] , \tag{5.16}$$

$$I_{PV}(x^2<0) = \frac{i}{(2\pi)^3\sqrt{|x^2|}}\mathrm{PV}\int_0^\infty dp\, p^2\left[2\pi\frac{\mathcal{F}(-p^2)}{p^2+m^2}Y_1\left(p\sqrt{|x^2|}\right) + 4\frac{\mathcal{F}(p^2)}{p^2-m^2}K_1\left(p\sqrt{|x^2|}\right)\right] . \tag{5.17}$$

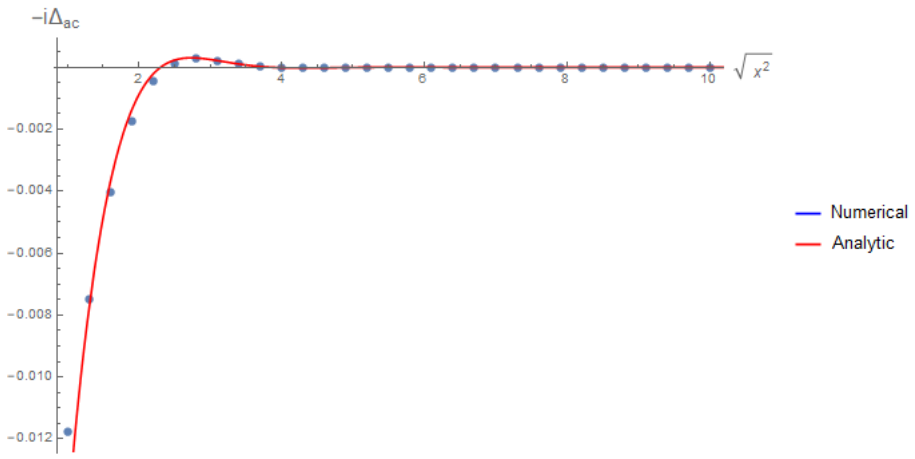


Figure 5.1: The acausal part of a particular effective propagator. The analytic expression of its asymptotic (5.13) is compared to numerical evaluation using (5.16), and indeed they agree well for large x^2. The parameters are set to $m = 1$ and $\ell = 1/2$.

The integral is numerically well behaved without any divergence or oscillatory ambiguity, thanks to the exponential decay of $\mathcal{F}$ for large p^2. Since I_{PV} is the imaginary part of the effective propagator, from (5.9) one finds $\Delta_{ac} = I_{PV} - \text{Im}\Delta$, where Δ is given in (5.3). We numerically evaluated Δ_{ac} and compared it to (5.13), as shown in Fig. 5.1 for large timelike separation. One sees that they indeed match well for $|x^2| \gg \ell^2$.

5.1 Asymptotic Behavior for General Kernel

For a generic nonlocal kernal of type (2.11) and the text following that, we shall argue that the delocalized vertex (2.8) and the acausal part of a propagator (5.8) decays faster than any power of ℓ^2/x^2. We'll do so first for the vertex and then use the trick analogous to (5.10) for the propagator. We'll introduce Mellin transform and use that for asymptotic expansion. A detailed presentation of the method can be found in [39], but we reproduce below a self-contained introduction to the techniques that we'll need. Because we are studying the Fourier transform of Lorentz invariant functions, the integrals we will be studying is of the form (E.3) and (E.5).

5.1.1 Asymptotic Expansion Using Mellin Transform

We wish to find the asymptotic expansion of integrals of the form

$$I(\lambda) = \int_0^\infty h(\lambda p) f(p) dp \tag{5.18}$$

as λ becomes large. The Mellin transformation is defined as

$$M[h; z] = \int_0^\infty h(p) p^{z-1} dz. \tag{5.19}$$

The associated fundamental strip is the area in the complex z plane in which the above integral converges. Outside the strip, $M[h; z]$ is defined by analytic continuation. In general, $M[h; z]$ is analytic in the fundamental strip and meromorphic outside. The Parseval formula for Mellin transform states that, if the fundamental strips of $M[h; z]$ and $M[f; 1-z]$ overlap, then

$$I(\lambda) = \frac{1}{2\pi i} \int_{c-i\infty}^{c+i\infty} dz\, \lambda^{-z} M[h; z] M[f; 1-z] \,, \tag{5.20}$$

where c is any real number in the overlap of the fundamental strips. For the exact conditions for which the Parseval formula holds, see [39]. (It will be satisfied in our application.) The asymptotic expansion for large λ can then be obtained by shifting the vertical contour to the right, from $\mathrm{Re} z = c$ to $\mathrm{Re} z = R$ for some R, picking up residues along the way.

$$I(\lambda) \sim - \sum_{R > \mathrm{Re} z > c} \mathrm{Res}\, \lambda^{-z} M[h; z] M[f; 1-z] \tag{5.21}$$

In the above asymptotic expansion, the terms in the summation come from the residues, while the vertical contour at $\mathrm{Re} z = R$ contributes $O(\lambda^{-R})$, provided that it converges. In order for the above procedure to work, R must be such that

$$M[h; x+iy] M[f; 1-x-iy] \to 0 \quad \text{as } |y| \to \infty \,, \tag{5.22}$$

for all $c < x < R$ and that

$$\left| \int_{-\infty}^{\infty} dy\, M[h; R+iy] M[f; 1-R-iy] \right| < \infty \,. \tag{5.23}$$

If R can be made arbitrarily large, then the sum in (5.21) is over all $\mathrm{Re} z > c$.

5.1.2 Asymptotic of (Minkowski) Fourier Transform

The integral of interest is (E.3), reproduced here for convenience,

$$A(x^2>0)=\frac{1}{\sqrt{x^2}}\int_0^\infty dp\,p^2\left[2\pi A(p^2)Y_1\left(p\sqrt{x^2}\right)-4A(-p^2)K_1\left(p\sqrt{x^2}\right)\right]. \tag{5.24}$$

It is the Fourier transform of some Lorenz invariant function $A(p^2)$ to position space with time-like x^2. (We've dropped the inessential $1/(2\pi)^3$). The large parameter here is $\lambda=\sqrt{x^2}$. Technically the large parameter should be dimensionless, but it can be achieved by a simple rescaling of p. For now we will pretend that we've already rescaled p such that λ is dimensionless. Following the form of (5.18), let

$$\begin{aligned}h_1(p)&=2\pi p^2Y_1(p)\\ h_2(p)&=4p^2K_1(p).\end{aligned} \tag{5.25}$$

The Mellin transforms of h_1,h_2 are [2] [41]

$$M_1\equiv M\left[h_1;z\right]=2^{z+2}\sin\frac{\pi z}{2}\Gamma\left(\frac{z+3}{2}\right)\Gamma\left(\frac{z+1}{2}\right),\quad -\frac{1}{2}>\mathrm{Re}\,z>-1 \tag{5.26}$$

$$M_2\equiv M\left[h_2,z\right]=2^{z+2}\Gamma\left(\frac{z+3}{2}\right)\Gamma\left(\frac{z+1}{2}\right),\quad \mathrm{Re}\,z>-1. \tag{5.27}$$

with their fundamental strips stated on the right. (5.26) can be straightforwardly continued to $\mathrm{Re}z>-\frac{1}{2}$ as a holomorphic function. On the other hand, $A(\pm p^2)$ is so far general, but the locations of the poles of its Mellin Transform are determined solely by the small p^2 behavior of $A(\pm p^2)$, which could be different as p^2 approach 0 from the left or right. (The $p^2\to\infty$ behavior also creates poles, but they are to the left of the fundamental strip of $M[A;1-z]$, which is not relevant in the asymptotic expansion.) Suppose that $A(p^2)$ has the following asymptotic expansion

$$f_1(p)\equiv A(p^2)\sim\sum a_np^{r_n}\ , \tag{5.28}$$

[2] In (5.18), the argument of $h(\lambda p)$ is scaled by the large parameter; while in (5.24), only Y_1 and K_1 have arguments scaled by λ. This is easily resolved by including a factor $1/\lambda^2$ to (5.24), so that now both h_1,h_2 have arguments scaled by λ

$$f_2(p) \equiv A(-p^2) \sim \sum b_n p^{s_n} \ . \tag{5.29}$$

as $p^2 \to 0^+$. The fundamental strip of $M[f_1; 1-z]$ is then $\mathrm{Re}z < r_0 + 1$ and has poles at $z = r_n + 1$ with residues $-a_n$. Similarly, the fundamental strip of $M[f_2, 1-z]$ is $\mathrm{Re}z < s_0 + 1$ and has poles at $z = s_n + 1$ with residues $-b_n$. If $r_0, s_0 > -2$, then the fundamental strips of $M[h_{1,2}; z]$ and $M[f_{1,2}; 1-z]$ overlap, respectively. Given the poles and residues of the Mellin transforms, one now has sufficient information to write down the asymptotic expansion using (5.21), and that is

$$\begin{aligned} A(\lambda) \sim & -\sum_n a_n \frac{1}{2} \left(\frac{2}{\lambda}\right)^{r_n+4} \cos\frac{\pi r_n}{2} \Gamma\left(\frac{r_n}{2}+2\right) \Gamma\left(\frac{r_n}{2}+1\right) \\ & + \sum_n b_n \frac{1}{2} \left(\frac{2}{\lambda}\right)^{s_n+4} \Gamma\left(\frac{s_n}{2}+2\right) \Gamma\left(\frac{s_n}{2}+1\right) . \end{aligned} \tag{5.30}$$

The number of terms in the expansion depends on the R for which (5.22) and (5.23) are satisfied. (5.26) is $O(|y|^{\lceil x+3/2 \rceil})$ as $|y| \to \infty$ for $x > -1$, where $z = x + iy$ and $\lceil \cdot \rceil$ is the ceiling function. So $M[f_1; 1-z]$ needs to decay fast enough in y for (5.22) and (5.23) to hold. In particular, if and only if for any fixed x, $M[f_1; 1-z]$ decays faster than any power of $1/y$, then the asymptotic expansion (5.30) is true for all n, which is desired for out application. This puts some constraint on $A(p^2)$, which we will discuss in the next section. On the other hand, (5.27) is already exponentially decaying for large y, so if $M[f_2; 1-z]$ decays as fast as $M[f_1; 1-z]$ in y, then (5.22) and (5.23) are automatically satisfied.

5.1.3 Asymptotic for Nonlocal Kernel and the Acausal Part of the Propagator

For nonlocal theories, we find the following theorem particularly suitable.

Theorem 2 *Let $f(p)$ be n times continuously differentiable on $(0, \infty)$. Suppose $f(p)$ has the following asymptotic expansion as $p \to 0$:*

$$f(p) \sim \sum_{m=0}^{\infty} a_m p^{r_m} \ . \tag{5.31}$$

and the asymptotic expansion of the derivatives $f^{(j)}(p)$ is obtained by differentiating the above term by term. Furthermore, suppose that for all $x > -r_0$ and for $q = 0, 1, 2, ..., n$,

$$\left(p\frac{d}{dp}\right)^q p^x f(p) \tag{5.32}$$

vanishes as $p \to \infty$. Then for all x

$$M[f; z] = \mathcal{O}(|y|^{-n}) \quad as\ |y| \to \infty\ , \tag{5.33}$$

where $z = x + iy$. In particular, if the above holds true for all n, then $M[f; z]$ decays faster than any power of $1/y$ for large y.

The proof of this theorem is in [39]. As an example, consider the nonlocal kernel

$$f(p) = e^{-p^4\ell^4} \sim \sum_{n=0}^{\infty}(-1)^n\frac{p^{4n}\ell^{4n}}{n!}\ . \tag{5.34}$$

It satisfies the conditions of the theorem and one would expect its Mellin transform to decay faster than any power of $1/y$ for large y. Indeed, its Mellin transform is explicitly

$$M[f; z] = \frac{1}{4}\ell^{\frac{3}{2}+z}\Gamma\left(\frac{z}{4}\right)\ , \tag{5.35}$$

which decays exponentially for large y for all x. It is not hard to see that any nonlocal kernel of the type (2.11) will satisfy the conditions of the theorem. Therefore, for the Fourier transform of a nonlocal kernel, there are infinite terms in the asymptotic expansion (5.30).

In addition to the condition of the above theorem, we further assume that $A(p^2)$ is infinitely differentiable with respect to p^2 around $p^2 = 0$. This means that $A(p^2)$ has the same asymptotic expansion as $p^2 \to 0^+$ and $p^2 \to 0^-$, and that the asymptotic expansions are in even powers of p. Explicitly, $f_{1,2}$ as defined in (5.28), (5.29) now become

$$\begin{aligned} f_1(p) &\sim \sum_{n=0}^{\infty} a_n p^{2n} \\ f_2(p) &\sim \sum_{n=0}^{\infty}(-1)^n a_n p^{2n}. \end{aligned} \tag{5.36}$$

The Mellin transforms $M[f_{1,2}; 1-z]$ have fundamental strips $\mathrm{Re}(z) < 1$ [3], which overlaps with those of $M[h_{1,2}; z]$, as noted in (5.26), (5.27). Thus one may use (5.30) and get

$$\begin{aligned} A(x^2) \sim & -\sum_{n=0}^{\infty} \frac{1}{2} \left(\frac{2}{\sqrt{x^2}} \right)^{4+2n} a_n \cos(n\pi) \Gamma(2+n) \Gamma(1+n) \\ & + \sum_{n=0}^{\infty} \frac{1}{2} \left(\frac{2}{\sqrt{x^2}} \right)^{4+2n} a_n (-1)^n \Gamma(2+n) \Gamma(1+n) \\ \sim & \, o\left(\frac{1}{\sqrt{x^2}^N} \right), \quad \forall N \in \mathbb{N}. \end{aligned} \tag{5.37}$$

The first and second line cancels exactly, thus meaning that $A(x^2)$ decays faster than any power of $1/x^2$. For large spacelike separation, since (E.5) and (E.3) have similar forms, the exact same argument goes through. We summarize our result in the following proposition.

Proposition 5.1.1 *If a function $A(p^2)$ is locally integrable on $p^2 \in (0, \infty)$ and $p^2 \in (-\infty, 0)$, satisfies the conditions of theorem 2 (for all n), and is infinitely differentiable around $p^2 = 0$, then the asymptotic behavior of its Fourier transform decays faster than any power of $1/x^2$.*

Arbitrary delocalized vertex (2.8), with kernels of the form (2.11), satisfies all the conditions in Proposition 5.1.1. Thus it decays faster than any power of ℓ^2/x^2. Next we study the large separation behavior of the acausal part of a effective propagator, which can be written in the form (5.9). we use the same trick as in (5.10). By assumption, we write $\mathcal{F}(p^2) = e^{\mathcal{P}(p^2)}$ [4], where $\mathcal{P}$ is some entire function, and let

$$e^{\mathcal{P}} - 1 = \int_0^1 d\xi \, \exp(\xi \mathcal{P}) \, \mathcal{P}. \tag{5.38}$$

Using (E.3), we can write the acausal part of the nonlocal propagator, for timelike separation,

[3] If the first few a_n's are zero, the fundamental strip covers even more ground.

[4] This definition differs from 2.11 by a factor of -2, which can be easily acounted for.

as

$$\begin{aligned}\Delta_{ac}(x^2>0) =& \frac{i}{(2\pi)^3\sqrt{x^2}}\mathrm{PV}\int_0^1 d\xi\int_0^\infty dp\, p^2 \\ &\times\left[2\pi\frac{\left(e^{\xi\mathcal{P}(p^2)}\mathcal{P}(p^2)\right)}{p^2-m^2}Y_1\left(p\sqrt{x^2}\right)+4\frac{\left(e^{\xi\mathcal{P}(-p^2)}\mathcal{P}(-p^2)\right)}{p^2+m^2}K_1\left(p\sqrt{x^2}\right)\right] \\ =& \frac{i}{(2\pi)^3\lambda\ell^2}\mathrm{PV}\int_0^1 d\xi\int_0^\infty dp\, p^2 \\ &\times\left[2\pi\frac{\left(e^{\xi\hat{\mathcal{P}}(p^2)}\hat{\mathcal{P}}(p^2)\right)}{p^2-m^2\ell^2}Y_1\left(p\lambda\right)+4\frac{\left(e^{\xi\hat{\mathcal{P}}(-p^2)}\hat{\mathcal{P}}(-p^2)\right)}{p^2+m^2\ell^2}K_1\left(p\lambda\right)\right],\end{aligned} \tag{5.39}$$

where in the second equality, we've rescaled $p\to p/\ell$ and defined $\hat{\mathcal{P}}(p^2\ell^2)\equiv\mathcal{P}(p^2)$ and $\lambda\equiv\sqrt{x^2}/\ell$, which is dimensionless and will be taken to be large.

We now check that the conditions of proposition 1 are satisfied. $A(p^2)=\frac{e^{\xi\hat{\mathcal{P}}}\hat{\mathcal{P}}}{p^2-m^2\ell^2}$. It is locally integrable on $(0,\infty)$ because the only possible pole from the denominator $p^2-m^2\ell^2$ is canceled by $\hat{\mathcal{P}}(m^2\ell^2)=0$. The function is infinitely differentiable on $p\in(0,\infty)$ and satisfies the conditions of theorem 1 because $e^{\xi\hat{\mathcal{P}}}$ is exponentially decaying for large p. And finally, $A(p^2)$ is infinitely differentiable around $p^2=0$. That these conditions are met means that for fixed ξ, the Fourier transform decays faster than any power of $1/\lambda$. Then, for the asymptotic behavior of Δ_{ac}, one has to integrate over ξ, but that doesn't change the nature of rapid decay of the asymptotic behavior. We will argue the last point in more detail below.

Before the final step of (5.37), where one cancels the two asymptotic series, we will first integrate over ξ. The a_n's are obtained from Taylor expanding $A(p^2)$ around $p^2=0$. Clearly ξ appears in positive powers in a_n. Integrating over ξ doesn't produce any singularity in each term in the asymptotic series. Thus the two summations still cancel after the ξ integration, and Δ_{ac} decays faster than any power of $1/\lambda^2=\ell^2/x^2$.

For massless nonlocal propagators, the same argument goes through as well. In fact, we see from the explicit example in the previous section that the leading acausal part is the same for massless and massive propagators.

For kernels described in section 2.3.1, the small s expansion (5.28) and (5.29) do not have

the form (5.36). With the example (2.24), f_1 includes a term $-(p\ell)^{4\rho}$, while the same order term in f_2 is $-e^{i2\pi\rho}(p\ell)^{4\rho}$. Their contributions do not cancel in (5.30), and so the asymptotic behavior is some power in ℓ^2/x^2. For other examples of how this Mellin transform method can be applied to ordinary propagators and amplitudes, see appendix F. There will also be cases where the conditions in Proposition 5.1.1 are not all satisfied and we discuss the consequences thereof.

5.1.4 Kernels with polynomial decay

We now turn to kernels described in section that are exponentials of entire functions, but which decay polynomially for large momentum, as described in section 2.3.2. Though $\mathcal{F}(p^2)$ is infinitely differentiable around $p^2 = 0$, the result from the last sections doesn't apply directly, because a condition in Theorem 2 no longer holds. There is no $-r_0$ such that for all $x > -r_0$, $p^x\mathcal{F}(p^2) \to 0$ for large p. We will find another way to show that this type of kernel also has a similar result as Theorem 2.

Assume that a particular kernel of this type decays as $1/p^B$ for large $|p^2|$. Since it is entire it is infinitely differentiable. Further assume that for small p^2, it has the following asymptotic expansion,

$$\mathcal{F} \sim \sum_{m=0}^{\infty} a_m p^{2m}, \tag{5.40}$$

where $a_0 \neq 0$ since the kernel approaches some constant for small p; and assume that for large p, it has the following asymptotic expansion,

$$\mathcal{F} \sim \sum_{m=B/2}^{\infty} b_m p^{-2m}, \tag{5.41}$$

and that the asymptotic of the derivatives of $\mathcal{F}$ is the derivative of the above series term by term. Given the large p and small p behavior, the fundamental strip of $M[\mathcal{F}; z]$ is in $0 < \mathrm{Re} z < B$. It vanishes as $y \to 0$ in this strip ($z = x + iy$). To do asymptotic expansion, we want to know how fast it goes to zero for all $x < B$.

Consider $f_k \equiv \mathcal{F} - s_k$ for some positive integer k, where

$$s_k \equiv e^{-p^\delta} \sum_{m=0}^{k-1} a_m p^{2m} \ , \tag{5.42}$$

and $\delta = 2k+1$. Given this decomposition, the Mellin transform can also be decomposed as

$$M[\mathcal{F}; z] = M[f_k; z] + M[s_k; z] \ . \tag{5.43}$$

$M[s_k; z]$ can be computed explicitly to be

$$M[s_k; z] = \sum_{m=0}^{k-1} \frac{a_m}{\delta} \Gamma\left(\frac{z+a_m}{\delta}\right) \ . \tag{5.44}$$

which vanishes exponentially as $|y| \to \infty$ for all x. On the other hand, because of the choice of δ, $f_k \sim \mathcal{O}(p^{2k})$ for small p. The fundamental strip of $M[f_k; z]$ is in $-2k < x < B$. In this strip, the Mellin transform is

$$\begin{aligned} M[f_k; x+iy] &= \int_0^\infty f_k(p) p^{x-1} p^{iy}\, dp \\ &= \frac{1}{iy} f_k(p) p^x p^{iy}\Big|_0^\infty - \int_0^\infty \frac{1}{iy} \frac{d}{dp}\Big(f_k(p)p^x\Big) p^{iy}\, dp \\ &= \sum_{j=0}^{N-1} (-1)^j \left(\frac{1}{iy}\right)^{j+1} p^{iy} \left(p\frac{d}{dp}\right)^j \Big(f_k(p)p^x\Big)\Big|_0^\infty \\ &\quad + (-1)^N \left(\frac{1}{iy}\right)^N \int_0^\infty \frac{p^{iy}}{p} \left(p\frac{d}{dp}\right)^N \Big(f_k(p)p^x\Big)\, dp \ , \end{aligned} \tag{5.45}$$

for some N. Given the asymptotic series (5.40) and (5.41), and given s_k, we see that all the boundary terms in the third line vanishes when $-2k < x < B$. The remaining integral can be written as

$$(-1)^N \left(\frac{1}{iy}\right)^N \int_{-\infty}^\infty \left[\left(p\frac{d}{dp}\right)^N \Big(f_k(p)p^x\Big)\right]_{p=e^q} e^{iqy}\, dq \ . \tag{5.46}$$

Because $\mathcal{F}$ is the exponential of an entire function and has the asymptotic expansions (5.40) and (5.41), the term inside the bracket is in $L(-\infty < q < \infty)$, and by Riemann-Lebesque, the integral is of $o(1)$. Therefore $M[f_k; x+iy] = o(1/y^N)$ as $|y| \to \infty$ for $-2k < x < B$. But the choice of N and k is arbitrary, so $M[f; x+iy]$ decays faster than any power of $1/y$ for all $x < B$. Combining this result with (5.43) and (5.44), we get that $M[\mathcal{F}; 1-z]$ decays faster

than any power of $1/y$ for $x > 1 - B$. This is a similar result as Theorem 2 (except not for all x), and we can apply the same technique as that in the last section. We conclude that for the kernel considered in this section, the delocalized vertex (2.8) and the acausal part of the nonlocal propagator (5.8) decay faster than any power of ℓ^2/x^2.

CHAPTER 6

Amplitudes and causality

6.1 Bogoliubov Causality Condition

A general statement of the requirement of causality in quantum field theory is provided by the BCC [7]. It formulates the notion of causality as the requirement that variations in the strength of the coupling g at some spacetime point x_2 do not affect the dynamics at a spacetime point x_1 if $x_1 \prec x_2$, i.e., x_2 is in the future lightcone of x_1, or if the two points are separated by a spacelike distance. This requirement is then expressed in terms of the S-matrix operator (evolution operator) in the form [7]:

$$\frac{\delta}{\delta g(x_2)}\left(S^\dagger \frac{\delta S}{\delta g(x_1)}\right) = 0 \qquad \text{if } x_1 \prec x_2 \ . \tag{6.1}$$

This may be written in the equivalent form

$$\frac{\delta}{\delta g(x_2)}\left(\frac{\delta S^\dagger}{\delta g(x_1)} S\right) = 0 \qquad \text{if } x_1 \prec x_2 \ , \tag{6.2}$$

since $\dfrac{\delta S^\dagger}{\delta g(x)} S = -S^\dagger \dfrac{\delta S}{\delta g(x)}$ as implied by the unitarity condition $S^\dagger S = 1$. The BCC is a general formulation of the causality condition in QFT. The usual 'microcausality condition', i.e., that of the commutativity of field operators at spacelike separations, is implied by the BCC and thus can be obtained from it [34], [37].

The BCC formulates the condition of causality in terms of amplitudes. Expanded in perturbation theory it can be expressed in terms of graphs. In local theories (6.1) can in fact be derived within perturbation theory from Veltman's largest time equation [42], [37], or, in momentum space, from tree-loop duality [34]. These derivations do not carry through in the presence of nonlocal vertices.

Violation of the condition in a theory will result in a nonvanishing r.h.s. in (6.1). Such a nonzero r.h.s. provides a direct estimate of the extent of the violation. The physically relevant question then is how large the violation is at distances long compared to the nonlocality scale ℓ.

(6.1) has a diagrammatic representation as sum over diagrams with Cutkosky cuts [37]. Another representation of amplitudes in terms of retarded and advanced propagators, suitable for exhibiting causal relations, has been obtained in [43] from the Hamiltonian operator formalism. Such derivations, however, like the ones based on the largest time equation or tree-loop duality, are not applicable in the presence of nonlocal vertices. In this paper we will derive a representation in terms of (non-local extensions of) 'retarded' and 'advanced' propagators by direct diagrammatic analysis, which holds in the nonlocal as well as the local theory. In the nonlocal case one obtains (6.1) or (6.2) but with a nonvanishing r.h.s., which, of course, vanishes in the local limit.

As discussed in section 2.2, beyond tree level, amplitudes $A^{(M)}(p)$ computed directly in Minkowski space do not generally coincide with the amplitude $A(p)$, which is the correct one and obtained by analytic continuation in the external momenta $\{p_i\}$ from the Euclidean amplitude $A^{(E)}(p)$, cf. (2.22). For brevity, in the following we will often refer to the $A^{(M)}$ as the 'Minkowski-defined' amplitudes or theory and to the A as the 'Euclidean-defined' amplitudes or theory.

Consider a general diagram with N vertices. To discuss causality properties one can straightforwardly Fourier transforms $A^{(M)}(p)$ to obtain the position space n-point amplitude with truncated legs:

$$\begin{aligned}\mathcal{A}^{(M)}M(x_1,\dots,x_n) &= \int \prod_{i=1}^{n}\left(\frac{d^4p_i}{(2\pi)^4}e^{-ip_ix_i}\right)(2\pi)^4\delta\left(\Sigma p\right)A^{(M)}(p)\\ &= \int \prod_{j=n+1}^{N} d^4x_j\,\mathcal{I}(x_1,...,x_N)\ . \end{aligned} \tag{6.3}$$

The integrations are over the internal vertices, here labeled $j = n+1,\dots,N$. The integrand $\mathcal{I}$ is simply a product of position-space propagators and vertex factors. If we take the vertices to be of the type (2.6), which in fact will the basis of our discussion, they can be combined

with the propagators to form the effective propagators (5.1), so that, assuming, for simplicity, no extra polynomial derivative interactions, $\mathcal{I}$ is simply a product of $\tilde{\Delta}(x_i - x_j) \equiv \tilde{\Delta}_{ij}$ factors. This makes working with (6.3) in coordinate space rather more convenient than working with the FT of the analytically continued $A(p)$. So we first work with (6.3) and then examine how it differs from the analytically continued amplitudes.

We now define a set of operations on $\mathcal{I}$ that should be familiar to those acquainted with the approach to unitarity and causality based on Veltman's largest time equation [37], which is just (6.1) FT into position space. The presentation, though, is largely self-contained. Given $\mathcal{I}(x_1, \ldots, x_N)$, we introduce new functions denoted by underlining one or more of their arguments: $\mathcal{I}(x_1, \ldots, \underline{x}_j, \ldots, \underline{x}_k, \ldots, x_N)$. They are defined by the following rules: (i) a factor of $\tilde{\Delta}_{ij}$ if neither x_j nor x_i are underlined ; (ii) a factor of $\tilde{\Delta}^*_{ij}$ if both x_j and x_i are underlined; (iii) a factor of $\tilde{\Delta}^+_{ij}$ if x_i is but x_j is not underlined; (iv) a factor of $\tilde{\Delta}^-_{ij}$ if x_i is not but x_j is underlined; and (v) a factor of (-1) for every underlined vertex.[1] The effective propagator $\tilde{\Delta}_{ij}$ is given by (5.5) and the other various propagators in position space are explicitly given by:

$$\Delta^{\pm}_{ij} \equiv \int \frac{d^4p}{(2\pi)^4} 2\pi\delta^{\pm}(p^2 - m^2) e^{-ip(x_i - x_j)} \tag{6.4}$$

$$\tilde{\Delta}^*_{ij} = \int \frac{d^4p}{(2\pi)^4} \frac{-i\mathcal{F}(p^2)}{p^2 - m^2 - i\epsilon} e^{-ip(x_i - x_j)} \ , \tag{6.5}$$

where the $\delta^{\pm}$ denotes taking the support of either the positive or negative value of p^0 only. We will also introduce:

$$\tilde{\Delta}_{A,ij} \equiv \int \frac{d^4p}{(2\pi)^4} \frac{i\mathcal{F}(p^2)}{p^2 - m^2 - ip^0\epsilon} e^{-ip(x_i - x_j)} \tag{6.6}$$

$$\tilde{\Delta}_{R,ij} \equiv \int \frac{d^4p}{(2\pi)^4} \frac{i\mathcal{F}(p^2)}{p^2 - m^2 + ip^0\epsilon} e^{-ip(x_i - x_j)} \ . \tag{6.7}$$

Note the relations $\tilde{\Delta}_{A,ij} = \tilde{\Delta}_{R,ji}$, $\Delta^+_{ij} = \Delta^-_{ji}$.

[1] This comes from letting $i \to -i$ for the factor of i assigned to each vertex in the Minkowski space Feynman rules.

In the local limit, $\mathcal{F} \to 1$, (6.6) and (6.7) reduce to the usual advanced and retarded propagators. In the nonlocal case, however, one no longer can perform the p^0 integration by closing the contour at infinity to extract an overall factor of $\theta(\pm(x^0_- - x^0_j))$, and thus $\tilde{\Delta}_{A,R}$ do *not* imply any time ordered propagation. Their only resemblance to their local counterpart is the locations of poles relative to the contour. By locally deforming the contour around the poles, one gets the identities:

$$\tilde{\Delta}_{ij} - \Delta^+_{ij} = \tilde{\Delta}_{A,ij} \qquad \tilde{\Delta}_{ij} - \Delta^-_{ij} = \tilde{\Delta}_{R,ij} \tag{6.8}$$

$$-\tilde{\Delta}^*_{ij} + \Delta^-_{ij} = \tilde{\Delta}_{A,ij} \qquad -\tilde{\Delta}^*_{ij} + \Delta^+_{ij} = \tilde{\Delta}_{R,ij} \ . \tag{6.9}$$

The other important relation for what follows is the decomposition

$$\tilde{\Delta}_R(x) = \Delta_R(x) + \Delta_{ac}(x) \ . \tag{6.10}$$

In (6.10) this is the *same* $\Delta_{ac}(x)$ as in (5.8) because the nonlocal factor only affects the propagator away from the pole, while $\tilde{\Delta}(x)$ and $\tilde{\Delta}_{A,R}(x)$ differs only at the poles; also, cf. (5.15) and remark following it.

Now given the set of vertices with associated spacetime $\{x\}$, we single out one of them, say, vertex i and consider the sum: $\sum_i \mathcal{I}(x_1, \ldots, x_N)$. The summation is over all underlinings of vertices except for the vertex i, indicated by the index i under the sum, which is never underlined; thus the sum includes a term with no vertices underlined, a term with all vertices underlined except i, $N-1$ terms with one vertex other than i underlined, and so on. Now single out a second vertex j and impose the restriction on the time components $x^0_i < x^0_j$, or, more generally, $x_i \prec x_j$. In the *local* theory, i..e, when $\tilde{\Delta} = \Delta$, the above sum equals zero:

$$\sum_i \mathcal{I}(x_1, \ldots, x_N) = 0 \qquad \text{if} \quad x_i \prec x_j \ , \qquad \text{local theory} \ . \tag{6.11}$$

This is an immediate consequence of the largest time equation [37]. (6.11), when multiplied by the appropriate wave functions for each external vertex and integrated over all x_k except the singled out x_i and x_j vertices, becomes precisely (the single diagram version of) the BCC equation (6.1).

Similarly, one may consider the sum over all underlinings with the vertex i kept always underlined (denoted by $\underline{i}$ below the summation), and obtain the analogous statement

$$\sum_{\underline{i}} \mathcal{I}(x_1, \ldots, \underline{x}_i, \ldots, x_N) = 0 \qquad \text{if} \quad x_i \prec x_j \ , \qquad \text{local theory} \ , \tag{6.12}$$

which, after integration over vertices except for x_i and x_j, gives the equivalent BCC form (6.2).

Our goal then is to determine how the sum on the l.h.s. of (6.11), or (6.12), which represents the l.h.s. of the (6.2), deviates from zero when $x_i \prec x_j$ in the *nonlocal* theory. This will give a measure of any acausal effects in terms of amplitudes. We will obtain a representation of the sum in terms of $\tilde{\Delta}_{A,R}$ and $\Delta_{\pm}$. In the local theory, the representation is simply obtained by replacing $\tilde{\Delta}_{A,R}$ with $\Delta_{A,R}$, which makes the causal relationships in the local theory and the differences in the nonlocal theory transparent.

The BCC equation can also be related to the unitarity condition [37], [34]. Adding (6.1) and (6.2) one obtains

$$\frac{\delta}{\delta g(x_1)} \frac{\delta}{\delta g(x_2)} \left(S^\dagger S \right) = 0 \ , \tag{6.13}$$

Now, the unitarity condition $S^\dagger S = S S^\dagger = 1$ requires that the r.h.s. in (6.13) vanishes regardless of whether the r.h.s in (6.1) and (6.2) vanish; and the corresponding statement can then be made in terms of the sum of the l.h.s. of (6.11) and (6.12). Thus, non-vanishing r.h.s. in (6.13), or

$$\left(\sum_{i} \mathcal{I}(x_1, \ldots, x_N) + \sum_{\underline{i}} \mathcal{I}(x_1, \ldots, x_N) \right) \neq 0 \ , \tag{6.14}$$

gives us another handle on any unitarity violations.

6.2 Tree Amplitudes

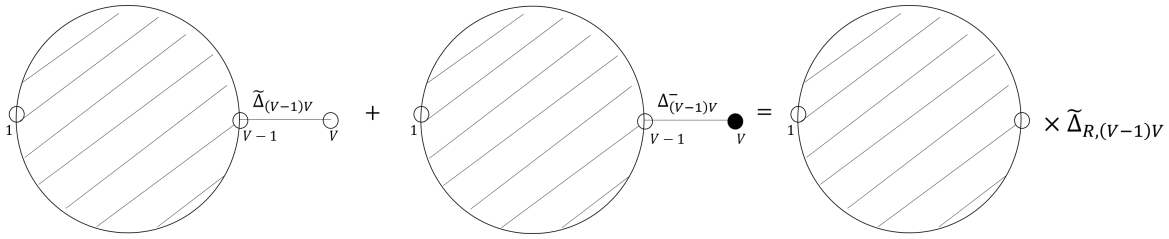
For tree diagrams one has $\mathcal{A}^{(M)} = A$. Consider first the simplest case of lowest order tree-level 2-2 scattering. There are only two vertices connected by an internal propagator. If

vertex x_1 is singled out, one has

$$\sum_1 \mathcal{I}(x_1, x_2) = \tilde{\Delta}_{12} - \Delta^-_{12} = \tilde{\Delta}_{R,12} \tag{6.15}$$

by (6.8). In the local case $\tilde{\Delta}_{R,12} = \Delta_{R,12} = 0$ when x_1 is not in the future light cone of x_2, so BCC is indeed satisfied. But for the nonlocal $\tilde{\Delta}_{R,12}$ one has the decomposition (6.10). When $x_1 \prec x_2$, the causal part Δ_R vanishes but Δ_{ac} does not, which signals violation of causality. Detecting such a violation, however, say, production at x_1 before annihilation at x_2, in any realistic experiment requires $(x_1 - x_2)^2 \gg \ell^2$. This is the situation studied in section 2.13 with the result that $\tilde{\Delta}_{ac}$ is exponentially small. (The same holds for spacelike separation.) The case where $(x_1 - x_2)^2$ is near the light cone, though x_2 still in the future lightcone of x_1, would still be zero in the local theory, but needs to be specially considered in the nonlocal case; this is done in section 6.3 in generality.

We now consider a general tree graph G with N vertices and for convenience, let vertex 1 be the singled out vertex with associated spacetime x_1. Consider a vertex different from 1 and attached to only one internal line. This implies that any other lines attached to it are external legs (truncated external lines). Labeling this vertex V and the vertex at the other end of the internal line by $V-1$, one has the following relation:

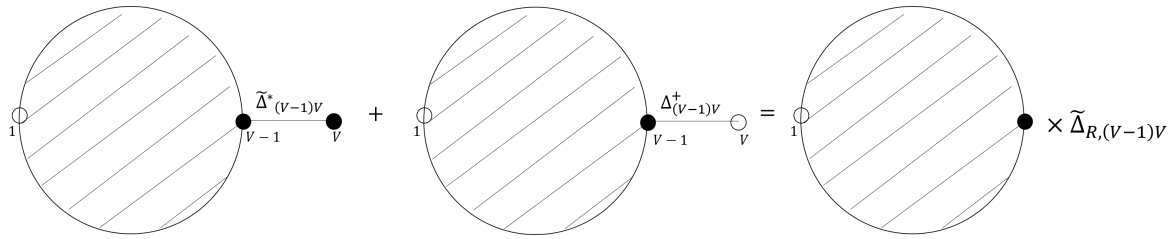


(6.16)

In (6.16) and the subsequent diagrammatically represented equations the following graphical conventions are used. The internal line with the vertex V is explicitly shown. The rest of the tree diagram is represented by the striped circle. External legs are not shown. Summation over all underlinings of all vertices is not explicitly shown (i.e., vertices inside the stripped circle is implied). For the explicitly depicted vertices, i.e., vertices 1, V, and $V-1$ in (6.16), the following convention is used. If the vertex is not underlined, it is shown as an unfilled

circle; if it is underlined it is shown as a filled circle. A vertex explicitly shown as a dot (i.e., neither as a filled nor as an unfilled circle) is summed over underlinings. (6.16) is obtained by a simple application of (6.8). Note that, by the rules above, an underlined (filled circle) vertex gets a factor of (-1) in the Feynman rules associated with these graphical equations, which takes care of minus signs such as in (6.8).

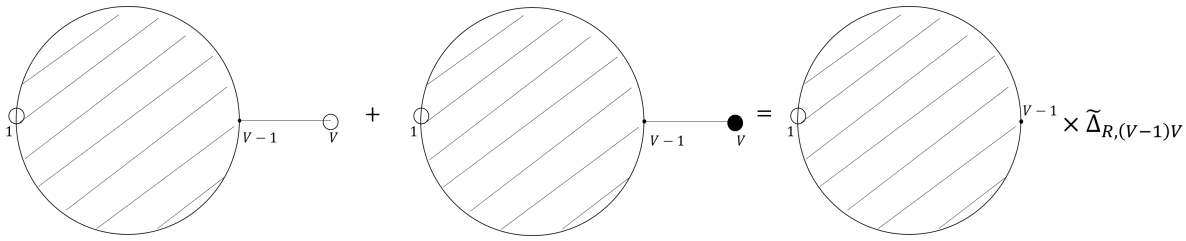
Similarly, one obtains



(6.17)

Summing (6.16) and (6.17) then gives

$$\sum_1 \mathcal{I}_G(x_1,\ldots,x_N) =$$



(6.18)

Thus, summing over the underlinings of V, we have reduced the sum to summing over the underlinings of the remaining $N-2$ vertices (x_1 is always not underlined), while one propagator with one end attached only to external legs has been replaced by $\tilde{\Delta}_{R,(V-1)V}$.[2]

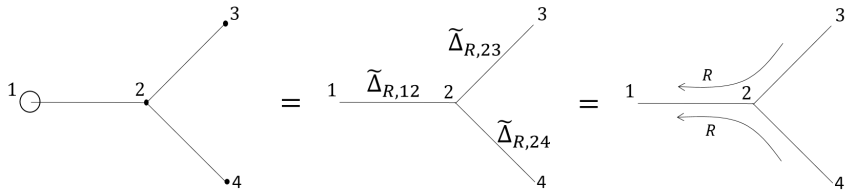
One can now iterate, applying the same argument to the rest of the tree diagram, i.e., the striped circle on the r.h.s. of (6.18), with the leg carrying the propagator replaced by $\tilde{\Delta}_R$ treated as an external leg. In this manner one can recursively reduce the sum to a product

[2]It is easily verified that it is irrelevant whether momentum flow is assigned from V to $V-1$ or vice versa in obtaining (6.18).

involving only $\tilde{\Delta}_R$, and such that for every vertex it contains a chain of $\tilde{\Delta}_R$ that connects that vertex to the vertex x_1:

$$\sum_{1} \mathcal{I}_G(x_1, x_2, \ldots, x_N) = \prod_{\substack{i,j \in G \\ i<j}} \tilde{\Delta}_{R,ij} \ . \tag{6.19}$$

(The vertices are numbered such that if $j > i$, then the distance from vertex j to 1 is no less than the distance from i to 1, where distance means the number of edges connecting the two vertices.) A simple example is given by:



. (6.20)

(In (6.20) the arrows carrying the R label indicate chains of $\tilde{\Delta}_R$ connecting vertices along the course of the arrow by factors of $\tilde{\Delta}_{R,ij}$ in the arrow direction.) The representation (6.19) renders the causality relations transparent.

Choose an arbitrary vertex m with associated position x_m. Let the vertices between 1 and m be labeled $2, 3, ..., m-1$. In the local theory the chain of retarded propagators between x_m and x_1 in (6.19) forces $x_1 \succ x_2 \succ ... \succ x_{m-1} \succ x_m$. When we demand $x_1 \prec x_m$, the r.h.s. of (6.19) vanishes, which is the statement (6.1).

In contrast, in the nonlocal theory $\tilde{\Delta}_R$ has an acausal part. Inserting the decomposition (6.10) in (6.19) the r.h.s. may be expanded in a series of terms, each a product of Δ_R and Δ_{ac} factors, starting with the term with only Δ_R factors (which vanishes when $x_1 \prec x_m$) and ending with the term with only Δ_{ac} factors. One then expects some causality violation and the question is how big it is. This is addressed in section 6.3 below.

If the singled out vertex x_1 is instead kept underlined, the analogous argument now leads to

$$\sum_{\underline{1}} \mathcal{I}_G(\underline{x}_1, x_2, \ldots, , x_N) = - \prod_{\substack{i,j \in G \\ i<j}} \tilde{\Delta}_{R,ij} \ . \tag{6.21}$$

instead of (6.19). In (6.21) the sum is over all underlinings of all vertices except x_1 which is kept underlined. There is an extra minus sign on the r.h.s. because x_1 is always underlined. If one singles out another vertex m with position x_m and demands that $x_1 \prec x_m$, the r.h.s. vanishes in the local case. This corresponds to the alternative form of the BCC (6.2). Again, in the nonlocal case the r.h.s. of (6.21) will be non-vanishing but exponentially suppressed.

If one adds (6.19) and (6.21) one obtains

$$\sum \mathcal{I}_G(z_1, ..., z_V) = 0 \ , \tag{6.22}$$

where now the sum is over all underlinings of all vertices. The important point here is that (6.22) holds equally well in the local as in the nonlocal case. One should note, however, that in the nonlocal case (6.22) *cannot* be obtained from application of the largest time equation. This should be obvious from the fact that the r.h.s. of both (6.19) and (6.21) are non-vanishing. It is only by deriving the representations (6.19), (6.21) in terms of $\tilde{\Delta}_R$ that their sum is found to cancel. (6.22) corresponds to the statement (6.13), which shows that the tree amplitudes satisfy unitarity.

6.3 Causality violation for Tree Amplitudes

In any scattering experiment, particles are created and detected at sources and detectors, and one can measure causality violation with respect to these spacetime points. For each external leg, which represents propagation from a source/detector to the interaction region, there is a factor of propagator multiplying the S-matrix element.

$$G(k) = \left(\prod_i \frac{i\mathcal{F}(k_i^2)}{k_i^2 - m^2 + i\epsilon} \right) \left\langle k_1, k_2, ... | ..., k_{n-1}, k_n \right\rangle \ . \tag{6.23}$$

We then Fourier transform to position space to get the n-point Green's function as a function of the spacetime points of the sources/detectors.

$$G(y_1, y_2, ...y_n) = \int \left(\prod_i \frac{d^4 k_i}{(2\pi)^4} e^{ik_i y_i} \right) G(k) \ . \tag{6.24}$$

Since spacetime points, in particular, locations of created/detected particles can be localized only within somee uncertainty, (6.24) must be integrated over wave packets to get the amplitude:

$$A_{det}(x) = \int \left(\prod_i d^4 y_i f_i(y_i - x_i) \right) G(y) \ , \tag{6.25}$$

where the x_i's are the center of space-time locations of the sources/detectors. The $f_i(x_i)$'s are wave packets centered at zero and, correspondingly, their Fourier transforms are centered at momentum p_i:

$$\begin{aligned} f(y-x) &= \frac{1}{\pi^2 L^4} e^{-\frac{\|y-x\|^2}{L^2}} e^{-ip(y-x)} \\ \hat{f}(q) &= e^{-\frac{\|q-p\|^2 L^2}{4}} e^{iqx} \ . \end{aligned} \tag{6.26}$$

(6.26) are Gaussian wavepackets of characteristic width L. The $\|\cdot\|^2$ denotes Euclidean distance, and so the wave packets are localized in space *and* time.

To measure the amount of causality violation using BCC for tree diagrams, we apply the sum of (6.11) for $G(y)$ of (6.25). Since a tree diagram with untruncated external legs is, of course, still a tree diagram, (6.19) applies, and all the propagators are just replaced by $\tilde{\Delta}_R$. The local part of it, where all propagators are Δ_R, is causal, and the rest is acausal. Thus the detected acausality, with wavpacket, is

$$\mathcal{I}_{ac}(x) = \int \left(\prod_i d^4 y_i f_i(y_i - x_i) \right) \left(\sum_1 G(y) - \text{local part} \right) \ . \tag{6.27}$$

Take the simplest example, where a single propagator connects a source to a detector. The physical question we are asking is, when we vary the coupling constant at the source, can the detector detect the change in amplitude before that. Using the wavepackets (6.26) and the results (6.15) and (6.10), we get that the potential violation is

$$\begin{aligned} \mathcal{I}_{ac}(x) &= \int d^4 y_1 \, d^4 y_2 \, \frac{1}{\pi^4 L^8} e^{-\frac{\|y_1 - x_1\|^2}{L^2} - \frac{\|y_2 - x_2\|^2}{L^2}} e^{-ip(y_1 - x_1) + ip(y_2 - x_2)} \Delta_{ac}(y_2 - y_1) \\ &= \int \frac{d^4 q}{(2\pi)^4} \frac{i(\mathcal{F}(q^2) - 1)}{q^2 - m^2} e^{-\frac{\|q-p\|^2 L^2}{2} - iqx} \ , \end{aligned} \tag{6.28}$$

where $x \equiv x_2 - x_1$. We always assume the nonlocality scale to be of the order of some unification or Planck scale and thus $L \gg \ell$. Note also that, for any two spacetime points x_1

and x_2, one must have $(x_1 - x_2)_\mu > L$ (in the laboratory frame) since, otherwise, one cannot experimentally resolve the two points. We use Laplace's method to find the asymptotic behavior of (6.28) for $L/\ell \gg 1$. The extremum of the exponent is found to be located at $q = \hat{q}$ given by:

$$\hat{q}^0 = \left(p^0 - i\frac{x^0}{L^2}\right) \quad , \qquad \hat{\mathbf{q}} = \left(\mathbf{p} + i\frac{\mathbf{x}}{L^2}\right) \ . \tag{6.29}$$

We thus arrive at:

$$\mathcal{I}_{ac}(x) \sim \frac{1}{(2\pi)^2 L^4} \frac{i(\mathcal{F}(\hat{q}^2) - 1)}{\hat{q}^2 - m^2} \exp\left[-\frac{\|x\|^2}{2L^2} - ipx\right] \ . \tag{6.30}$$

The magnitude of the detected violation is

$$|\mathcal{I}_{ac}|^2 \sim \frac{1}{(2\pi)^4 L^8} \left|\frac{(\mathcal{F}(\hat{q}^2) - 1)}{\hat{q}^2 - m^2}\right|^2 \exp\left[-\frac{\|x\|^2}{L^2}\right] \ . \tag{6.31}$$

In the frame of any experiment at momenta scales much lower than $1/\ell$, one has $p_\mu \ell \ll 1$ and $\ell/L \ll 1$. Then there are two dimensionless quantities at work here: $x^2\ell^2/L^4$ and $\|x\|^2/L^2$. Suppose $x^2\ell^2/L^4$ is small, then $|\hat{q}^2\ell^2|$ is small, and $\mathcal{F}(\hat{q}^2) - 1$ is some polynomial in ℓ. E.g., with $\mathcal{F}(p^2) = e^{m^4\ell^4 - p^4\ell^4}$ as the nonlocal kernel, $\mathcal{F}(\hat{q}^2) - 1 \sim (m^4 - \rho^4)\ell^4$ and the magnitude of detected violation would be

$$|\mathcal{I}_{ac}|^2 \sim \frac{1}{(2\pi)^4} \left|\hat{q}^2 + m^2\right|^2 \frac{\ell^8}{L^8} e^{-\frac{\|x\|^2}{L^2}} \ . \tag{6.32}$$

This goes at least as $(\ell/L)^8$. If furthermore $\|x\|/L \gg 1$ but not to the extent that $x^2\ell^2/L^4$ is large, which in fact would be the case in almost any realistic experiment, then (6.31) shows that the violation is exponentially suppressed. Finally, if $x^2\ell^2/L^4 \sim 1$ or larger, then $\mathcal{F}(\hat{q}^2) - 1 \sim 1$; but since $\|x\|^2 \geq x^2$ and $\|x\|/L \geq L/\ell$, (6.31) is exponentially suppressed in at least L^2/ℓ^2.

In obtaining (6.31), we have not made any assumption on $|x^2|$. Even when x^2 is close to null (within order ℓ^2), the causality violation is still suppressed at least in powers of ℓ/L. Without the wave packet, the causality violation would have blown up as $x^2 \to 0$. When $|x^2|$ is large, (6.31) still holds as a bound on the causality violation, though the bound could be improved by replacing the Δ_{ac} of (6.28) with its asymptotic, e.g. (5.13) for the $e^{-p^4\ell^4}$ kernel.

Since Δ_{ac} decays faster than any power of ℓ^2/x^2, after integrating over the wave packet, the detected acausality also decays faster than any power of ℓ^2/x^2.

We now turn to causality violation for general tree diagram. The $\sum G(y)$ of (6.27) is a product of $\tilde{\Delta}_R$'s as shown in (6.19). After subtracting out the local (which is causal) part, there is a sum of terms, each a product of Δ_{ac}'s and Δ_R's. Let some connected chain of vertices be labeled $x_1, x_2, ..., x_m$, and suppose one wants to detect acausality with respect to x_1 and x_m, i.e. the non-vanishing of (6.19) when $x_1 \prec x_m$. When $x_m - x_1$ is time-like, first consider the terms that contain only products of Δ_R except for one factor of Δ_{ac}. The Δ_R's must obey $x_1 \succ x_2 \succ ... \succ x_m$, and only the factor of Δ_{ac} factor can break this pattern, say between x_i and x_{i+1}, to allow for non-vanishing (6.19). But this means the argument $(x_i - x_{i+1})^2$ of Δ_{ac} must be greater than $(x_m - x_1)^2$. (Fig. 6.1(a)). Thus if $(x_1 - x_m)^2 \gg \ell^2$, the causality violation would be exponentially suppressed since Δ_{ac} is, as discussed in detail in section 2.13 and 5.1 above. For terms with more factors of Δ_{ac}, basically the factors of Δ_R can only connect x_1 and x_m to points of even larger separation, which are then connected by factors of Δ_{ac}. (Fig. 6.1(b)). If the arguments of Δ_{ac} are not close to light-like (within ℓ^2), one can approximate them by their asymptotic, which is exponentially decaying, and integrating over the wave packets doesn't change their exponentially decaying behavior.

There are, however, extreme cases where the x's are carefully arranged such that all Δ_{ac}'s have light-like arguments. For example, $m = 3$ and both propagators are the acausal part, and while $x_3 - x_1$ is time-like, both $x_2 - x_1$ and $x_3 - x_2$ are light-like. (Fig. 6.1)(c)). One would expect the order of the detected acausality to be roughly the square of that of a single propagator, i.e. (6.31). Another example is $m - 3$, $x_3 - x_1$ is space-like, and there is one factor of Δ_R and one factor of Δ_{ac}. The Δ_R connects x_1 to some x_2 in the past of x_2 but such that $x_3 - x_2$ is light-like. (Fig. 6.1)(d)). Then one would expect the acausality to be of the same order as (6.31). We shall emphasize that while in principal one can conceive experiments where all of the Δ_{ac}'s have close to light-like arguments, this has to be very fine-tuned since as soon as any separation $|(x_i - x_{i+1})^2| \gg \ell^2$, the probability of detection is exponential suppressed in $(x_i - x_{i+1})^2/\ell^2$. Nevertheless, we will show that even when such

fine-tuning can be achieved, the acausality will be at most some power of ℓ/L. We will first consider the graph where all factors are Δ_{ac}'s, and then consider the graph where there is a mix of Δ_{ac}'s and Δ_R's. We will apply the result of the former case to the latter by treating the sub-diagram of just Δ_{ac}'s and showing that the Δ_R's do not enhance the acausality.

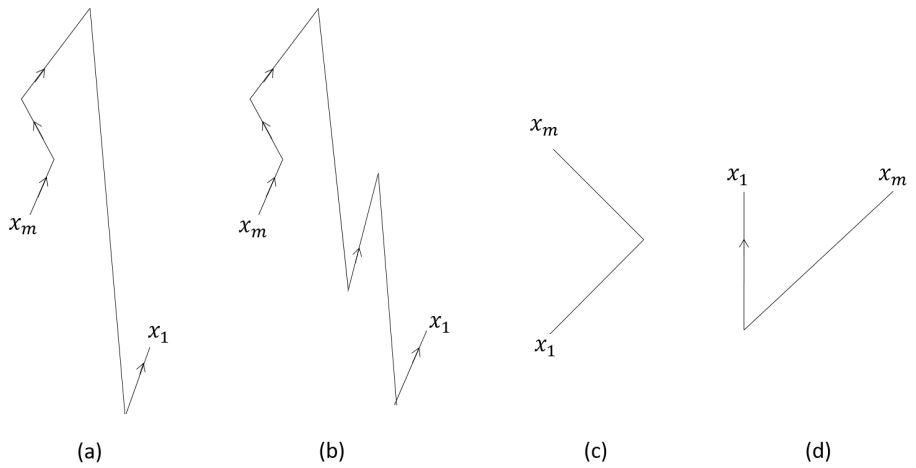


Figure 6.1: Propagation by a chain of Δ_R (arrowed segments) and Δ_{ac} (non-arrowed segments). (a) - (b): acausal propagation due to one or more Δ_{ac} segments; (c) - (d): carefully arranged space-time such that all Δ_{ac} have (nearly) null-like arguments connecting points with $|(x_1 - x_m)^2| \gg \ell^2$.

Let N be the number of vertices of the tree and n the number of vertices located at the sources/detectors with spacetime positions $x_1, x_2, ...x_n$, and each with its associated wave packets. The remaining $N - n$ vertices are internal ones that are to be integrated over. The contribution to (6.27) from the term where all propagators are the acausal part is

$$\mathcal{I}_{ac}^{(N-1)} = \int \left(\prod_{a=1}^{N} d^4 y_a \right) \left(\prod_{a=1}^{n} f_a(y_a - x_a) \right) \left(\prod_{i}^{N-1} \Delta_{ac}(y) \right) \ . \tag{6.33}$$

The superscript $(N-1)$ denotes that there are $N-1$ factors of Δ_{ac}. Suppose the wave packets are Gaussian with size $L_1, L_2, ..., L_n$. For the sake of calculation, for each internal vertex, we also include a Gaussian factor, with sizes $L_{n+1}, ..., L_N$, which will be taken to infinity later. The centers of these auxiliary Gaussians are denoted $x_{n+1}, ..., x_N$, but they

are just a handle and have no physical meaning. Let the momentum of each wave packet be p_a, which represents the total external momentum flowing into each vertex and $\sum p_a = 0$ by overall momentum conservation. The auxiliary wave packets have $p_a = 0$. A Feynman graph is entirely described by its incident matrix ϵ_{ia}, as defined in (3.3). (6.33) is then

$$\mathcal{I}_{ac}^{(N-1)} = \int \prod_{a=1}^{N} d^4 y_a \prod_{i=1}^{N-1} \Delta_{ac}(\epsilon_{ia} y_a) \prod_{a=1}^{n} \frac{1}{\pi^2 L_a^4} e^{-\frac{\|y_a - x_a\|^2}{L_a^2} - i p_a (y_a - x_a)} \prod_{a=n+1}^{N} e^{-\frac{\|y_a - x_a\|^2}{L_a^2}} . \tag{6.34}$$

We rewrite the Δ_{ac} as Fourier integrals and integrate over y_j's to get

$$\mathcal{I}_{ac}^{(N-1)} = \int \prod_{i=1}^{N-1} \frac{d^4 q_i}{(2\pi)^4} \frac{i(\mathcal{F}(q_i^2) - 1)}{q_i^2 - m^2} \prod_{a=1}^{N} e^{\frac{-\left\|\epsilon_{aj} q_j + p_a\right\|^2 L_a^2}{4} - i \epsilon_{aj} q_j x_a} \prod_{a=n+1}^{N} \pi^2 L_a^4 . \tag{6.35}$$

Defining the matrix

$$[d_G]_{ij} \equiv \sum_{a=1}^{N} \epsilon_{ia} L_a^2 \epsilon_{aj} , \text{[3]} \tag{6.36}$$

we follow Laplace's method by taking L/ℓ large. The extremum of the exponent is located at

$$\hat{q}_i = -\sum_a \left[d_G^{-1}\right]_{ij} \epsilon_{ja} \left(L_a^2 p_a + 2 i \eta x_a \right) , \tag{6.37}$$

where η is the Minkowski metric and the spacetime index is suppressed. Thus we find the asymptotic

$$\begin{aligned} \mathcal{I}_{ac}^{(0)} \sim \frac{1}{\pi^{2N-2} \left(\det d_G\right)^2} \left(\prod_{a=n+1}^{N} \pi^2 L_a^4 \right) \left(\prod_i \frac{i(\mathcal{F}(\hat{q}_i^2) - 1)}{\hat{q}_i^2 - m^2} \right) \\ \times \exp\left[\frac{1}{4} \hat{q}_i^0 [d_G]_{ij} \hat{q}_j^0 + \frac{1}{4} \hat{\mathbf{q}}_i [d_G]_{ij} \hat{\mathbf{q}}_j - \sum_a \frac{1}{4} \|p_a\|^2 L_a^2 \right] \end{aligned} . \tag{6.38}$$

We then let L_a go to infinity for $a = n+1, ..., N$. (The factors of infinite L_a's in $\det d_G$ will cancel the factors of L_a in the numerator). For a general tree graph, there is a graphical rule for the result, which is

$$\mathcal{I}_{ac}^{(0)} \sim \frac{1}{\pi^{2n-2} \left(\prod_a^n L_a^2\right)^2 \mathscr{P}^2} \left(\prod_i \frac{i(\mathcal{F}(\hat{q}_i^2) - 1)}{\hat{q}_i^2 - m^2} \right) e^{-\mathscr{Q} + i p_a x_a} , \tag{6.39}$$

[3] This is similar to (3.15) but here we summed over the vertex index instead of the propagator index.

where

$$\mathscr{P} = \left(\sum_{a=1}^{n} \frac{1}{L_a^2} \right), \tag{6.40}$$

$$\mathscr{Q} = \frac{1}{\mathscr{P}} \sum_{a<b}^{n} \frac{\|x_a - x_b\|^2}{L_a^2 L_b^2}, \tag{6.41}$$

For $\hat{q}_i$, the graphical rule is, if removing edge i separates the graph into two trees $\mathscr{T}_1$ and $\mathscr{T}_2$ and edge i points from $\mathscr{T}_1$ to $\mathscr{T}_2$, then

$$\hat{q}_i = \sum_{a \in \mathscr{T}_1} p_a + \frac{2i}{\mathscr{P}} \eta \sum_{\substack{a \in \mathscr{T}_1,\, b \in \mathscr{T}_2 \\ a,b \leq n}} \frac{x_a - x_b}{L_a^2 L_b^2} \,. \tag{6.42}$$

The detected violation of causality is suppressed because if all $\hat{q}_i^2 \ell^2 \ll 1$, then each factor of $\mathcal{F}(\hat{q}_i^2) - 1$ contributes some power of ℓ/L, thus the violation is at least polynomially suppressed in ℓ/L, with higher order diagrams having higher order polynomial suppression. If some $\hat{q}_i^2 \ell^2$ is not much less than 1, then it must be that some linear combination of $(x_a - x_b)/L$ is comparable to L/ℓ, which is large by assumption. Then the exponent (6.41) must be large and (6.39) is exponentially suppressed. Again, we've used no reference of the spacetime separations of the x's and so this derivation shows the suppression of acausality even where there are null separations.

We then turn to terms that have a mix of Δ_R's and Δ_{ac}'s in (6.27). The graph can be split up into two parts G_1 and G_2 where G_1 consists of the Δ_{ac} and G_2 consists of the Δ_R's. We will apply the result (6.39) to G_1 and then show that performing the integrals of G_2 will not change the suppression of the acausality. Let $G = (E, V)$ be the overall graph where E is the set of edges and V is the set of vertices. It's split into $G_1 = (E_1, V_1)$ and $G_2 = (E_2, V_2)$ as described above and while $E_1 \cap E_2 = 0$, $V_1 \cap V_2 \equiv V_s$ is nonempty and is the set of vertices connecting the two graphs. Let G_1, G_2 be described by their respective incident matrices ϵ^1, ϵ^2, let V_E be the set of vertices with external legs, and let V_I be the set of internal vertices, which are to be integrated over. We will apply the same trick in giving auxiliary Gaussians to the V_I vertices and then taking their size to infinity. Suppose $|E_1| = m$, i.e. there are m

factors of acausal parts. The contribution to acausality for this mixed term is

$$\begin{aligned}\mathcal{I}_{ac}^{(m)} &= \int \prod_{a\in V} d^4y_a \prod_{i\in E_1} \Delta_{ac}(\epsilon^1_{ia}y_a) \prod_{j\in E_2} \Delta_R(\epsilon^2_{jb}y_b) \\ &\qquad \prod_{a\in V_E} \frac{1}{\pi^2 L_a^4} e^{-\frac{\|y_a-x_a\|^2}{L_a^2} - ip_a(y_a-x_a)} \prod_{a=V_I}^{N} e^{-\frac{\|y_a-x_a\|^2}{L_a^2}} \\ &= \int \prod_{i\in E_1} \frac{d^4q_i}{(2\pi)^4}\, i\frac{\mathcal{F}(q_i)-1}{q_i^2-m^2} \prod_{j\in E_2} \frac{d^4k_j}{(2\pi)^4}\, \frac{i}{k_j^2-m^2+i\epsilon k_j^0} \\ &\qquad \prod_{a\in V} \exp\left[-\frac{\left\|\epsilon^1_{ai}q_i+\epsilon^2_{aj}k_j+p_a\right\|^2 L_a^2}{4} - i(\epsilon^1_{ai}q_i+\epsilon^2_{aj}k_j)x_a \right] \prod_{a\in V_I} \pi^2 L_a^4 \,.\end{aligned} \tag{6.43}$$

We then find the asymptotic for the q integrals as $L/\ell \to \infty$. We split $\epsilon^2 = \epsilon' + \epsilon''$ where ϵ' have the information for the vertices only in $V_2\backslash V_s$ while ϵ'' have the information for how edges in E_2 connect to vertices in V_s. Thus $\epsilon''_{aj}k_j + p_a$ acts like the set of external momentum for G_1 and we can apply the asymptotic (6.39). Let $V_{1E} = V_1 \cap V_E$ with cardinality n and let $V_{1I} = V_1 \cap V_I$. We get

$$\begin{aligned}\mathcal{I}_{ac}^{(m)} \sim \int \prod_{j\in E_2} \frac{d^4k_j}{(2\pi)^4}\, \frac{i}{k_j^2-m^2+i\epsilon k_j^0} \prod_{a\in V\backslash V_1} \exp\left[-\frac{\left\|\epsilon'_{aj}k_j+p_a\right\|^2 L_a^2}{4} - i\epsilon'_{aj}k_j x_a \right] \prod_{a\in V_I\backslash V_{1I}} \pi^2 L_a^4 \\ \frac{1}{\pi^{2n-2}\left(\prod_{a\in V_{1E}} L_a^2\right)^2 \mathscr{P}_1^2} \left(\prod_{i\in E_1} i\frac{(\mathcal{F}(\hat{q}_i^2)-1)}{\hat{q}_i^2-m^2} \right) e^{-\mathscr{Q}_1 + i\sum_{a\in V_{1E}} p_a x_a} \,.\end{aligned} \tag{6.44}$$

$\mathscr{P}_1$ and $\mathscr{Q}$ are as defined in (6.40) and (6.41) but restricted to G_1. $\hat{q}_i$ is slightly modified to become

$$\hat{q}_i = \left(\sum_{a\in\mathscr{T}_1} p_a + k_j\epsilon''_{ja} \right) + \frac{2i}{\mathscr{P}}\eta \sum_{\substack{a\in\mathscr{T}_1,\, b\in\mathscr{T}_2 \\ a,b\in V_{1E}}} \frac{x_a - x_b}{L_a^2 L_b^2} \,. \tag{6.45}$$

Indeed the k_j's of the propagators of G_2 that are immediately connected to G_1 act as the external momentum for G_1. For the above rule, we'd like to point out a special case when a particular vertex a connects G_1 and G_2 and is connected to only a particular edge i of

G_1. If furthermore, vertex a is to be integrated over, that means its L_a and x_a should have no meaning. Since either the set $\mathscr{T}_1$ or $\mathscr{T}_2$ has no intersection with V_{1E}, the second sum of (6.45) is simply 0. $\hat{q}_i$ is then just the sum of external momentum and momentum from G_2 that flows into edge i. This is expected because an internal vertex just means that there is momentum conservation at that vertex.

(6.44) is at least polynomially suppressed. In most realistic experiment, $(\mathcal{F}-1)/(q^2-m^2)$ is polynomial in ℓ/L, given the size of p, x, and k. As before, if the x's are large such that the second term of (6.45) is large and so that $\mathcal{F}-1 \sim \mathcal{O}(1)$, then $e^{-\mathscr{Q}}$ is exponentially suppressed, which is a stronger suppression. If k is large such that $\mathcal{F}-1 \sim \mathcal{O}(1)$, then $k \sim 1/\ell$ but the exponent in the first line of (6.44) shows that there would be exponential suppression. To conclude, the acausality of G is at most that of G_1, and the retard propagators of G_2 will not enhance the order of the asymptotic behavior of the acausality.

In conclusion, for a general tree diagram, each term that contributes to acausality will have at least one factor of the acausal part of the effective propagator. Even when the space-time are fine-tuned such that the acausal parts have arguments that are light-like, the acausality will be at most some power of ℓ/L.

In [44], it was shown that one could infer the spacetime location of interactions provided that each interaction vertex is connected to two or more external legs. Basically, given the spacetime and momentum (with uncertainties) of two particles (or more) at the sources/detectors, the inferred interaction spacetime is where the two classical trajectories collide. It was shown in [44] that effectively, the detected amplitude is the same form as (6.25) but with the understanding that $G(y)$ is now the truncated n-point amplitude and the f_i's are effective wavepackets centered around the inferred interaction points. Then the same calculation for causality violation using BCC follows and one arrives at (6.39), with the x's now being the inferred interaction spacetime. The causality violation with respect to these interaction points is expected to be more prominent than when looking at the causality violation with respect to the spacetime points of the sources/detectors. Specifically, the exponent (6.41) may be $\mathcal{O}(1)$ because the separation of the interaction points are not necessarily much

larger than L. Still, the violation is at most polynomial in ℓ/L, and exponentially suppressed once $\|x\|^2/L^2$ become large.

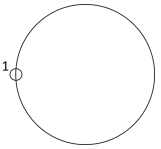
6.4 Loop amplitudes

As discussed in section 2.2, in theories with nonlocal vertices, Wick rotations of integration contours are no longer possible, and, hence, at loop level the relation (2.22) holds: amplitudes $A^{(M)}(p)$ do not coincide with $A(p)$. As we find in the following, a major implication of this is that the amplitudes $A^{(M)}(p)$ are actually not unitary, as first argued in [19]. This shows that the amplitudes A, obtained by continuation of the Euclidean amplitudes and known to be unitary, do indeed provide the correct definition of the theory in Minkowski space as discussed in [10], [1], [19]. We will proceed as before by Fourier transforming $A^{(M)}(p)$ to position space by (6.3) and extend the tree level results of section 6.2, first to one loop and then to multi-loop graphs. These will allow us to estimate the small causality violations and then discuss the relation between the Euclidean- and Minkowski-defined theories.

6.4.1 One Loop Amplitudes

Consider a 1-loop graph with N vertices. We consider again the sum over all underlinings of the integrand $\mathcal{I}$ (cf. 6.3)) of the Minkowski-defined amplitude, with vertex 1 being the singled out vertex which is kept not underlined. This is represented diagrammatically as:

$$\sum_1 \mathcal{I}(x_1, x_2, ...x_N) = \quad .$$ (6.46)



Consistent with our previous conventions, the circle represents the loop with all internal lines (propagators) and all vertices other than 1, as well as all external legs, not explicitly shown. Summation over all underlinings of all vertices on the circle other than 1 is implied. The vertex 1 is explicitly shown and is not underlined as indicated by the unfilled little circle.

To evaluate this sum in terms of retarded propagators we first need the following result. Let T_N be a tree diagram with N vertices consisting of $(N-1)$ internal lines in a linear

chain. Any number of external legs may be attached at each vertex. Consider the sum

$$\sum_{1,N} \mathcal{I}_{T_N} \ ,$$

where the summation is over all underlining of the $(N-2)$ vertices other than vertices 1 and N, which are kept not underlined. For $N=3$, which has just two propagators, we get

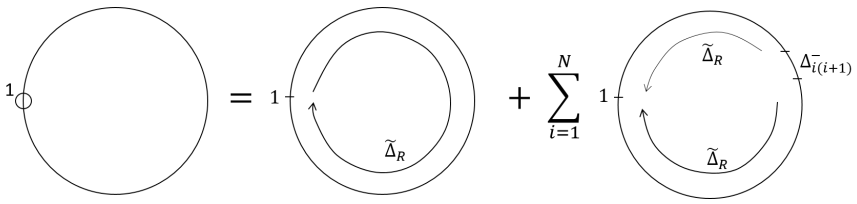
$$\begin{aligned}\sum_{1,3} \mathcal{I}_{T_3} &= \tilde{\Delta}_{32}\tilde{\Delta}_{21} - \Delta^-_{32}\Delta^+_{21} \\ &= \left(\Delta^-_{32} + \tilde{\Delta}_{R,32}\right)\left(\Delta^+_{21} + \tilde{\Delta}_{A,21}\right) - \Delta^-_{32}\Delta^+_{21} \\ &= \tilde{\Delta}_{R,32}\Delta^+_{21} + \Delta^-_{32}\tilde{\Delta}_{A,21} + \tilde{\Delta}_{R,32}\tilde{\Delta}_{A,21} \\ &= \tilde{\Delta}_{R,32}\tilde{\Delta}_{R,21} + \tilde{\Delta}_{R,32}\Delta^-_{21} + \Delta^-_{32}\tilde{\Delta}_{A,21} \ , \end{aligned} \tag{6.47}$$

by use of (6.8). The generalization to any N then, obtained by induction, is:

$$\begin{aligned}\sum_{1,N} \mathcal{I}_{T_N} = \quad & \tilde{\Delta}_{R,12}...\tilde{\Delta}_{R,(N-3)(N-2)}\,\tilde{\Delta}_{R,(N-1)N} \\ & + \tilde{\Delta}_{R,12}\ldots\tilde{\Delta}_{R,(N-3)(N-2)}\,\tilde{\Delta}_{R,(N-2)(N-1)}\,\Delta^-_{(N-1)N} \\ & + \tilde{\Delta}_{R,12}\ldots\tilde{\Delta}_{R,(N-3)(N-2)}\,\Delta^-_{(N-3)(N-2)}\,\tilde{\Delta}_{A,(N-1)N} \\ & + \tilde{\Delta}_{R,12}\ldots\tilde{\Delta}_{R,(N-4)(N-3)}\,\Delta^-_{(N-3)(N-2)}\,\tilde{\Delta}_{A,(V-2)(N-1)}\,\tilde{\Delta}_{A,(N-1)N} \\ & + \ldots \\ & + \Delta^-_{12}\,\tilde{\Delta}_{A,23}\ldots\tilde{\Delta}_{A,(N-1)N} \ . \end{aligned} \tag{6.48}$$

We can now apply (6.48) to the sum (6.46) by setting $x_N = x_1$ i.e., identifying the location of the first and last vertices in the chain. (Thus a N-vertex tree graph becomes a $(N-1)$-vertex 1-loop graph). Relabeling N as the number of vertex in the loop and noting that $\tilde{\Delta}_{A,ij} = \tilde{\Delta}_{R,ji}$, we get

$$\sum_{1} \mathcal{I}(x_1, x_2, ...x_N) =$$

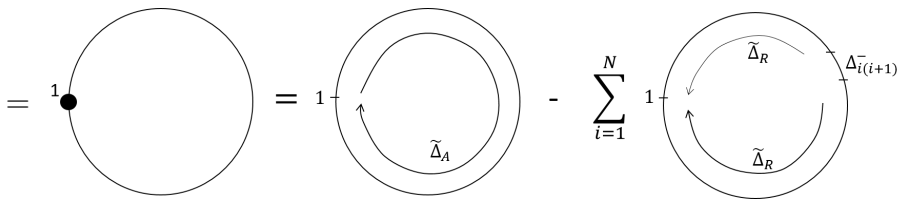


(6.49)

with the cyclic convention $N+1 \equiv 1$. Each term in the above sum has indeed a chain of retarded propagator between vertex 1 and every other vertex.

A similar derivation shows that,

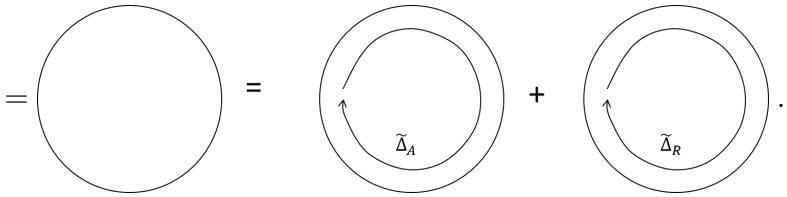
$$\sum_{\underline{1}} \mathcal{I}(\underline{x_1}, x_2, ..., x_N)$$



(6.50)

If we now sum (6.49) and (6.50), i.e., sum over underlinings of vertex 1, we get

$$\sum \mathcal{I}(x_1, x_2, ..., x_N)$$



(6.51)

In the local theory, the r.h.s. of (6.51) would be exactly zero because vertex 1, or any other vertex in the loop, has a loop of retarded (or advanced) propagator back to itself. But for a non-local theory, the acausal part in $\tilde{\Delta}_{A,R}$ contributes, so the r.h.s. is nonzero. This is in contrast to the tree-level result, i.e., (6.22), and signifies that at loop-level the Minkowski-defined theory is non-unitary: multiplying by external wave-functions and integrating over the positions of the vertices in (6.51) except for x_1 and another picked out vertex x_2, one obtains (6.13) but with non-vanishing r.h.s. We show explicitly in the next section that these unitarity-violating terms are absent in the Euclidean-defined theory.

6.4.2 Unitarity of the Euclidean-defined theory

The r.h.s. of (6.51) exhibits the non-unitary contributions in the Minkowski-defined theory. The Euclidea-defined theory, on the other hand, is known to be unitary and we now demon-

strate this explicitly by showing that the difference between the Minkowski- and Euclidean-defined theories is given precisely by the r.h.s. of (6.51). Consider the bubble graph (Fig.

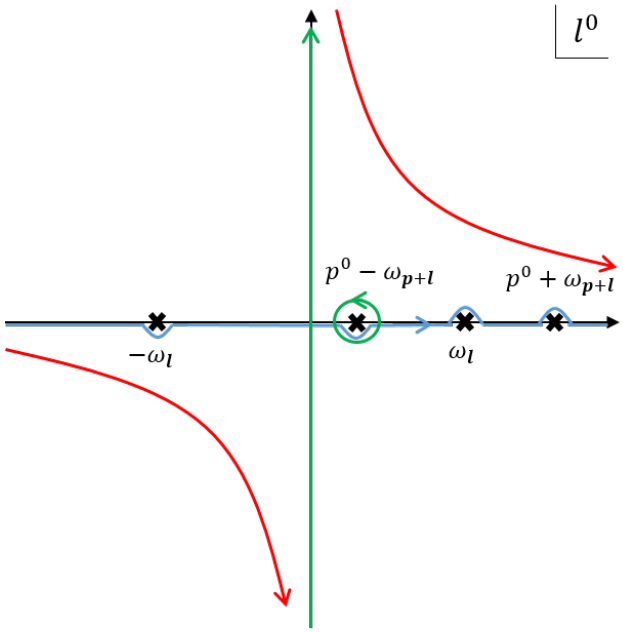


Figure 6.2: Contours for the bubble graph: blue for Minkowski-defined theory; green for Euclidean defined theory. Integration along the red contour gives the difference.

2.1). The generalization to any other one loop diagram is straightforward. The amplitude is given by

$$A(p) = \int_{\mathcal{C}} \frac{d^4 l}{(2\pi)^4} \frac{-\mathcal{F}(l)\mathcal{F}(p-l)}{(l^2 - m_1^2)((p-l)^2 - m_2^2)} \,. \tag{6.52}$$

The choice of the l-contour $\mathcal{C}$ depends on the theory. With real space-like components, the l^0 contour $\mathcal{C}$ for the Euclidean-defined (green) versus the Minkoski-defined (blue) amplitude is shown in Fig. 6.2. As easily seen, the difference between these two contours is given by the the contour shown in red. The graph resulting from having all vertices underlined in the integrand is given by the same integral as (6.52) except the contours are complex conjugated. It then gives the corresponding difference between the Minkowski- and Euclidean-defined amplitudes by the complex conjugate of the red contours in Fig. 6.2. These two are in fact the only contributions to the difference between the Minkowski- and Euclidean defined amplitudes for the quantity appearing on the l.h.s. of (6.13) (the sum of the l.h.s. of

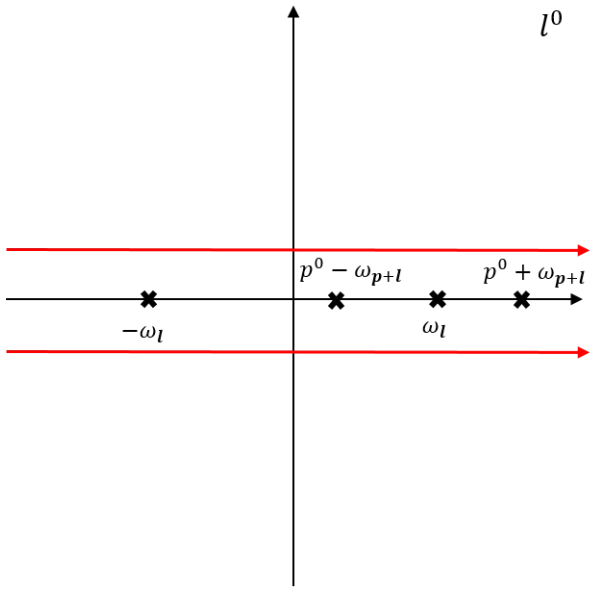


Figure 6.3: Integration along contour (red) giving the difference between Minkowski- and Euclidean-defined amplitude for the l.h.s. of (6.13).

(6.1) and (6.2)). The contributions to the difference from graphs resulting from the other combinations of underlined vertices cancel for these 1-loop graphs.[4] The result of adding these two contributions then is given by integration over the red contour shown in Fig. 6.3. This is precisely the sum of products of only $\tilde{\Delta}_R$ and products of only $\tilde{\Delta}_A$, i.e., the r.h.s. of (6.51).

The extension to a general 1-loop diagram, i.e., one with more than two propagators forming the loop, is straightforward. The difference between the Minkowski- and Euclidean-defined theory for the quantity given by the l.h.s. of (6.13) is again obtained by adding the contour in the first and third quadrant, far away from all poles, analogous to the red contour in Fig. 6.2 to its complex conjugate contour. This sum is again represented by integration along a contour as in Fig. 6.3 but with generally more poles sandwiched between the two branches of the contour. This corresponds precisely to the r.h.s. of (6.51).

[4]This is perhaps more easily seen in the representation [37] of the BCC equation in terms of cut graphs.

6.4.3 Multi-loop Amplitudes

We now consider multi-loop graphs. Note that general multi-loop amplitudes also include IPR graphs consisting of several one-loop graphs connected by trees - a case not covered in the previous section where only a single 1-loop diagram with external trees attached was treated. We will obtain the direct generalization of the results obtained for trees and 1-loop graphs. Specifically, we will prove the following two statements for the integrands of the general multi-loop diagram (6.3) defined directly in Minkowski space:

(i) The sum over all underlinings keeping a singled-out vertex, labeled x_1, not underlined (or underlined) equals a sum of terms, where each term has a chain of $\tilde{\Delta}_R$ from every other vertex to vertex x_1, modulo the possible addition of extra terms, which contain at least one closed loop formed out of $\tilde{\Delta}_R$ propagators.
(ii) The sum over all underlinings of all vertices gives a sum of terms, each of which contains at least one closed loop formed out of the $\tilde{\Delta}_R$ propagators.

The proof of (i) and (ii), which is obtained by induction in the number N of internal lines in a graph, is given in Appendix C.

The same conclusions, therefore, follow as in the previous sections 6.2, 6.4.1 and in the exactly same manner. (i) implies that a causality violation, i.e., a non-vanishing r.h.s. of the BCC equations (6.1) or (6.2). This violation, for separations $(x_1 - x_2)^2 \gg \ell^2$ between any two picked out vertices x_2, x_2, is exponentially suppressed by application of the results in section 5.1. (ii) implies that the nonlocal theory defined directly in Minkowski space has unitarity violations at loop level.

6.5 Difference between Euclidean-defined and Minkowski-defined theory

We've shown that the causality violation of the Minkowski-defined theory, (6.3), is at least polynomially suppressed at all orders in perturbation. We now show that the difference

between Euclidean-defined theory (the correct theory) and the Minkowski-defined theory is suppressed at large spacetime separation, so any causality violation of the correct theory is also suppressed. We first work out the explicit example of the bubble graph of a massive $\mathcal{F} = Ne^{-p^4\ell^4}$ nonlocal theory. Then make some general arguments towards why the difference should be suppressed at all loops.

The Euclidean-defined amplitude of the bubble graph (Fig 2.1) is given in (6.52), and the integration contour is the green curve in Fig. 6.3. Following the steps leading up to (3.11), we get

$$A^{(E)}(s) = \frac{iN^2}{64\pi^3\ell^4}\int_0^\infty d\alpha_1 d\alpha_2 \int_{-\infty}^\infty d\beta_1 d\beta_2 \frac{1}{(\tilde{w}_1+\tilde{w}_2)^2} \exp\left[\frac{\tilde{w}_1\tilde{w}_2}{\tilde{w}_1+\tilde{w}_2}s - \frac{\beta_1^2}{4\ell^4} - \frac{\beta_2^2}{4\ell^4} - (\alpha_1+\alpha_2)m^2\right] , \tag{6.53}$$

where $\tilde{w}_i = \alpha_i + i\beta$, and s is negative. We will defer continuing to positive s to later. On the other hand, the Minkwoski-defined theory also starts with (6.52) but its contour is the blue curve in Fig. (6.3). Again, using generalized (rotated) Schwinger parameter :

$$\frac{i}{p^2-m^2+i\epsilon} = \int_0^\infty d\alpha e^{i\alpha(p^2-m^2+i\epsilon)} , \tag{6.54}$$

we get,

$$A^{(M)}(s) = \frac{iN^2}{16\pi^3\ell^4}\int_0^\infty d\alpha_1 d\alpha_2 \int_{-\infty}^\infty d\beta_1 d\beta_2 \frac{\mathrm{sgn}(w_1+w_2)}{(w_1+w_2)^2} \exp\left[i\frac{w_1w_2}{w_1+w_2}s - \frac{\beta_1^2}{4\ell^4} - \frac{\beta_2^2}{4\ell^4} - i(\alpha_1+\alpha_2)m^2\right] . \tag{6.55}$$

where $w = \alpha + \beta$. This expression is true for all s. To compare the Euclidean-defined and Minkowski-defined theory, we rotate $\alpha \to i\alpha$ through the first quadrant in (6.53), and subtract from (6.55). The rotation is justified because the integrand goes to zero at the infinties of α. The difference is

$$A_{dif}(s<0) = \frac{iN^2}{16\pi^3\ell^4}\int_0^\infty d\alpha_1 d\alpha_2 \int_{-\infty}^\infty d\beta_1 d\beta_2 \frac{1-\mathrm{sgn}(w_1+w_2)}{(w_1+w_2)^2} e^{i\frac{w_1w_2}{w_1+w_2}s} \exp\left[i\frac{w_1w_2}{w_1+w_2}s - \frac{\beta_1^2}{4\ell^4} - \frac{\beta_2^2}{4\ell^4} - i(\alpha_1+\alpha_2)m^2\right] . \tag{6.56}$$

We shift $\beta \to \beta - \alpha$ and integrate over α to get

$$A_{dif}(s) = \frac{i}{16\pi^2} \int_{\beta_1+\beta_2<0} d\beta_1 d\beta_2 \left(1 - \text{Erf}\left(im^2\ell^2 - \frac{\beta_1}{2\ell^2}\right)\right)\left(1 - \text{Erf}\left(im^2\ell^2 - \frac{\beta_2}{2\ell^2}\right)\right) \frac{2}{(\beta_1+\beta_2)^2} \exp\left[i\frac{\beta_1\beta_2}{\beta_1+\beta_2}s - i(\beta_1+\beta_2)m^2\right] . \tag{6.57}$$

Initially, this expression is only defined for $s < 0$, but it can be continued to $s > 0$ through the upper half plane without deforming the contour. When s takes on positive imaginary value, there would be a singularity if the exponent goes to positive infinity. Since $\beta_1 + \beta_2$ is restricted to be negative, as $\beta_1 + \beta_2 \to 0^-$, the numerator $\beta_1\beta_2$ is also negative, making the exponent go to negative infinity, which suppresses the integrand. If both $\beta_1, \beta_2 \to -\infty$, the exponent does go to positive infinity, but the suppression from $1 + \text{Erf}(\frac{\beta}{2\ell^2})$ is more rapid, ensuring that the integrand still go to 0.

We then Fourier transform this into position space to get

$$A_{dif}(x^2) = \frac{1}{8} \int_{\beta_1+\beta_2>0} d\beta_1 d\beta_2 \left(1 - \text{Erf}\left(im^2\ell^2 - \frac{\beta_1}{2\ell^2}\right)\right)\left(1 - \text{Erf}\left(im^2\ell^2 - \frac{\beta_2}{2\ell^2}\right)\right) \frac{\text{sgn}(\beta_1\beta_2)}{\beta_1^2\beta_2^2} \exp\left[-i\left(\frac{1}{\beta_1} + \frac{1}{\beta_2}\right)\frac{x^2}{4} - i(\beta_1+\beta_2)m^2\right] . \tag{6.58}$$

Because of the *sgn* function, we split the integral into three parts, $A_{dif} = A_1 + A_2 + A_3$, corresponding to the integral domains: 1) $\beta_1, \beta_2 < 0$, 2) $\beta_1 < 0$, $\beta_2 > 0$, and 3) $\beta_1 > 0$, $\beta_2 < 0$, respectively. We will find the asymptotic of (6.58) for large time-like x^2 using stationary phase. For all the $A_i's$, the peaks are located at large positive or negative β, so the $1 - Erf$ function can be approximated by its asymptotic.

$$1 - \text{Erf}\left(im^2\ell^2 - \frac{\beta}{2\ell^2}\right) \sim \begin{cases} 2 & \beta \to \infty \\ \frac{1}{\sqrt{\pi}\left(im^2\ell^2 - \beta/2\ell^2\right)} \exp\left[-\frac{\beta^2}{4\ell^4} + i\beta m^2 + m^4\ell^4\right] & \beta \to -\infty \end{cases} \tag{6.59}$$

Following the usual procedure, we find the stationary points of the exponent are located at

$$\hat{\beta}_{1,2} = \left(\frac{ix^2\ell^4}{2}\right)^{1/3} . \tag{6.60}$$

The root in the second quadrant is the one which the integral contour can be deformed and passed through. Performing the method of stationary phase, we get

$$A_{dif} \sim A_1 \sim \frac{-64N^2}{3x^4} \exp\left[-\left(\frac{x^2}{2\ell^2}\right)^{2/3} \left(\frac{3}{4} + i\frac{\sqrt{3}}{4}\right)\right] . \tag{6.61}$$

For A_2 and A_3, the peaks are located outside the integration domain. Thus the leading contribution to the asymptotic of A_{dif} is that of A_1 only, and indeed this difference is exponentially suppressed for large x^2/ℓ^2.

In general, $A_{dif}(s)$ for a general graph cannot be written down in integral forms with simple contours like (6.57) after continuing s through the upper half plane. We will argue why the difference should decay rapidly for large spacetime separation for all graphs. For one loop, we've showned that $A_{dif}(p)$ is

$$A_{dif}(p) = \int \frac{d^4k}{(2\pi)^4} \prod_i \frac{i\mathcal{F}(q_i)}{q_i^2 - m^2} , \tag{6.62}$$

where the q_i's are appropriate sums of the external momentum and the loop momentum. The contour of k^0 is two arcs at infinity in the first and third quadrant, like the red curve in Fig. 6.2. Both arcs are far away from the poles in the k^0 plane. We will apply Proposition 1 to argue that the Fourier Transform of $A_{dif}(p)$ is suppressed for large x^2. To be precise, previously, p is shorthand for the set of total external momentum flowing into each vertex, and s the set of external invariants. Now we pick out two vertices, the spacetime of which will be used to check acausality. We Fourier transform only the total external momentum flowing into the first vertex, and by momentum conservation, that momentum goes through the second vertex too. Below we will refer to p as that particular momentum, and $s = p^2$.

When s approach 0 from left or right, that corresponds to, for example, $\mathbf{p} = 0$ and p^0 approaching 0 from the imaginary direction and from the real direction. Clearly, $A_{dif}(s)$ will be the same as $s \to 0^{\pm}$. And since the poles will not pinch the contour no matter how p changes (i.e. two poles approaching the same point from different sides of the contour), $A_{dif}(s)$ is analytic in s. Finally, due to the nonlocal factor, both the Euclidean-defined and Minkowski-defined amplitude decrease exponentially in $|s|$ for $s \to \pm\infty$, and so must $A_{dif}(s)$.

Thus the requirements for Proposition 1 are satisfied and the Fourier Transform of $A_{dif}(s)$ into position space shows that $A_{dif}(x_2 - x_1)$ decays faster than any power of $\frac{1}{(x_2-x_1)^2}$. Since the propagator masses are not needed in the above argument, it must be that the decay is faster than any power of $\frac{\ell^2}{(x_2-x_1)^2}$.

When discussing causality violation, for the sum (6.11) for one loop diagrams, only the loop diagram differs for Euclidean- and Minkowski- defined theory. The cut diagrams are the same since they are just tree diagrams integrated over physical intermediate states. The Minkowski-defined theory has suppressed acausality and since $A_{dif}(x)$ is also suppressed, the acauslity for the Euclidean-defined theory is also suppressed. For higher loops, we speculate that the same argument applies.

APPENDIX A

Non-vanishing of the Symanzik polynomial for the nonlocal theory

In this Appendix we prove (3.22). To this end we use the following known fact. Let A be an $n \times n$ complex matrix, and $H(A) \equiv \frac{1}{2}(A + A^\dagger)$. Then if $H(A)$ is a positive definite matrix, the following inequality holds:

$$\det H(A) \leq |\det A| \,. \tag{A.1}$$

Equality holds iff $A = H(A)$, i.e., A is hermitian. To prove (A.1) write $A = H(A) + S(A)$, where $S(A) = \frac{1}{2}(A - A^\dagger)$. Now, the asserted inequality (A.1) is the statement:

$$1 \leq |\det[H(A)^{-1}A]| = |\det[I + H(A)^{-1}S(A)]| \,. \tag{A.2}$$

But

$$H(A)^{-1}S(A) = H(A)^{-1/2}\big[H(A)^{-1/2}S(A)H(A)^{-1/2}\big]H(A)^{1/2} \,,$$

i.e., $H(A)^{-1}S(A)$ is related by a similarity transformation to the matrix $[H(A)^{-1/2}S(A)H(A)^{-1/2}]$, which is anti-hermitian. Hence, it has purely imaginary eigenvalues $i\lambda_i$. But then, since for any real number λ one has $|(1 + i\lambda)| = (1 + \lambda^2)^{1/2} \geq 1$,

$$|\det[I + H(A)^{-1}S(A)]| = \prod_{i=1}^{n} |(1 + i\lambda_i)| \geq 1 \,, \tag{A.3}$$

which proves (A.1). Note that equality obtains if all $\lambda_i = 0$, i.e., $S(A) = 0$.

We apply (A.1) to the matrix $d(w)$ given by (3.15). One has

$$H(d(w))_{rs} = \sum_{i=1}^{I} \varepsilon^{(V)}_{ri}\gamma_i(\varepsilon^{(V)})^T_{is} \,, \tag{A.4}$$

where, with $\bar{\ell} > 0$,

$$\gamma_i = \frac{\alpha_i + \bar{\ell}^2}{[(\alpha_i + \bar{\ell}^2)^2 + \ell_2^4 \beta_i^2]} > 0 \tag{A.5}$$

for all $\alpha \geq 0$, $-\infty < \beta_i < \infty$. $H(d(w))$ is manifestly positive definite, since

$$z^\dagger \cdot H(d(w)) \cdot z = \sum_{i=1}^{I} \gamma_i \Big| \sum_{s=1}^{V-1} \varepsilon_{si}^{(V)} z_s \Big|^2 > 0 \tag{A.6}$$

for any vector $z \in \mathbb{C}^{(V-1)}$. Applying (A.1) then:

$$|\det d(w)| > 0\,. \tag{A.7}$$

It follows that

$$|\Delta(w)| = |\det d(w)| \prod_{i=1}^{I} |w_i| > 0\,, \tag{A.8}$$

since $|w_i| = \big((\alpha_i + \bar{\ell}^2)^2 + \ell_2^4 \beta_i^2\big)^{1/2} > 0$, all i.

In the local case, where $\ell_1 = \ell_2 = 0$, (A.8) fails at $\alpha_i = 0$. This is the source of UV divergences. The introduction of nonlocality then through either or both $\ell_i \neq 0$ regulates all UV divergences as remarked in the main text.

APPENDIX B

Equivalence of the Landau equations for the amplitudes in different forms

We next show the equivalence of the Landau equations (3.34) - (3.35) to their parametric form (3.53) - (3.54). Let C_i, $i = 1, \cdots, L$, be a set of independent loops in the Feynman diagram G. The internal momenta q_j may, if need be by a relabeling, be taken to be: $q_j = l_j$, for $j = 1, \cdots, L$, whereas each q_j for $j = L+1, \cdots, I$ is a linear combination of the loop momenta l_i and the external momenta P_r such that the momentum conservation system (2.14), (3.4) is satisfied.

Introduce the vector I-component K by

$$K_j = l_j\,, \quad j = 1, \cdots, L\,; \qquad K_{L+r} = P_r\,, \quad r = 1, \cdots, (V-1)\,. \tag{B.1}$$

One can then write

$$q = RK\,, \quad \text{or} \quad K = R^{-1}q\,, \tag{B.2}$$

where the $(I \times I)$ matrix R^{-1} is given by

$$\begin{aligned} R^{-1}_{ij} =& \delta_{ij}\,, \qquad i = 1, \cdots, L; \quad j = 1, \cdots, I\,, \\ R^{-1}_{(L+r)j} =& \varepsilon_{rj}\,, \qquad r = 1, \cdots, (V-1); \quad j = 1, \cdots, I\,, \end{aligned} \tag{B.3}$$

i.e., it has the structure

$$R^{-1} = \begin{pmatrix} \mathbf{1}_L & \vdots & \mathbf{0} \\ \cdots\cdots & & \\ \varepsilon^{(V)} & & \end{pmatrix}. \tag{B.4}$$

Here, $\varepsilon^{(V)}$ denotes the incidence matrix with the V-th row deleted. Then, defining the quadratic form

$$\mathcal{Q}(l,P) \equiv \sum_{i=1}^{I} \alpha_i q_i^2 \,, \tag{B.5}$$

and introducing the $I \times I$ matrix A:

$$A_{ij} = \alpha_i \, \delta_{ij} \,. \tag{B.6}$$

one has

$$\mathcal{Q}(l,P) = K^T R^T A R K \,. \tag{B.7}$$

Now, given a quadratic form $\mathcal{Q}(z) = z^T M z$, where M is an invertible matrix, the conjugate, or inverse, quadratic form is defined to be $\tilde{\mathcal{Q}}(z) = z^T M^{-1} z$. If $z = (y, x)$, given the quadratic form $\mathcal{Q}(z) = \mathcal{Q}(y, x)$ and its inverse $\tilde{\mathcal{Q}}(y, x)$, define $\mathcal{Q}(x) \equiv \mathrm{extr}_y \, \mathcal{Q}(y, x)$.

The following fact then holds [45]: If $\tilde{\mathcal{Q}}(x)$ denotes the inverse of $\mathcal{Q}(x)$, one has

$$\tilde{\mathcal{Q}}(x) = \tilde{\mathcal{Q}}(0, x) \,. \tag{B.8}$$

Hence, $\mathcal{Q}(x)$ is given by the inverse of $\tilde{\mathcal{Q}}(0, x)$.

Now, from (B.7) and using (B.3), (B.4), a simple computation gives

$$\begin{aligned} \tilde{\mathcal{Q}}(l,P) &= K^T R^{-1} A^{-1} (R^T)^{-1} K \\ &= \sum_{i=1}^{L} \frac{1}{\alpha_i} \Big(l_i + \sum_{r=1}^{V-1} \varepsilon_{ri} P_r \Big)^2 + \sum_{i=L+1}^{I} \frac{1}{\alpha_i} \Big(\sum_{r=1}^{V-1} \varepsilon_{ri} P_r \Big)^2 . \end{aligned} \tag{B.9}$$

Hence,

$$\begin{aligned} \tilde{\mathcal{Q}}(0,P) &= \sum_{i=1}^{I} \frac{1}{\alpha_i} \Big(\sum_{r=1}^{V-1} \varepsilon_{ri} P_r \Big)^2 \\ &= P d(\alpha) P \,. \end{aligned} \tag{B.10}$$

Thus,

$$\mathcal{Q}(P) = P d^{-1}(\alpha) P \,, \tag{B.11}$$

i.e., the extremum of (B.5) over the loop momenta equals the quadratic form $Q(\alpha; P)$ in (3.40). Recalling the definition (3.2) of $\psi(\alpha, l, P)$ then, it immediately follows that equations (3.53) - (3.54) are equivalent to (3.34) - (3.35).

APPENDIX C

Leading asymptotic behavior of the effective propagator

Recall that the stationary phase method gives the leading behavior of an integral $I(\lambda)$ as:

$$I(\lambda) = \int_{\mathcal{D}} d^n x\, g(x) e^{i\lambda\phi(x)} \sim \sqrt{\frac{(2\pi)^n}{\lambda^n |\det \phi_{ij}(x_0)|}} g(x_0) e^{i\lambda\phi(x_0)} e^{i\frac{\pi}{4}\text{sig}}\,, \tag{C.1}$$

assuming there is an extremum x_0 of ϕ within $\mathcal{D}$. Here sig is the number of positive minus the number of negative eigenvalues of the Hessian ϕ_{ij}. We use the method to evaluate (5.6) for large $x^2 > 0$. . After rescaling $\alpha \to \lambda\alpha$ and $x \to \lambda x$, (5.6) becomes

$$\tilde{\Delta}(x) = \lambda \int \frac{d^4p}{(2\pi)^4} \int_0^\infty d\alpha\, \mathcal{F}(p^2) e^{i\lambda(\alpha p^2 - \alpha m^2 - px)}\,. \tag{C.2}$$

Writing the exponent as $\lambda\phi(p,\alpha)$, the gradient of ϕ is $(2\alpha p_\mu - x_\mu,\, p^2 - m^2)$. Setting this to zero, we get the stationary point to be

$$\begin{pmatrix} \hat{p}^\mu \\ \hat{\alpha} \end{pmatrix} = \begin{pmatrix} x^\mu \sqrt{\frac{m^2}{x^2}} \\ \frac{1}{2}\sqrt{\frac{x^2}{m^2}} \end{pmatrix}\,. \tag{C.3}$$

For large positive x^2, the stationary point lies within the integration domain of (C.2). The Hessian evaluated at the stationary point is

$$\phi_{,p\alpha}(\hat{p},\hat{\alpha}) = \begin{pmatrix} \sqrt{\frac{x^2}{m^2}}\eta_{\mu\nu} & 2x_\mu\sqrt{\frac{m^2}{x^2}} \\ 2x_\mu\sqrt{\frac{m^2}{x^2}} & 0 \end{pmatrix}\,. \tag{C.4}$$

Its determinant is $4x^2\sqrt{\frac{x^2}{m^2}}$ and its signature is -3. Using (C.1), one finds

$$\tilde{\Delta}(x) \sim \lambda \sqrt{\frac{(2\pi)^5}{\lambda^5 4x^2\sqrt{x^2/m^2}}} \frac{1}{(2\pi)^4} \mathcal{F}(m^2) e^{-i\lambda m\sqrt{x^2}} e^{-i3\pi/4}\,, \tag{C.5}$$

which, after rescaling back $\lambda x \to x$, is (5.7).

APPENDIX D

Explicit asymptotic behavior of the acausal part of a particular effective propagator

We study the explicit example where $\mathcal{F} = Ne^{-p^4\ell^4}$, where $N = e^{m^4\ell^4}$. The delocalized vertex is

$$\tilde{V}(x) = \int \frac{d^4p}{(2\pi)^4} N e^{-p^4\ell^4} e^{-ipx} \ . \tag{D.1}$$

By Lorentz invariance, we can set $x = (\lambda\, 0\, 0\, 0)$ for any time-like x. After a change of variable to $u = p^0$ and $v = |\mathbf{p}|$, we get

$$\tilde{V}(x) = \int_0^\infty dv \int_{-\infty}^\infty du\, g(u,v) e^{\phi(u,v)} \ , \tag{D.2}$$

where

$$g(u,v) = \frac{N}{4\pi^3} v^2 \ , \tag{D.3}$$

$$\phi(u,v) = \left(-(u^2-v^2)^2\right)\ell^4 - i\lambda u \ . \tag{D.4}$$

By solving $\partial_u\phi = \partial_v\phi = 0$, one finds the saddle points to be $v = 0$ and $u = \frac{1}{\ell}\left(\frac{-i\lambda}{4\ell}\right)^{1/3}$. However, it is not clear how the integration contour, which is a 2 real-dimensional surface in a 2 complex-dimensional space, is deformed to pass through the saddle points in the direction of steepest descent while keeping the contour at infinity fixed. Thus we'll study one integration variable at a time, first finding the asymptotic for a fixed v, and then finding the asymptotic after integrating over v. For fixed v, the saddle points of u are located at

$$\partial_u\phi = -4u(u^2-v^2)\ell^4 - i\lambda = 0 \ . \tag{D.5}$$

There are three solutions to this equation, namely

$$\begin{aligned}
\hat{u}_1 &= e^{-i\frac{5\pi}{6}}\frac{1}{2\ell}\left(\frac{2\lambda}{\ell}\right)^{1/3} + e^{i\frac{5\pi}{6}}\frac{2}{3}\ell v^2\left(\frac{\ell}{2\lambda}\right)^{1/3} + \mathcal{O}(v^6) \\
\hat{u}_2 &= e^{-i\frac{\pi}{6}}\frac{1}{2\ell}\left(\frac{2\lambda}{\ell}\right)^{1/3} + e^{i\frac{\pi}{6}}\frac{2}{3}\ell v^2\left(\frac{\ell}{2\lambda}\right)^{1/3} + \mathcal{O}(v^6) \\
\hat{u}_3 &= e^{i\frac{\pi}{2}}\frac{1}{2\ell}\left(\frac{2\lambda}{\ell}\right)^{1/3} + e^{-i\frac{\pi}{2}}\frac{2}{3}\ell v^2\left(\frac{\ell}{2\lambda}\right)^{1/3} + \mathcal{O}(v^6)
\end{aligned} \tag{D.6}$$

.

To avoid cluttering, the exact form of the solution is replaced with the solution in the limit $v \to 0$, and because we know that the asymptotic is determined by the integral around $v = 0$. For each saddle point $\hat{u}_i$, the curves with constant $Im(\phi)$ that passes through the point are found. In most cases, there will be two such curves for each saddle point, but only one is along the direction of steepest descent, i.e. $Re(\phi)$ peaks at the saddle point along that curve; the other curve is along the direction of steepest ascent. We denote $\mathcal{C}_i$ as the steepest descent curve that passes through $\hat{u}_i$. For $v = 0$, the curves are plotted in Fig. D.1.

The qualitative features are essentially the same for small nonzero v. The original contour of u, which is the real line, can then be deformed to $\mathcal{C}_1 \cup \mathcal{C}_2$. This unambiguously determines the direction at which the contour passes through the saddle points and we denote the directions as $e^{i\psi_1(v)}, e^{i\psi_2(v)}$, respectively. For $v = 0$, $\psi_1 = -\pi/6$ and $\psi_2 = \pi/6$, which agrees with the contour in Fig. D.1. By the standard procedure of method of steepest descent, the integral is asymptotically

$$\tilde{V}(x) \sim \int dv\, g(\hat{u}_1, v)\sqrt{\frac{2\pi}{|\phi_{uu}(\hat{u}_1, v)|}}e^{\phi(\hat{u}_1,v)}e^{i\psi_1(v)} + g(\hat{u}_2, v)\sqrt{\frac{2\pi}{|\phi_{uu}(\hat{u}_2, v)|}}e^{\phi(\hat{u}_2,v)}e^{i\psi_2(v)} \ , \tag{D.7}$$

where

$$\begin{aligned}
\phi(\hat{u}_1, v) &= e^{i2\pi/3}3\left(\frac{\lambda}{4\ell}\right)^{4/3} + e^{i\pi/3}\left(\frac{\lambda^2\ell^4}{2}\right)^{1/3} v^2 + \mathcal{O}(v^4) \\
, \phi(\hat{u}_2, v) &= e^{-i2\pi/3}3\left(\frac{\lambda}{4\ell}\right)^{4/3} + e^{-i\pi/3}\left(\frac{\lambda^2\ell^4}{2}\right)^{1/3} v^2 + \mathcal{O}(v^4) \ ,
\end{aligned} \tag{D.8}$$

$$g(\hat{u}_1, v) = g(\hat{u}_2, v) = \frac{N}{4\pi^3}v^2 \ , \tag{D.9}$$

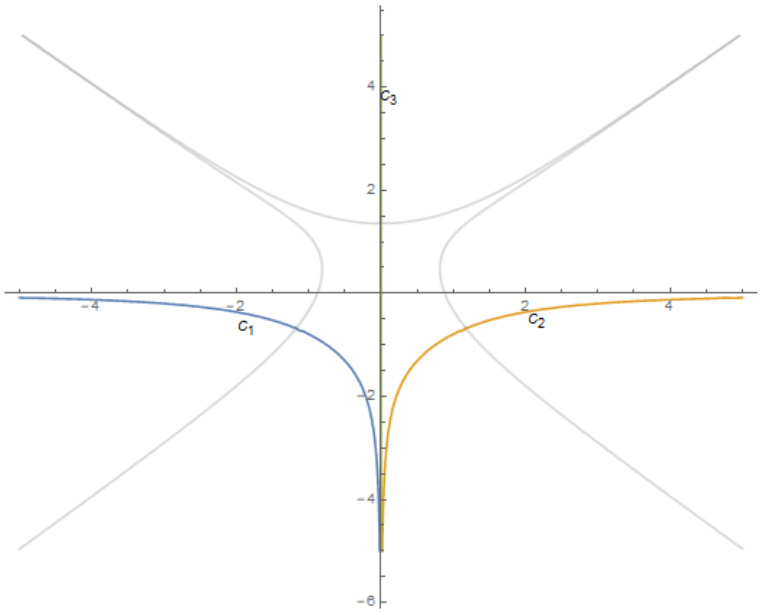


Figure D.1: Curves of steepest descent (in colors) and ascent (gray) of (D.4) in the complex u plane with $v = 0$. The saddle points (D.6) are located at the intersections. The original u contour of (D.2) can be deformed to $\mathcal{C}_1 \cup \mathcal{C}_2$.

and

$$\phi_{uu}(u, v) = 4(-3u^2 + v^2)\ell^4. \tag{D.10}$$

For the first term in (D.7), the saddle point is at $v = 0$ and we rotate $v \to e^{i\pi/3}v$ so that the contour is along the direction of steepest descent. One can show analytically that

$$\phi(\hat{u}_1, v) \to i\lambda v, \quad \text{as } v \to \infty. \tag{D.11}$$

and so the v contour is free to rotate in the upper half plane, justifying our deformation. We'd like to approximate the integral as a Gaussian around v, but the prefactor $g(\hat{u}_1, v) \propto v^2$ vanishes at $v = 0$. So the integral is really approximated by the second moment of a Gaussian integral, i.e

$$\int_0^\infty dv\, v^2 e^{-av^2} = \frac{1}{4}\sqrt{\frac{\pi}{v^3}}\,. \tag{D.12}$$

We then find the first term of (D.7) is asymptotically,

$$\begin{aligned} &-\frac{N}{16\pi^3}\sqrt{\frac{2\pi}{|\phi_{uu}(\hat{u}_1,0)|}}\sqrt{\frac{2\pi}{\lambda^2\ell^4}}e^{\phi(\hat{u}_1,0)}e^{i\psi_1(0)} \\ =&-\frac{N}{8\pi^2\sqrt{3}\lambda\ell^3}\left(\frac{\ell}{2\lambda}\right)^{1/3}e^{-i\pi/6}\exp\left[(-1+i\sqrt{3})\frac{3}{2}\left(\frac{\lambda}{4\ell}\right)^{4/3}\right] . \end{aligned} \tag{D.13}$$

Combining this with the second term of (D.7), which is exactly the complex conjugate of (D.13), and rewriting $\lambda=\sqrt{x^2}$, we get

$$\tilde{V}(x)\sim-\frac{N}{2\pi^2\sqrt{3}}\left(\frac{1}{4x^2\ell^4}\right)^{2/3}\exp\left[-\frac{3}{2}\left(\frac{x^2}{16\ell^2}\right)^{2/3}\right]\cos\left[\frac{3\sqrt{3}}{2}\left(\frac{x^2}{16\ell^2}\right)^{2/3}-\frac{\pi}{6}\right] . \tag{D.14}$$

We briefly sketch the derivation for large space-like separation. The vertex can be recast to

$$\tilde{V}(x)=\int_{-\infty}^{\infty}du\int_0^{\infty}dv\,g(u,v)e^{\phi(u,v)} , \tag{D.15}$$

$$\phi=-(u^2-v^2)^2\ell^4-i\lambda u , \tag{D.16}$$

$$g=\frac{iN}{4\pi^3\lambda}u . \tag{D.17}$$

where $\lambda=\sqrt{|x^2|}$. (We used $v=p^0$ and $u=|\mathbf{p}|$ and wrote it such that the integral bound looks exactly the same as (D.2)) Since the exponent is the same as for time-like separation, one can readily show that the saddle points are the same as (D.6), and that the asymptotic is also (D.7). The only difference is that

$$g(\hat{u}_{1,2},v)=\frac{iN}{4\pi^3\lambda}\hat{u}_{1,2} . \tag{D.18}$$

Then one can perform the approximation of v integral (which is now just a Gaussian instead of the second moment of Gaussian). The result is

$$\tilde{V}(x)\sim\frac{N}{2\pi^2\sqrt{3}}\left(\frac{1}{4|x^2|\ell^4}\right)^{2/3}\exp\left[-\frac{3}{2}\left(\frac{|x^2|}{16\ell^2}\right)^{2/3}\right]\cos\left[\frac{3\sqrt{3}}{2}\left(\frac{|x^2|}{16\ell^2}\right)^{2/3}-\frac{\pi}{6}\right] . \tag{D.19}$$

For both large space-like and time-like separation, $\tilde{V}(x)$ decays exponentially in $\left(\frac{|x^2|}{\ell^2}\right)^{2/3}$.

The calculation can be easily extended to find the asymptotic behaviour of the acausal part of the nonlocal propagator. Everything above is the same except, by (5.10) and (5.11), we replace $\ell^4 \to \xi\ell^4$ everywhere, multiply g in (D.3) by a factor of $p^2 + m^2 = u^2 - v^2 + m^2$, and integrate over ξ. The additional factor in g means that in (D.7), there's an additional factor of $\hat{u}_1^2$ in the first term and a factor of $\hat{u}_2^2$ to the second term. ($-v^2 + m^2$ is omitted because they are much smaller.) Explicitly, we get

$$\Delta_{ac} \sim i\ell^4 \int_0^1 d\xi \, \frac{e^{\xi m^4 \ell^4}}{8\pi^2\sqrt{3}} \frac{1}{(4x^2\xi^4\ell^{16})^{1/3}} \exp\left[-\frac{3}{2}\left(\frac{x^4}{256\xi\ell^4}\right)^{1/3}\right] \cos\left[\frac{3\sqrt{3}}{2}\left(\frac{x^4}{256\xi\ell^4}\right)^{1/3} + \frac{\pi}{6}\right] . \tag{D.20}$$

The ξ integral can be approximated asymptotically using Lapace's method and the result is shown in (5.13).

APPENDIX E

Fourier transform of Lorentz invariant functions

Supppose there's a Lorentz invariant function in momentum space, $A(p^2)$. Its Fourier transform into position space can be done partially by integrating out the angular part. The integral in question is

$$\begin{aligned} A(x^2) &= \int \frac{d^4p}{(2\pi)^4} A(p^2) e^{-ipx} \\ &= \frac{1}{(2\pi)^3} \int_{-\infty}^{\infty} dp^0 \int_0^{\infty} d|\boldsymbol{p}| \int_0^{\pi} d\theta \, |\boldsymbol{p}|^2 \sin\theta A(p^2) e^{-i(p^0x^0 - |\boldsymbol{p}||\boldsymbol{x}|\cos\theta)} \, . \end{aligned} \tag{E.1}$$

If x^2 is time-like, one can Lorentz transform so that $x = \begin{pmatrix} t & 0 & 0 & 0 \end{pmatrix}$, where $t \equiv \sqrt{x^2}$. One can then carry out the θ integral as followed:

$$\begin{aligned} A(x^2 > 0) &= \frac{1}{2\pi^3} \int_0^{\infty} dp^0 \int_0^{\infty} d|\boldsymbol{p}| \, |\boldsymbol{p}|^2 A(p^2) \cos(p^0 t) \\ &= \frac{1}{2\pi^3} \int_0^{\infty} dp d\eta \, p^3 \sinh^2\eta \, A(p^2) \cos\left(pt\cosh\eta\right) \\ &+ \frac{1}{2\pi^3} \int_0^{\infty} dp d\eta \, p^3 \cosh^2\eta \, A(-p^2) \cos\left(pt\sinh\eta\right) \\ &= \frac{1}{2\pi^3} \int_0^{\infty} dp d\eta \, A(p^2) p \left(-\frac{d^2}{dt^2} - p^2\right) \cos\left(pt\cosh\eta\right) \\ &+ \frac{1}{2\pi^3} \int_0^{\infty} dp d\eta \, A(-p^2) p \left(p^2 - \frac{d^2}{dt^2}\right) \cos\left(pt\sinh\eta\right) \\ &= \int_0^{\infty} \frac{dp}{(2\pi)^3} A(p^2) \pi p^3 \Big[Y_0(p\sqrt{x^2}) + Y_2(p\sqrt{x^2}) \Big] \\ &+ \int_0^{\infty} \frac{dp}{(2\pi)^3} A(-p^2) 2p^3 \Big[K_0(p\sqrt{x^2}) - K_2(p\sqrt{x^2}) \Big] \, , \end{aligned} \tag{E.2}$$

where Y is the Bessel function of the second kind and K is the modified Bessel function of the second kind. In the second equality , we did a change of variable $p^0 = p\cosh\eta$, $|\boldsymbol{p}| = p\sinh\eta$ and $p^0 = p\sinh\eta$, $|\boldsymbol{p}| = p\cosh\eta$, for the time-like and space-like domain, respectively. In

the fourth equality, one integrate out η to get the Y and K functions, the derivatives of which are also Y and K functions. Finally, the expression can be simplified by the recursion relation of the Bessel functions and we arrive at

$$A(x^2>0)=\frac{1}{(2\pi)^3\sqrt{x^2}}\int_0^\infty dp\,p^2\left[2\pi A(p^2)Y_1\left(p\sqrt{x^2}\right)-4A(-p^2)K_1\left(p\sqrt{x^2}\right)\right]\ . \tag{E.3}$$

If the separation is space-like, then one can Lorentz transform to $x=\begin{pmatrix}0 & r & 0 & 0\end{pmatrix}$ where $r\equiv\sqrt{-x^2}$. Then

$$\begin{aligned}A(x^2<0)&=\frac{1}{2\pi^3}\int_0^\infty dp^0\int_0^\infty d|\boldsymbol{p}|\,\frac{|\boldsymbol{p}|}{r}A(p^2)\sin(|\boldsymbol{p}|r)\\&=\frac{1}{2\pi^3}\frac{1}{r}\int_0^\infty dpd\eta\,p^2\sinh\eta\,A(p^2)\sin(pr\sinh\eta)\\&+\frac{1}{2\pi^3}\frac{1}{r}\int_0^\infty dpd\eta\,p^2\cosh\eta\,A(-p^2)\sin(pr\cosh\eta)\\&=-\frac{1}{2\pi^3}\frac{1}{r}\int_0^\infty dpd\eta\,p\,A(p^2)\frac{d}{dr}\cos(pr\sinh\eta)\\&-\frac{1}{2\pi^3}\frac{1}{r}\int_0^\infty dpd\eta\,p\,A(-p^2)\frac{d}{dr}\cos(pr\cosh\eta)\ .\end{aligned} \tag{E.4}$$

One can integrate over the η integral and differentiate. The result is

$$A(x^2<0)=\frac{1}{(2\pi)^3\sqrt{-x^2}}\int_0^\infty dp\,p^2\left[4A(p^2)K_1\left(p\sqrt{-x^2}\right)-2\pi A(-p^2)Y_1\left(p\sqrt{-x^2}\right)\right]\ . \tag{E.5}$$

APPENDIX F

Examples of asymptotic behavior using the Mellin Transform method

In this appendix, we apply the Mellin Transform method as described in section 5.1 to common expressions to check consistency and to point out the consequences when the conditions in section 5.1 are not met.

F.1 Ordinary massive propagator

We first study the asymptotic behavior of the ordinary massive propagator when the separation is large and space-like, which as shown in (5.4), should be exponentially suppressed in $\sqrt{x^2}$. By Lorentz invariance, we can write the propagator $\Delta(x)$ as (E.5) with

$$\begin{aligned} A(p^2) &= \frac{i}{p^2 - m^2} \equiv f_1(p) \ , \\ A(-p^2) &= \frac{-i}{p^2 + m^2} \equiv f_2(p) \ . \end{aligned} \tag{F.1}$$

Following the steps in section 5.1.2, we have to check that the conditions (5.22), (5.23) are satisfied and note that in (E.5), $h_1(p)$ of (5.25) is paired with $f_2(p)$ instead of $f_1(p)$. The Mellin Transform of $f_{1,2}(p)$ can be easily computed to be

$$M[f_1; z] = -i\frac{\pi}{2} m^{z-2} \left(i + \cot\frac{\pi z}{2} \right) \ , \tag{F.2}$$

$$M[f_2; z] = -i\frac{\pi}{2} m^{z-2} \csc\frac{\pi z}{2} \ . \tag{F.3}$$

The problematic one is $M[h_1; z]$, which grows polynomially in y for large y, where $z = x + iy$. But $M[f_2; 1 - z]$ is exponentially suppressed for large y, so conditions (5.22), (5.23) are

satisfied, and the asymptotic series (5.30) contains infinite number of terms. Then since f_1 and f_2 are defined from the same function $A(p^2)$, (5.36) holds and the cancellation in (5.37) can happen, which in turn means that $\Delta(x)$ decays faster than any power in $1/x^2$ for large space-like x, as we have expected.

On the other hand, for large time-like separation, the conditions (5.22), (5.23) are not satisfied. From (E.3), we see that h_1 is paired with f_1. $M[h_1, z]$ has the problem of polynomial growth for large y, but $M[f_1; 1-z]$ is only $O(1)$ for large y. Clearly then (5.22) does not hold. Thus although f_1, f_2 are defined from the same function and (5.36) holds, the asymptotic series (5.30) is not valid and we cannot conclude that $\Delta(x)$ decays faster than any power of $1/x^2$ for large time-like x. This is consistent with (5.4).

F.2 Bubble graph of massless particles

The second example will be about an amplitude where (5.36) does not hold and therefore the full cancellation in (5.37) does not happen. Consider the bubble graph amplitude for massless particles (e.g. Fig 2.1). The amplitude is

$$A(p^2) = -\int \frac{d^4k}{(2\pi)^4} \frac{1}{(p+k)^2 k^2} \,. \tag{F.4}$$

This amplitude is defined in Euclidean space with strictly negative p^2 and then continued into Minkowski space. After introducing the Schwinger parameter into the expression and appropriately regulating the ultraviolet divergence, we get

$$\begin{aligned} A(s) &= -\frac{i}{16\pi^2} \int_0^1 d\alpha_1 d\alpha_2 \, \delta(1-\alpha_1-\alpha_2) \ln\left[\frac{\alpha_1\alpha_2}{\alpha_1+\alpha_2} s\right] + Const. \\ &= -\frac{i}{16\pi^2} \ln(s) + Const. \end{aligned} \tag{F.5}$$

The constant depends on the regularization scheme and is not important. The amplitude can be straightforwardly continued to positive s. When we Fourier transform the amplitude into position space and study the asymptotic behavior for large x^2 following the method in section 5.1, we see that the expansions (5.28) and (5.29) do not satisfy (5.36). Instead, we

get

$$\begin{aligned} f_1(p) = A(p^2) &= a_0 - \frac{i}{16\pi^2}\ln(p^2) \\ f_2(p) = A(-p^2) &= a_0 + \frac{1}{16\pi} - \frac{i}{16\pi^2}\ln(p^2) \end{aligned} \tag{F.6}$$

The exact value of a_0 depends on the regulation scheme and won't matter. But the difference in the constant term means that the expansion in (5.30) don't cancel term by term and the remaining term is

$$A(x^2) \sim \frac{1}{16\pi^4 x^4}\ , \tag{F.7}$$

where we restored the factor of $1/(2\pi)^3$ that was omitted in all of section 5.1. To be precise, one has to do extra work in dealing with the $\ln(p)$ in $f_{1,2}$ because that changes the nature of the poles of $M[h;z]M[f;1-z]$, but it turns out that their contributions cancels as well like in (5.37). See [39] for details on how to deal with log terms.

From ordinary field theory, we know that the Fourier transform of (F.4) is just the position-space propagator squared, i.e.,

$$A(x^2) = D(x)^2 = \frac{1}{16\pi^2 x^4}, \quad \text{for} \quad x^2 > 0\ . \tag{F.8}$$

This agrees with the asymptotic behavior (F.7).

APPENDIX G

BCC argument for all loop

In this Appendix we prove statements (i) and (ii) of section 6.4.3. Consider a general graph with N internal lines. We proceed by induction in N.

Consider the case $N = 2$, i.e., two internal propagators. Keeping vertex 1 not underlined (unfilled circle) the possible graphs are shown in Fig. G.1, where, by our graphical conventions above, any number of external legs can be attached to the vertices. Statement

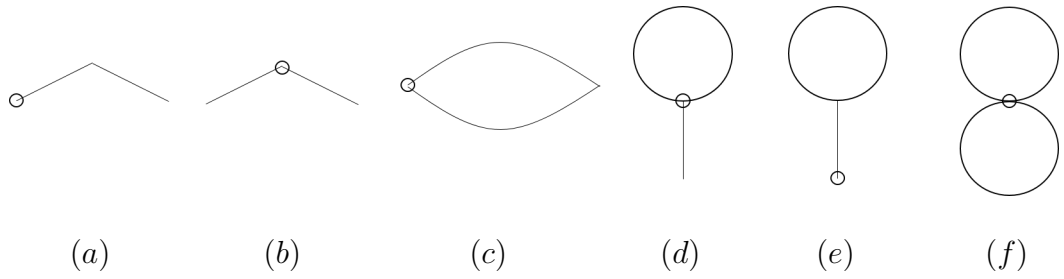


Figure G.1: Graphs with two internal propagators; external legs not explicitly shown.

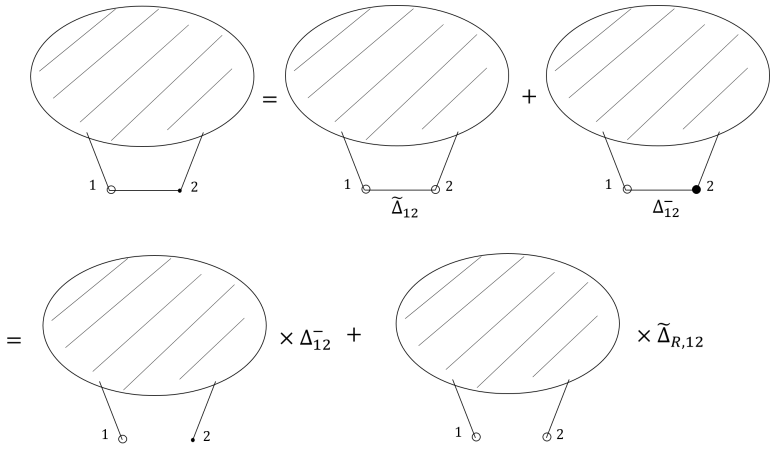
(i) holds for the two tree graphs (a) and (b) and for the one-loop graph (c) by the results in sections 6.2, 6.4.1 above. Graph (d) gives $\tilde{\Delta}_{11}\tilde{\Delta}_{R,12}$ by the tree argument of section 6.2. Graph (e) gives $\tilde{\Delta}_{12}\tilde{\Delta}_{22} - \Delta^{-}_{12}\tilde{\Delta}^{*}_{22} = \tilde{\Delta}_{R,12}\tilde{\Delta}_{22} + \Delta^{-}_{12}(\tilde{\Delta}_{R,22} + \tilde{\Delta}_{A,22})$ by use of the relations (6.8) - (6.9). So, the first term is a $\tilde{\Delta}_R$ connecting 2 to 1, and the second and third terms have a one-propagator loop of $\tilde{\Delta}_R$. Finally, graph (f) is a trivial case of (i), since there is no other vertex to be connected to x_1. The analogous expressions hold when vertex 1 is always underlined; e.g., graph (e) gives $-\Delta^{-}_{21}\tilde{\Delta}_{22} + \tilde{\Delta}^{*}_{21}\tilde{\Delta}^{*}_{22} = -\Delta^{+}_{21}(\tilde{\Delta}_{R,22} + \tilde{\Delta}_{A,22}) - \tilde{\Delta}_{R,12}\tilde{\Delta}^{*}_{22}$. Thus statement (i) holds for all graphs with $N = 2$.

Consider next the sum over underlinings of all vertices (i.e., including vertex 1) for the

graphs of Fig. G.1. Statement (ii) holds for graphs (a) -(c) by the results in sections 6.2, 6.4.1. Similarly, graph (d) gives $\tilde{\Delta}_{R,12}\tilde{\Delta}_{11} - \tilde{\Delta}_{R,12}\tilde{\Delta}^*_{11} = \tilde{\Delta}_{R,12}(\tilde{\Delta}_{R,11} + \tilde{\Delta}_{A,11})$. For graph (e), adding the expressions in the previous paragraph and using again (6.8) - (6.9) is shown to give $\tilde{\Delta}_{A,12}(\tilde{\Delta}_{R,22} + \tilde{\Delta}_{A,22})$. Finally graph (f) is easily seen to give $(\tilde{\Delta}_{A,11} + \tilde{\Delta}_{R,11})\tilde{\Delta}_{11} + \tilde{\Delta}^*_{11}(\tilde{\Delta}_{A,11} + \tilde{\Delta}_{R,11})$. Thus, since $\tilde{\Delta}_{A,ij} = \tilde{\Delta}_{R,ji}$, the integrands of graphs (d) - (f) all include a one-propagator $\tilde{\Delta}_R$ loop. Thus statement (ii) holds for all graphs with $N = 2$.

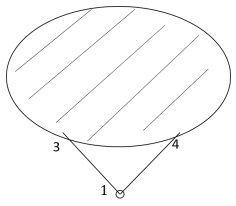
Now suppose that statements (i) and (ii) are true for the integrands of all graphs with $N - 1$ internal lines. We will show that they then hold true for those with N internal lines.

Consider the sum over all underlinings with singled-out vertex 1 kept not underlined. Assume first that there are two internal lines attached to it. One then has the relation:



. (G.1)

Again, the stripped blob represents the rest of the diagram, external legs are not shown, and it is assumed that vertex 1 and vertex 2 are connected to the blob as shown. The second line in (G.1) follows by (6.8). The first term in the second line has a chain of $\tilde{\Delta}_R$ from every other vertex to vertex 1 by induction. The second term in the second line can be compared to the following diagram

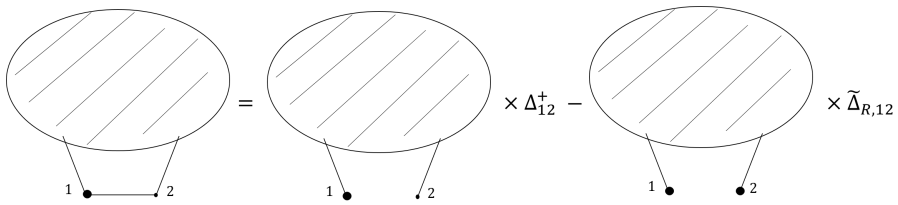


,

which also has a chain of $\tilde{\Delta}_R$ from every other vertex to vertex 1 by induction. The vertices

neighboring vertex 1 have also been labeled explicitly. The second term of the second line in (G.1) can be obtained from this diagram by simply replacing all the $\Delta^{\pm}_{41}$ and $\tilde{\Delta}_{R(A),41}$ by $\Delta^{\pm}_{42}$ and $\tilde{\Delta}_{R(A),42}$. Thus, the second term has a chain of $\tilde{\Delta}_R$ from every vertex, other than 1 and 2, to either vertex 1 or 2. This, together with the factor of $\tilde{\Delta}_{R,12}$ already explicitly separated in (G.1), means that there is a chain of $\tilde{\Delta}_R$ from every other vertex (including 2) to vertex 1.

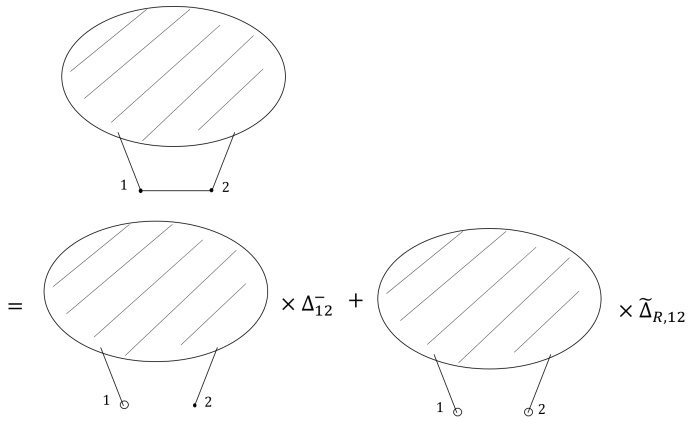
Similarly, if vertex 1 is always underlined, one obtains:

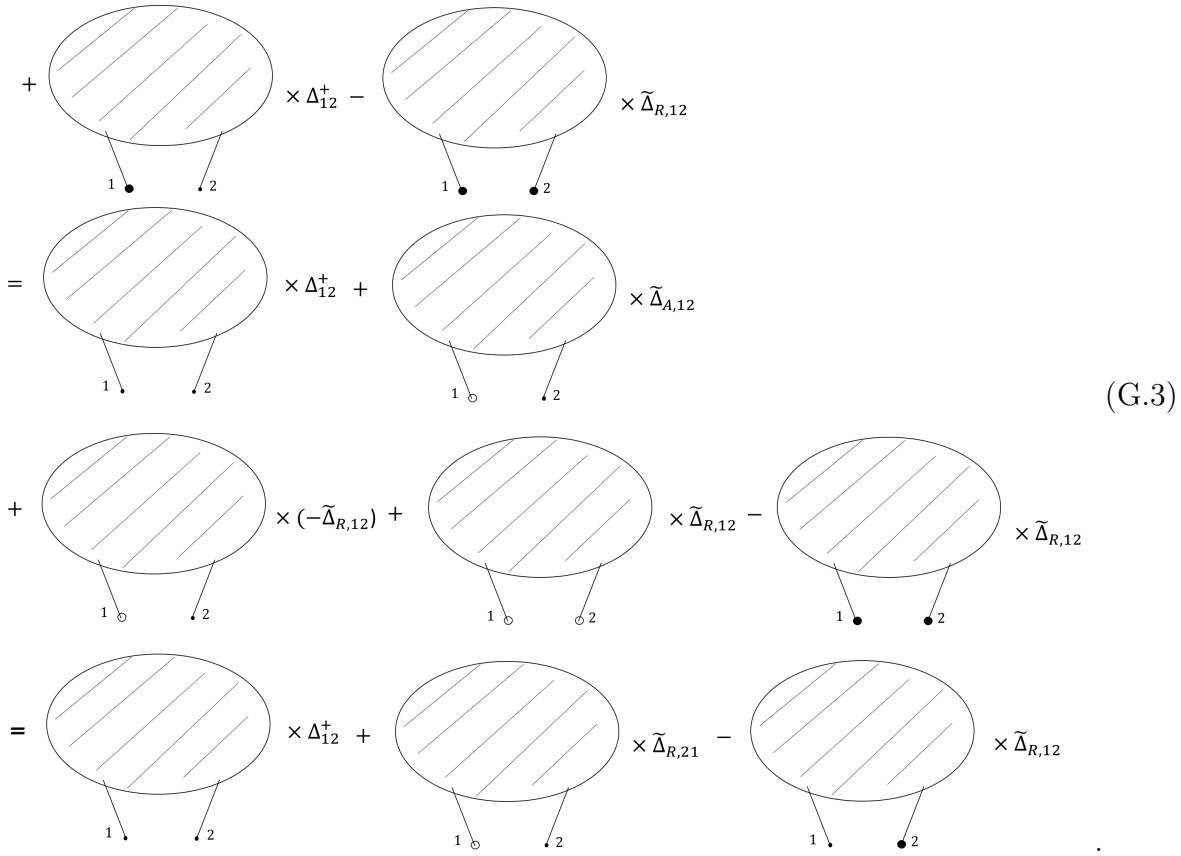


. (G.2)

Using the same comparison of the second term on the r.h.s. to the integrand of the graph compared obtained from merging vertex 1 and 2, one concludes by the induction hypothesis that there is a chain of $\tilde{\Delta}_R$ from every other vertex to vertex 1.

Next, consider the sum over underlinings of all vertices (including x_1). One gets:





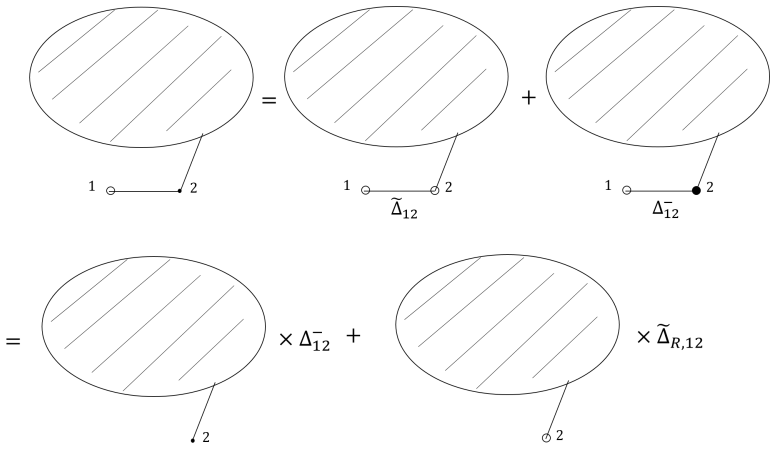
(G.3)

The first equality in (G.3) is obtained by summing (G.1) and (G.2). The second equality in obtained as follows. In the first term in the second line in (G.3) one uses the identity $\Delta^- = \Delta^+ + \tilde{\Delta}_A - \tilde{\Delta}_R$; then the Δ^+_{12} part is combined with the first term of the third line to get the first term of the fourth line. The third equality in (G.3) is obtained by noting that the three terms in the fifth line combine to give the last term in the sixth line.

In the final equality in (G.3), the first term contains at least one loop of $\tilde{\Delta}_R$ (or $\tilde{\Delta}_A$) by the induction hypothesis in (ii). The second term contains a chain of $\tilde{\Delta}_R$ from vertex 2 to vertex 1 by induction in (i). The chain combines with the explicit factor of $\tilde{\Delta}_{R,21}$ to form a closed loop of $\tilde{\Delta}_R$ propagators. Similarly, the third term has a chain of $\tilde{\Delta}_R$ from 1 to 2 (where now 2 is taken as the singled-out vertex) by induction in (i); this chain, together with the factor of $\tilde{\Delta}_{R,12}$, then forms a closed loop of $\tilde{\Delta}_R$ propagators. This completes the inductive proof of (i) and (ii) when vertex 1 is connected by two internal lines in the manner assumed in (G.1), (G.2).

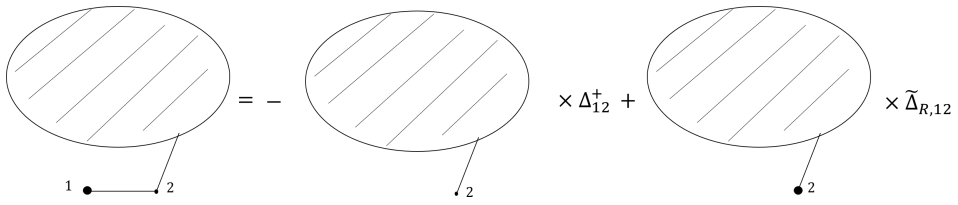
It is easily seen that the same argument carries through when vertices 1 and 2 are connected to the rest of the diagram (blob) by more than one internal line.

The case where vertex 2 is connected only to vertex 1 is a special case of the treatment of tree graphs above. In particular, summing over the underlinings of 2 results in a factor of $\tilde{\Delta}_{R,12}$. In the case where the vertex 1 is connected only to vertex 2 and vertex 1 is kept not underlined, the sum over all other underlinings gives:



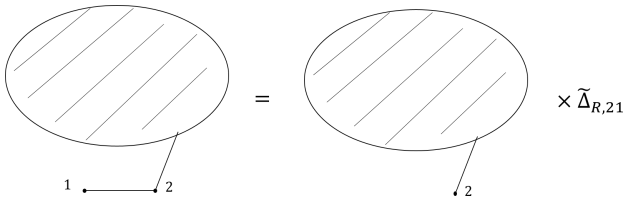
. (G.4)

The first term in the final equality has a closed loop of $\tilde{\Delta}_R$ propagators by the induction hypothesis. In the second term the graph contains a chain of $\tilde{\Delta}_R$ from every other vertex to vertex 2 by the induction hypothesis, which combines with the explicit $\tilde{\Delta}_{R,21}$ to form a chain from any other vertex to vertex 1. Similarly, when vertex 1 is kept underlined, one has:



. (G.5)

The sum over all underlinings, obtained by summing (G.4) and (G.5). Using again the identity $\Delta^- = \Delta^+ + \tilde{\Delta}_A - \tilde{\Delta}_R$ and $\tilde{\Delta}_{A,12} = \tilde{\Delta}_{R,21}$ one gets:



. (G.6)

Note that (G.6) may also be obtained directly by applying the tree level argument of section 6.2 to the sum over underlinings of 1 to get the factor of $\tilde{\Delta}_{R,21}$ on the r.h.s. Thus, by the induction hypothesis, the r.h.s. ends up containing a chain of $\tilde{\Delta}_R$ propagators connecting any other vertex to 1.

This completes the inductive proof of (i) and (ii) for all cases where vertices 1 and 2 are connected by one internal line. The extension when vertices 1 and 2 are connected by more than one line is obtained by repeated use of the same type of argument, and, in particular, systematic use of the identities (6.8), (6.9).

Bibliography

[1] P. Chin and E. T. Tomboulis, *Nonlocal vertices and analyticity: Landau equations and general Cutkosky rule*, *JHEP* **06** (2018) 014, [1803.08899].

[2] P. Chin and E. T. Tomboulis, "Nonlocal vertices and causality." to be published, 2022.

[3] E. T. Tomboulis, *Multigravity and the cosmological constant*, 2110.15516.

[4] R. J. Eden, P. V. Landshoff, D. I. Olive and J. C. Polkinghorne, *The analytic S-matrix*. Cambridge Univ. Press, Cambridge, 1966.

[5] R. F. Streater and A. S. Wightman, *PCT, spin and statistics, and all that*. Princeton University Press, 1989.

[6] S. Coleman, *Acausality*, in *7th International School of Subnuclear Physics (Ettore Majorana): Subnuclear Phenomena*, 1969.

[7] N. N. Bogolyubov and D. V. Shirkov, *Introduction to the theory of quantized fields*, vol. 3. John Wiley & Son, Inc, 1959.

[8] L. D. Landau, *On analytic properties of vertex parts in quantum field theory*, *Nucl. Phys.* **13** (1959) 181–192.

[9] R. E. Cutkosky, *Singularities and discontinuities of Feynman amplitudes*, *J. Math. Phys.* **1** (1960) 429–433.

[10] R. Pius and A. Sen, *Cutkosky rules for superstring field theory*, *JHEP* **10** (2016) 024, [1604.01783].

[11] E. T. Tomboulis, *Nonlocal and quasilocal field theories*, *Phys. Rev. D* **92** (2015) 125037, [1507.00981].

[12] G. V. Efimov, *Non-local quantum theory of the scalar field*, *Commun. Math. Phys.* **5** (1967) 42–56.

[13] A. Pais and G. E. Uhlenbeck, *On Field theories with nonlocalized action*, *Phys. Rev.* **79** (1950) 145–165.

[14] G. V. Efimov, *Quantization of non-local field theory*, *Int. J. Theor. Phys.* **10** (1974) 19–37.

[15] E. C. Titchmarsh, *The Theory of Functions*. Oxford University Press, Oxford, 1968.

[16] I. M. Gel'fand and G. E. Shilov, *Generalized functions*, vol. II. Academic Press, New York, 1964.

[17] D. I. Olive, *Unitarity and the evaluation of discontinuities*, *Il Nuovo Cimento* **26** (1962) 73–102.

[18] J. Glimm and A. Jaffe, *Quantum Physics*. Springer, New York, 1987.

[19] C. D. Carone, *Unitarity and microscopic acausality in a nonlocal theory*, *Phys. Rev. D* **95** (2017) 045009, [1605.02030].

[20] L. Keltner and A. J. Tolley, *UV properties of Galileons: Spectral Densities*, 1502.05706.

[21] L. Hormandor, *The Analysis of Linear Partial Differential Operators I*. Springer, Heidelberg, Berlin, 2 ed., 1990.

[22] N. Nakanish, *Graph Theory and Feynman Integrals*. Gordon and Breach, New York, 1971.

[23] J. Hadamard, *Théorème sur les séries entières*, *Acta Math.* **22** (1899) 55.

[24] J. C. Polkinghorne and G. R. Screaton, *The analytic properties of perturbation theory — i*, *Il Nuovo Cimento* **15** (1960) 289.

[25] J. C. Polkinghorne and G. R. Screaton, *The analytic properties of perturbation theory — ii*, *Il Nuovo Cimento* **15** (1960) 925.

[26] R. C. Hwa and V. L. Tplitz, *Homology and Feynman integrals*. W. A. Benjamin, New York, 1966.

[27] J. D. Bjorken, *Experimental tests of Quantum electrodynamics and spectral representations of Green's functions in perturbation theory*. PhD thesis, Stanford U., 1959.

[28] J. Tarski, *Analyticity of the fourth order scattering amplitude with two complex invariants*, *J. Math. Phys.* **1** (1960) 149.

[29] R. J. Eden, P. V. Landshoff, J. C. Polkinghorne and J. C. Taylor, *Mandelstam representation with anomalous thresholds*, *Phys. Rev.* **122** (1961) 307.

[30] R. J. Eden, P. V. Landshoff, J. C. Polkinghorne and J. C. Taylor, *Acnodes and cusps on landau curves*, *J. Math. Phys* **2** (1961) 656.

[31] D. I. Olive and J. C. Taylor, *Singularities of scattering amplitudes at isolated real points*, *Il Nuovo Cimento* **24** (1962) 814–822.

[32] T. T. Wu, *Properties of normal thresholds in perturbation theory*, *Phys. Rev.* **123** (Jul, 1961) 689–691.

[33] D. B. Fairlie, P. V. Landshoff, J. Nuttall and J. C. Polkinghorne, *Singularities of the second type*, *J. Math. Phys.* **3** (1962) 594.

[34] E. T. Tomboulis, *Causality and Unitarity via the Tree-Loop Duality Relation*, *JHEP* **05** (2017) 148, [1701.07052].

[35] R. P. Feynman, *Closed loop and tree diagrams*, in *Magic without magic* (J. R. Klauder, ed.), p. 355. Freeman, San Francisco, 1972.

[36] S. Catani, T. Gleisberg, F. Krauss, G. Rodrigo and J.-C. Winter, *From loops to trees by-passing Feynman's theorem*, *JHEP* **09** (2008) 065, [0804.3170].

[37] M. J. G. Veltman, *Unitarity and causality in a renormalizable field theory with unstable particles*, *Physica* **29** (1963) 186–207.

[38] R. Blankenbecler, M. L. Goldberger, S. W. MacDowell and S. B. Treiman, *Singularities of scattering amplitudes on unphysical sheets and their interpretation*, *Phys. Rev.* **123** (Jul, 1961) 692–699.

[39] N. Bleistein and R. Handelsman, *Asymptotic Expansions of Integrals*. Holt, Rinehar and Winston, New York, 1975.

[40] L. Buoninfante, G. Lambiase and A. Mazumdar, *Ghost-free infinite derivative quantum field theory*, *Nucl. Phys. B* **944** (2019) 114646, [1805.03559].

[41] I. S. Gradshtyn and I. M. Ryzhik, *Table of Integrals, Series, and Products*. Elsvier Inc, 8th ed., 2014.

[42] G. 't Hooft and M. J. G. Veltman, *Diagrammar*, *NATO Sci. Ser. B* **4** (1974) 177–322.

[43] R. Dickinson, J. Forshaw, P. Millington and B. Cox, *Manifest causality in quantum field theory with sources and detectors*, *JHEP* **06** (2014) 049, [1312.3871].

[44] B. Grinstein, D. O'Connell and M. B. Wise, *Causality as an emergent macroscopic phenomenon: The Lee-Wick O(N) model*, *Phys. Rev. D* **79** (2009) 105019, [0805.2156].

[45] K. Symanzik, *Dispersion Relations and Vertex Properties in Perturbation Theory*, *Progress of Theoretical Physics* **20** (1958) 690–702.